UT-GOM2-1 Hydrate Pressure Coring Expedition

Chapter 3. Hole GC 955 H002

Contents

List of Figures

List of Tables

Chapter 3. Hole GC 955 H002

Abstract

This chapter describes the operations, sample collection and handling, initial analyses, and preliminary interpretations developed by the UT-GOM2-1 Science Party for Hole GC 955 H002 (H002). This chapter describes the results of H002 pressure coring, physical property analysis, quantitative degassing, lithostratigraphic analysis, geochemical analysis, and wireline logging. All methods are described in Chapter 2 Expedition Methods.

3.1. Background and Objectives

H002 is located at 27^{o} 0.04154' N, -90^{o} 25.58715' W in Green Canyon 955 (Figure 1.3.2 of the UT-GOM2-1 Expedition Summary). H002 is 61.7 ft (18.8 m) SSW of the originally drilled JIP Leg 2 Hole GC 955 H001 (H001). The water depth is 6667 ft (2032.1 m).

The objectives of the work carried out at this site follow the general objectives of the UT-GOM2-1 expedition. Our goal was to:

- Test the DOE pressure coring tool with ball in the cutting shoe configuration (PCTB-CS)
- Recover pressure core samples throughout the main hydrate reservoir, including the top and base of hydrate contacts, as well as lithology both above and below the hydrate reservoir
- Recover gas samples for geochemical analysis
- Characterize the lithology and interpret the depositional environment of the hydrate reservoir
- Characterize hydrate saturation within the reservoir
- Characterize the pore water geochemistry and microbiology of the reservoir
- Run wireline logs across the cored section

Based on the depth of the seafloor observed by ROV at H002 and our mapping of seismic surfaces away from H001, the depths of events were predicted in H002 (Table 3.1.1). After correlating the seismic reflectors associated with the seafloor and the top of the hydrate-bearing coarse-grained interval, the top of the hydrate bearing zone was predicted to be one foot deeper relative to the rig floor and the same depth relative to the seafloor as encountered in H001.

Our goal was to sample in and near the sand-rich hydrate-bearing interval found by the JIP II logging while drilling (LWD) expedition (Boswell et al., 2012; Collett et al., 2010) and compare these results back to the previously acquired H001 LWD data.

Event	Depth below Rig Floor	Depth below Sea Level	Depth Below Seafloor	Seismic Reference Depth	Lithostratigraphic Unit
unit	fbrf	fbsl	fbsf	ft	
Sea floor	6,719	6,667	-	6,669	I
Top Fracture Filling Hydrates	7,329	7,277	610	7,279	
Fault	7,469	7,417	750	7,419	
5' thick sand	7,471	7,419	752	7,421	
Base Fracture Filling Hydrates	7,681	7,629	962	7,631	
Top Sand - rich section	8,033	7,981	1,314	7,983	II
Top Hydrate - Predicted	8,082	8,030	1,363	8,032	
Top Hydrate - Seismic Peak	8,163	8,111	1,444	8,113	
Base of Main Hydrate Reservoir - Predicted	8,311	8,259	1,592	8,261	
Base of Sand Unit	8,402	8,350	1,683	8,352	
Base of Channel System	8,551	8,499	1,832	8,501	III

Table 3.1.1 Mapped horizons at H002. H002 distance from the rig floor to the sea level was 52 ft. More information about the events and Lithostratigraphic Units can be found in Chapter 1. Expedition Summary Section 1.2.2 GC 955 Site Characterization and Selection and Section 1.4.1 Lithostratigraphy and Physical Properties. More information about the reference depths can be found in Chapter 2 Methods, Section the UT-GOM2-1 Methods Section 2.1.3. Depth References.

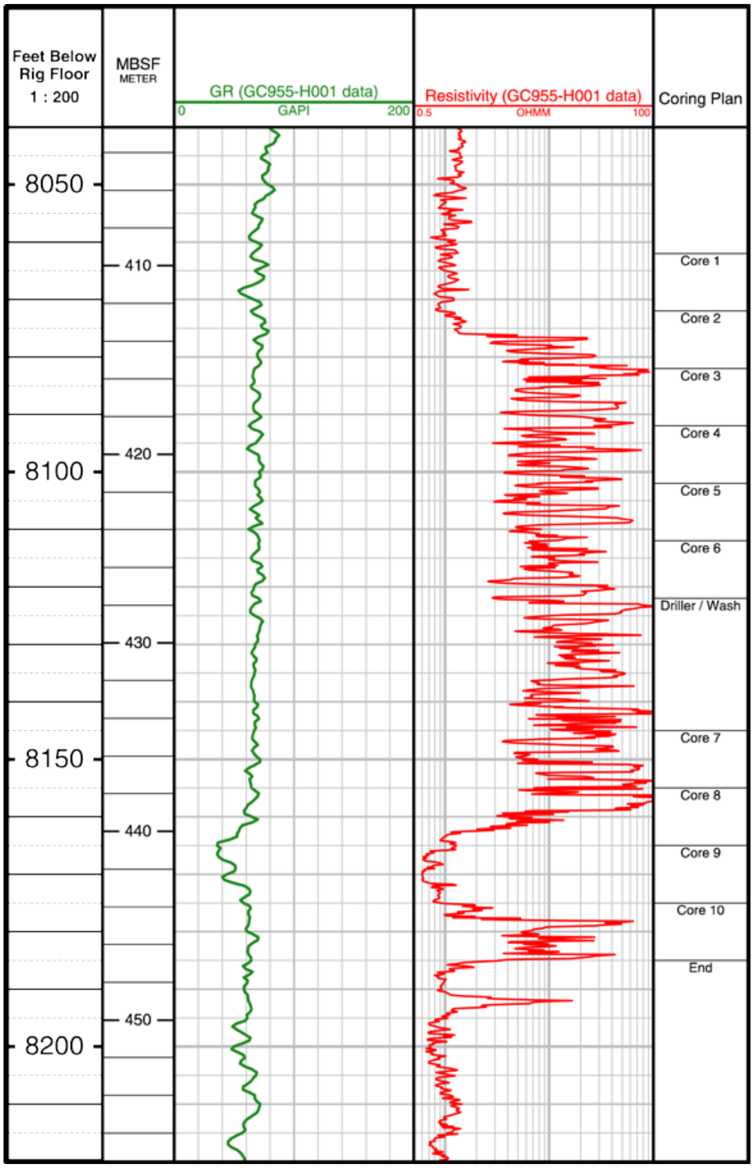

Figure 3.1.1 H002 coring plan versus H001 LWD data. Core 2 captures the upper boundary of hydrate. Core 8 captures the lower boundary.

Coring points (Figure 3.1.1) were picked based on the assumption that the stratigraphy encountered at H002 would be similar to that encountered at H001. The main target was the 87 ft thick main hydrate-bearing interval within the sand-rich unit. Ten, 10 ft, cores were planned in stratigraphic succession throughout this interval, with Core 1 being the shallowest and Core 10 the deepest. Core 2 was designed to encounter the top of hydrate within the center of the core. Core 8 was designed to encounter the base of hydrate within the center of the core. Cores 9 and 10 were designed to encounter water-bearing sands below hydrate. Overall, the coring plan called for coring the following: 15 ft of water-bearing sand/silt above the hydrate layer, 60 ft of interbedded hydrate sands, and 25 ft of water-bearing sands/silts below the base of the hydrate-bearing interval.

After completing the coring program, the plan was to drill ~250 ft further in order to extend the well far enough so that the logging tools could collect resistivity, velocity, density, gamma ray, and caliper measurements over the cored section. H002 would then be plugged and abandoned.

3.2. Operations

This section covers the operations associated with H002. Schedule and operational details for this drill and core hole can be found in Appendix A: UT-GOM2 Pre-Drill Operations Plan (activities, time estimates and forecast), and Appendix B: UT-GOM2 Post-Drill Operation Report and Daily Log (executed activities, drilling and coring statistics, and an event drilling-log) of Chapter 1 Expedition Summary.

The Helix *D/V Q4000* arrived within 1 nmi of the proposed location of H002 on 06-May-2017 at 1600 hr after completing required vessel sea trials and transiting 307 nmi from Brownsville, Texas. Upon arrival at H002, the *D/V Q4000* ROV was launched to deploy four Compatt seafloor transponders and to visually survey the seafloor at the site of the proposed well. H001 was found at 2247 hr at a location of 27° 00.05126’ N, 090° 25.58367’ W (WGS84 coordinate system). The borehole well-head at the seafloor was intact and in good condition. Also on 06-May-2017, the supply boat *M/V HOS Crockett* began the transfer of drilling mud, drilling gel, and the UT Mud Lab to the *D/V Q4000*. The transfer was completed at 1227 hr of 08-May-2017. On 09-May-2017 three Shallow Flow Tests of the DOE pressure coring tool with ball valve in the cutting shoe configuration (PCTB-CS) were conducted with the bottom hole assembly (BHA) hanging from the vessel just below the sea surface. Analysis of data from the instrumented core liner showed only small pressure differentials across the core liner during each of the three Shallow Flow Tests of the PCTB-CS (See Section 3.3 Pressure Coring). Upon visual inspection, the instrumented core liner did not exhibit any damage or deformation. The PCTB-CS Shallow Flow Tests 1 and 2 revealed a potential problem associated with the use of the on-board Hex mud pumps in that the pumps could not effectively work below a flow rate of about 125 gpm, which was required for controlled coring operations. The cement pumps used during Shallow Flow Test 3 were able to establish and maintain low flow rates in the range of 21-40 gpm. The operational plan was modified to include the use of the cement pumps during pressure coring operations.

The BHA was made up and run to the seafloor with drill collars and pipe reaching near the seafloor (6716 fbrf) at 2110 hr on 10-May-2017. Two Deep Flow Tests of the PCTB-CS were conducted with the BHA just above the seafloor. The two Deep Flow Tests were completed without any concerns, documenting only small pressure differentials across the core liner for all of the completed tests (See Section 3.3 Pressure Coring). Operations in support of spudding H002 began with offsetting the *D/V Q4000* 196 ft (15.8 m) SSW of H001. At 0830 hr on 11-May-2017, H002 was spudded at a water depth of 6667 ft (6719 fbrf) and the hole was advanced to a depth of 8032 fbrf (1313 fbsf) by midnight without any significant problems. By 0230 hr on 12-May-2017 the drill bit reached the depth of the first core point at 8062 fbrf (1343 fbsf). The hole was drilled to the first core point while pumping seawater with gel sweeps every fourth stand (double pipe-length stands).

In preparation for coring, the hole was circulated clean and was displaced with a 10.5 ppg water-based mud (WBM). All cores acquired in H002 were cut while pumping 10.5 ppg WBM.

Core UT-GOM2-1-H002-01CS was cut and recovered to the vessel at 0900 hr on 12-May-2017; the core barrel was recovered on deck with the ball valve closed but with little to no pressure in the autoclave (recovered 2.3 ft; 69 cm of core). In response to the results of the first core run, two Full Function Tests of the PCTB-CS were conducted with the drill bit off the bottom of hole. In both cases the pressure-boost failed and additional modifications were made to configuration of the internal seals within the PCTB-CS to deal with an apparent pressure-lock problem.

Core UT-GOM2-1-H002-02CS was cut and recovered to the vessel at 1945 hr on 12-May-2017; when recovered on deck the ball valve was not closed; one core liner extended through ball valve and the core failed to retract into the autoclave (i.e., the core was not recovered at pressure) (recovered 5.3 ft; 162 cm of core).

Core UT-GOM2-1-H002-03CS was cut and recovered to the vessel at 0345 hr on 13-May-2017. When attempting to recover the PCTB-CS outer barrel, the tool failed to unlatch from the BHA. A decision was made to use a special emergency release procedure that decoupled the tool from the BHA but also prevented the ball valve in the tool from closing, so the core barrel was recovered on deck with no pressure (recovered 1.1 ft; 33 cm of core).

On 13-May-2017 H002 was advanced from 8092 fbrf to 8112 fbrf with 2 PCTB-CS pressure cores. Core UT-GOM2-1-H002-04CS was cut and recovered to the vessel at 1330 hr on 13-May-2017; when recovered on deck the ball valve was closed and an internal autoclave pressure of 3372 psi was measured. This was the first core acquired during this expedition at pressure (recovered 4.6 ft; 140 cm of core).

Core UT-GOM2-1-H002-05CS was cut and recovered to the vessel at 2000 hr on 13-May-2017; when recovered on deck the ball valve was closed but not sealed. Silt and sand were found packed between the ball valve and seal, and the seal appeared to be damaged (recovered 3.1 ft; 94 cm of core).

On 14-May-2017 H002 was advanced from 8112 fbrf to 8142 fbrf with 3 PCTB-CS pressure cores. Core UT-GOM2-1-H002-06CS was cut and recovered to the vessel at 0230 hr on 14-May-2017. When recovered on deck, the ball valve was closed; however, the seal at top end of autoclave plug had failed (recovered 5.2 ft; 158 cm of core).

Core UT-GOM2-1-H002-07CS was cut and recovered to the vessel at 0830 hr on 14-May-2017; when recovered on deck the ball valve was closed but not sealed. Silt and sand were found packed between the ball valve and seal; and the seal appeared to be damaged (recovered 1.5 ft; 46 cm of core).

Core UT-GOM2-1-H002-08CS was cut and recovered to the vessel by 1400 hr on 14-May-2017; when recovered on deck it was observed that the ball valve failed to actuate or hold pressure. The ball valve release sleeve failed by sliding over its stop position, which resulted in the failure of the ball valve to seal (recovered 4.6 ft; 140 cm of core).

The decision was made to abandon H002 after the 8th pressure core in this hole. It was determined that the core recovery was so poor, it was not worth drilling the hole to the originally planned total depth in order to log the interval. However, it was necessary to log the hole in order to survey the hole position. The final depth of H002 was 8142 fbrf. After retrieval of the final core, the bit was raised to 7680 fbrf in preparation for the wireline logging operations. The logging string, including the EDTC, the HRLA and the GPIT logging tools, was not able to go deeper than 8057 fbrf. Later, the drill pipe was lowered to the total depth of the well indicating that the false bottom encountered during logging was most likely a bridge.

On 15-May-2017 H002 was plugged for abandonment. The plan was to emplace a 500 ft cement plug beginning 179 ft above the hydrate zone at a depth of 7900 fbrf and extending to a depth of 7400 fbrf.

With the bit positioned at total depth (TD) of 8142 fbrf, the bottom of the hole was displaced with 25 bbls of 11.5 Hi-Vis gel pad mud. Given a hole size of 9 ⅞ inch diameter, the top of the pad mud was at a depth 7879 ft. The bit was then pulled to a depth of 7900 fbrf and the hole was circulated clean with 200 bbls of 10.5 ppg mud. 20 bbls of 10.5 ppg neat spacer was then pumped, followed by 76.5 bbls of 16 ppg Class H cement, followed by 17 bbls of 10.5 ppg neat spacer. The cement slurry was then pumped into place within the hole with 170.9 bbls of seawater.

47.4 bbls of cement were required to create a 500 ft column in a 9.875 in borehole assuming the borehole was to gauge over its entire length. Since a caliper log of the borehole was not available the actual borehole diameter was not known. Thus, a 100% mean annular excess of cement was factored into the cementing plan. Figure 3.2.1 shows a schematic of the proposed cement plan and actual extent of the cemented interval.

The PCTB in the face bit configuration (PCTB-FB) BHA was used to re-enter H002 to tag and test the cement plug on 16-May-2017. The bit was lowered in the hole to the top of the cement plug at a depth of 6839 ft. The cement was confirmed by applying 11,000 lbs to the top of the cement plug. Tagging the top of cement at a depth of 6839 fbrf indicated a cement column height of 1061 ft. Given that 76.5 bbls of cement was pumped, the theoretical hole diameter was 8.615 in (the bit diameter was 9.875 in). This indicated the hole was probably very close to gauge over its entire length, and the pumping displacements may have been slightly off.

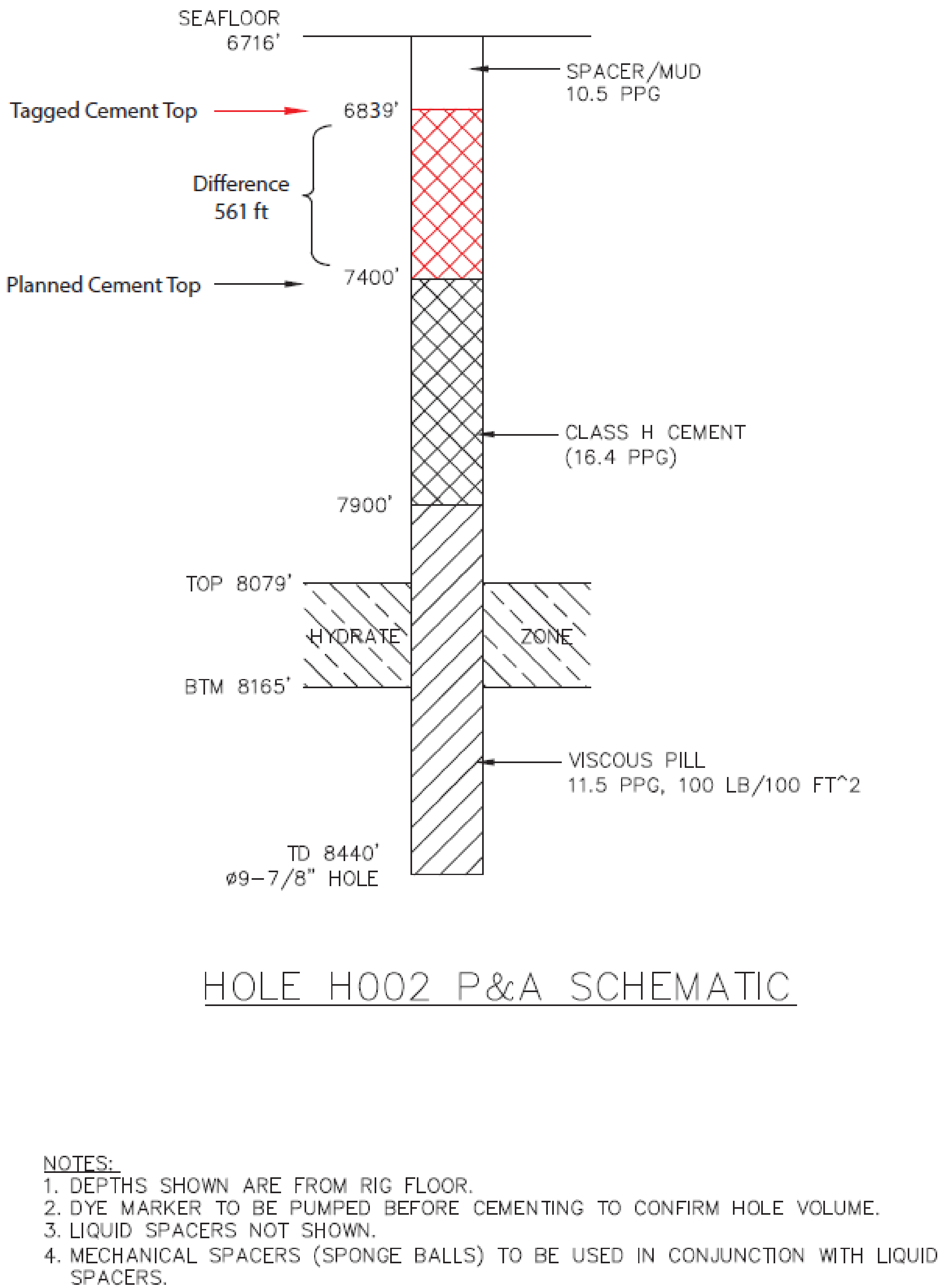

Figure 3.2.1 Proposed cement plan and actual extent of the cemented interval. All H002 Operational data can be found in the expedition data directory under H002 / Operations.

3.3. Pressure Coring

This section describes the coring operations for H002 from the UT-GOM2-1 hydrate pressure coring expedition. This section covers Flow Tests of the PCTB-CS with an instrumented core liner, Full Function Tests, pressure core runs, and PCTB failure analysis.

3.3.1 Flow Tests

Five flow tests were run with the PCTB in the cutting shoe configuration (PCTB-CS) with an instrumented core liner to characterize the relationship between flow rate and pressure differential across the core liner (Table 3.3.1 and Figure 3.3.1). Three of these tests, the Shallow Flow Tests, were run at ~50 fbrf and two, the Deep Flow Tests, at the mud line (6715 fbrf). Overall, these results indicate the pressure differential across the liner was less than 1.5 MPa and there was no damage to the liner.

Shallow Flow Tests

Shallow Flow Tests 1 and 2 were run with the bit just below the sea surface with the Hex mud pump rates of 0 to 140 strokes per minute (spm). However, below a rate of 40 spm, the values are unreliable (Table 3.3.1). Using the flow rate conversion of 5.04 gallons per stroke, the flow ranged from 0 to 650 gallons per minute (gpm). Shallow Flow Test 3 was run with Schlumberger cement pumps over a range of 0.5 to 8 barrels per minute (bpm) or 0 to 336 gpm.

The recorded pressure differential across the instrumented core liner was minor (see Chapter 2 Methods, Section 2.3 Pressure Coring) and no core liner deformation was evident. These results suggested that no large pressure differentials or liner damage should occur during coring operations.

Shallow Flow Tests	**Operational Depth (fbrf)**	**Outcome**
Shallow Flow Test 1 PCTB-CS	52	Only small pressure differential observed across core liner.
Shallow Flow Test 2 PCTB-CS	52	Only small pressure differential observed across core liner.
Shallow Flow Test 3 PCTB-CS w/ cement pump	52	Only small pressure differential observed across core liner.

Table 3.3.1 Results of shallow flow tests. All H002 DST data files for the shallow flow tests can be found in the expedition data directory under H002 / Pressure Coring / Starr-Oddi DST / Flow Tests / shallow.

Deep Flow Tests

Two Deep Flow Tests were completed near the seafloor, one with the Hex pump and one with the Schlumberger cement pump (Table 3.3.2). In Deep Flow Test 1 (with Hex pump) flow ranged from 0 to 650 gpm and 0 to 925 gpm in the Deep Flow Test 2 (with the Schlumberger cement pump).

Deep Flow Tests	Operational Depth (fbrf)	Outcome
Deep Flow Test X PCTB-CS	6715 - 6720	INCOMPLETE - electrical problems
Deep Flow Test 1 PCTB-CS	6715 - 6720	Only small pressure differential observed across core liner.
Deep Flow Test 2 PCTB-CS w/ cement pump	6715 - 6720	Only small pressure differential observed across core liner.

Table 3.3.2 Results of deep flow tests.

In both instances, the pressure differential across the core liner was minimal (Figure 3.3.1 and Figure 3.3.2) and no deformation was visible upon core recovery. Like the Shallow Flow Tests, these results suggest that no large pressure differentials or liner damage should occur during coring operations. A third deep flow test was abandoned due to an electrical malfunction in the Hex pump.

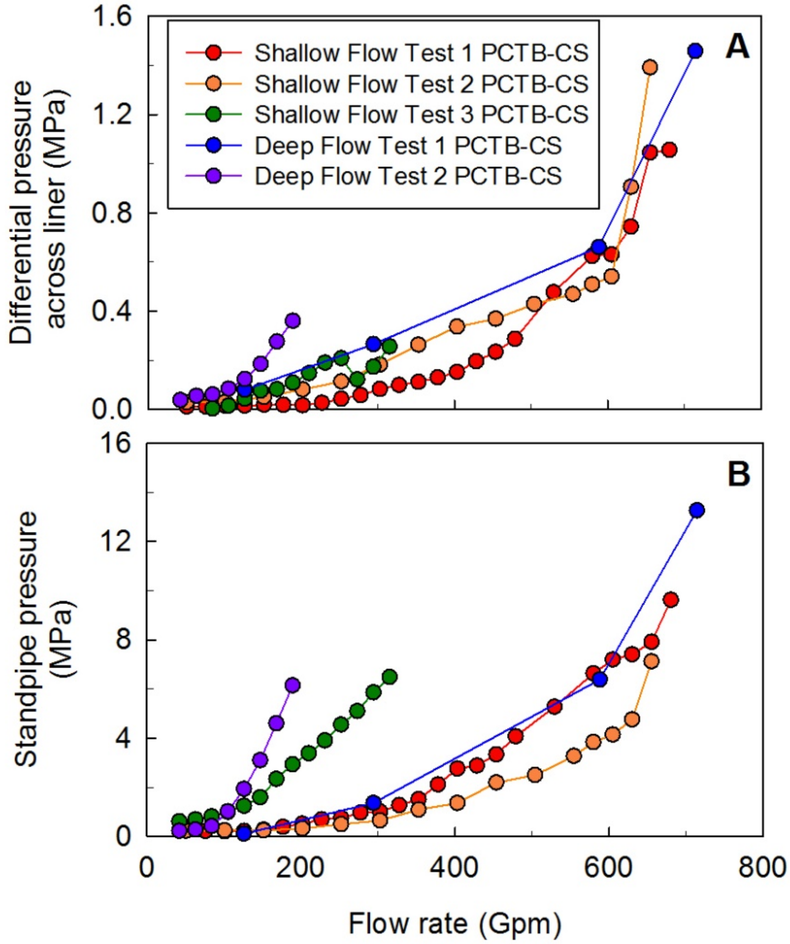

Figure 3.3.1 PCTB-CS flow test DST and standpipe pressure versus flow rate. See Chapter 2 Section 2.3.2 for more details. All H002 DST data files for the deep flow tests can be found in the expedition data directory under H002 / Pressure Coring / Starr-Oddi DST / Flow Tests / deep.

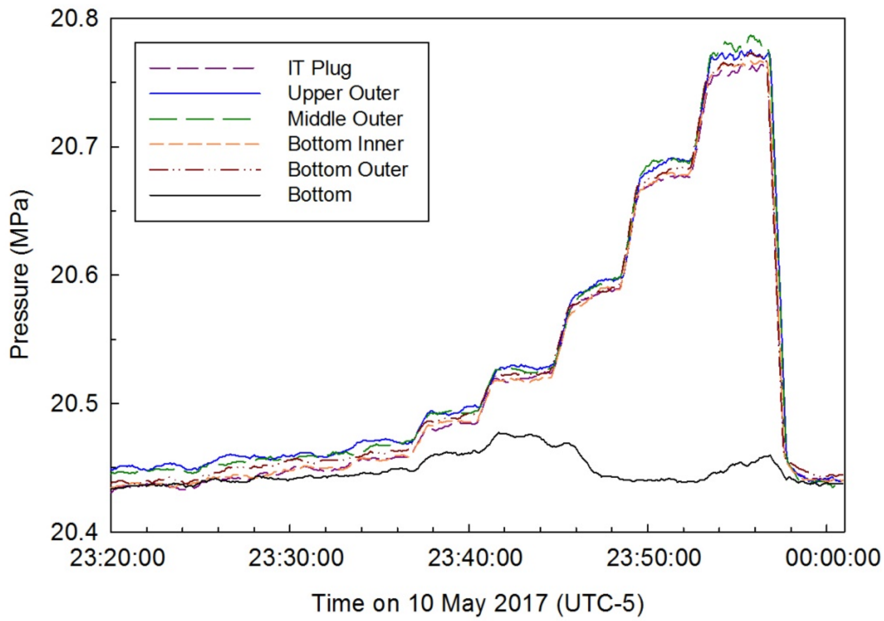

Figure 3.3.2: Pressure inside and outside the instrumented core liner as recorded by DSTs during Deep Flow Test 2. All H002 DST data files for the deep flow tests can be found in the expedition data directory under H002 / Pressure Coring / Starr-Oddi DST / Flow Tests.

3.3.2 Full Function Tests

Two full-function tests were completed between coring runs UT-GOM2-1-H002-01CS and UT-GOM2-1-H002-02CS (see 3.3.3 Pressure Core Acquisition below). These tests were conducted to determine the cause of failure after UT-GOM2-1-H002-01CS failed to maintain pressure.

Full Function Tests	Operational depth (fbrf)	Outcome
PCTB-CS Full-Function Test 1	8072	Pressure boost failed to charge PCTB-CS autoclave.
PCTB-CS Full-Function Test 2	8072	Pressure boost and seal occurred, however the middle section had lower pressure due to a hydraulic lock.

Table 3.3.3 Results from Full-Function Tests.

PCTB-CS Full-Function Test 1

Full Function Test 1 resulted in a hydraulic lock in the middle section of the PCTB, preventing the firing of boost pressure, which was interpreted to be the cause of failure encountered during coring run UT-GOM2-1-H002-01CS. The flow diverter was modified by replacing the PolyPak seal with an O-ring prior to Full Function Test 2, as it was thought to be the cause of the hydraulic lock (see Core UT-GOM2-1-H002-01CS).

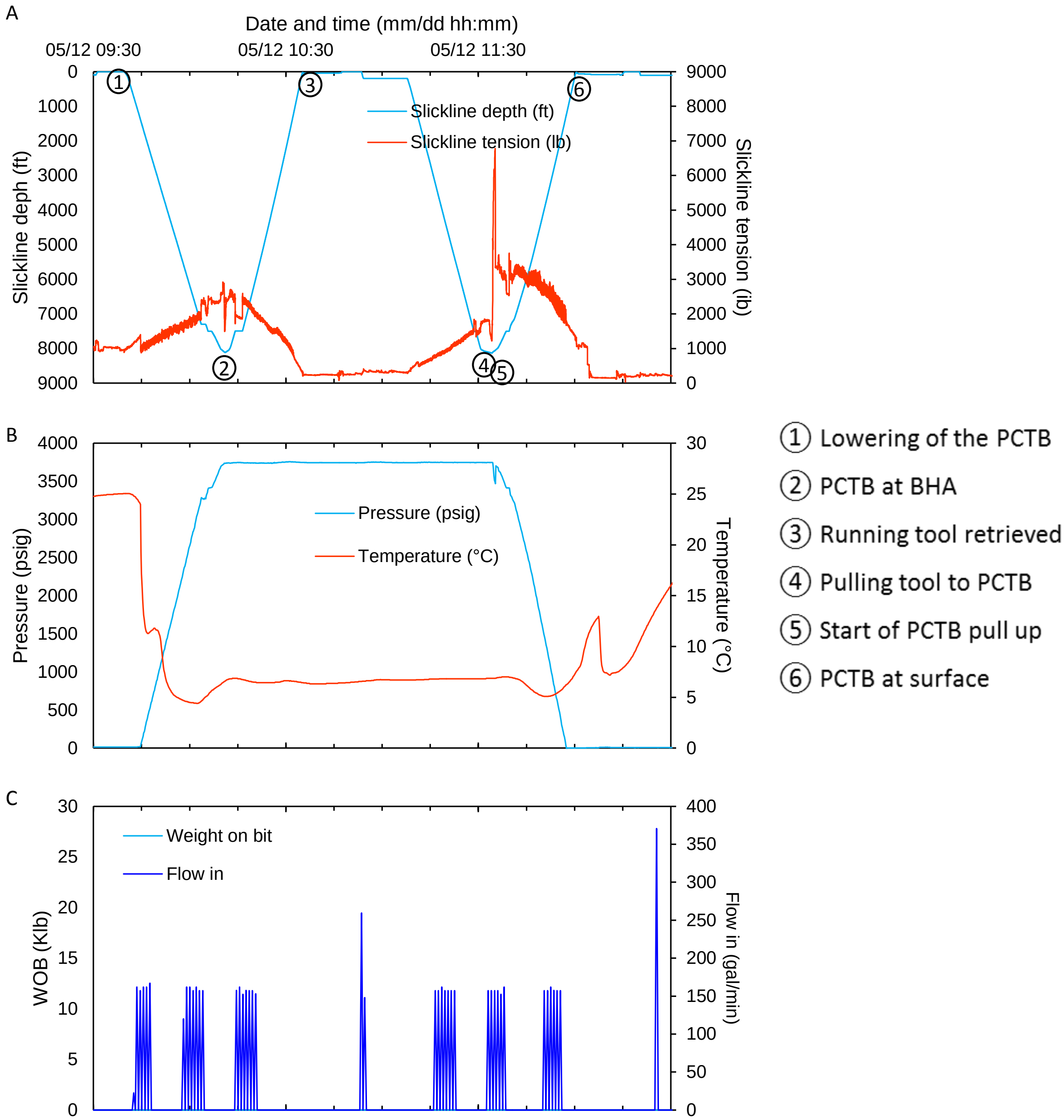

Figure 3.3.3 Deployment of PCTB-CS Full Function test 1. A) slickline tension and depth, B) pressure and temperature as measured by the rabbit DST and C) WOB and pump rate (flow in). WOB is zero because the BHA was suspended in the water column. All H002 pressure coring combined Weatherford, Schlumberger, and DST data can be found in the expedition data directory under H002 / Pressure Coring / Combined Datasets. See the readme file located there for more direction.

PCTB-CS Full-Function Test 2

The second test sealed and the autoclave was brought back at full pressure, though the pressure in the middle section was still low due to the hydraulic lock. At this point it was decided to remove the flow diverter seal completely for subsequent coring runs (UT-GOM2-1-H002-02CS and beyond). After Full

Function Test 2, pressure core acquisition was continued with UT-GOM2-1-H002-02CS. The pressure boost occurred late, after the PCTB was raised 2010 ft.

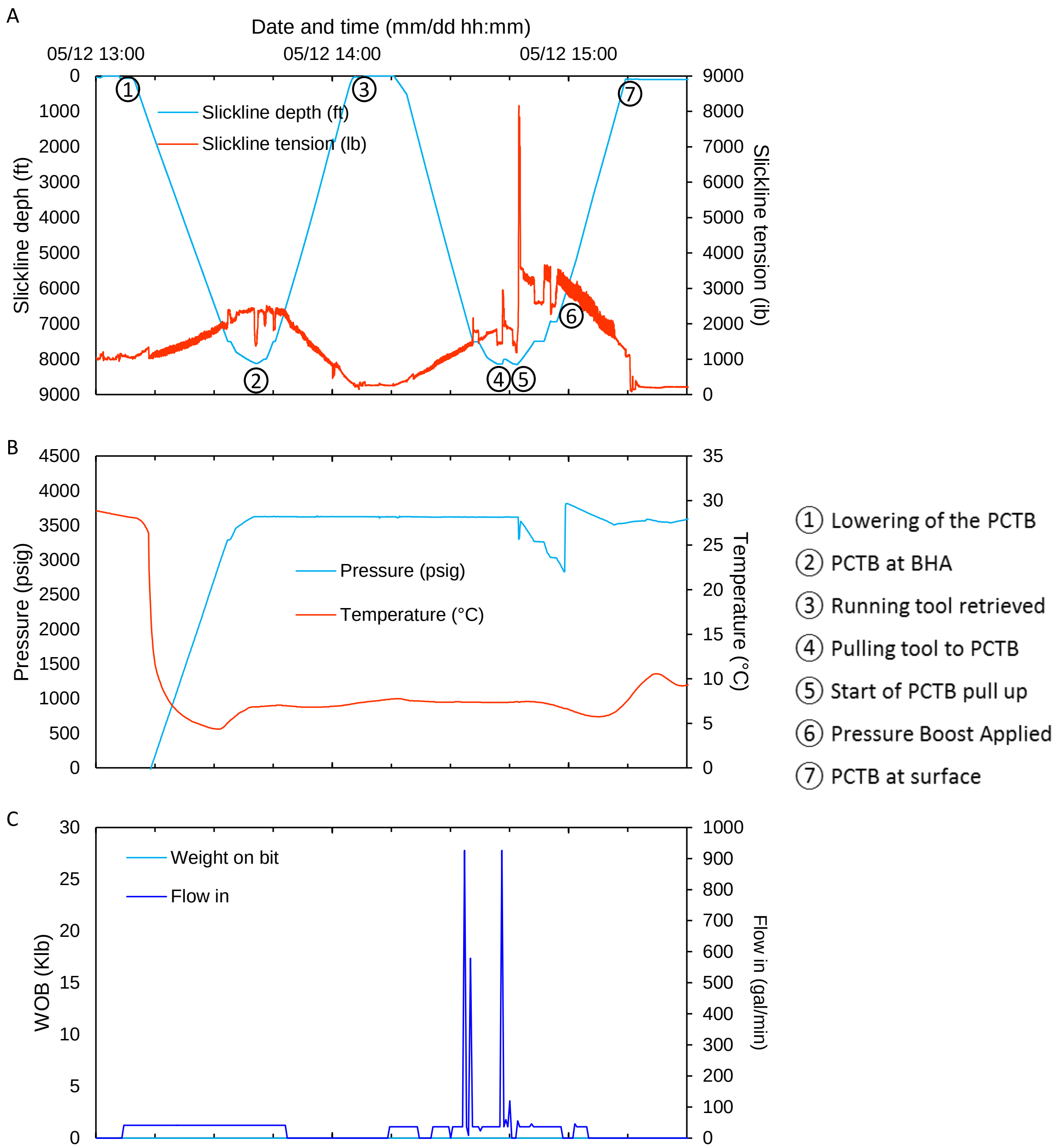

Figure 3.3.4 Deployment of PCTB-CS Full Function test 2. A) slickline tension and depth, B) pressure and temperature as measured by the rabbit DST and C) WOB and pump rate (flow in). WOB is zero because the BHA was suspended in the water column. All H002 pressure coring combined Weatherford, Schlumberger, and DST data can be found in the expedition data directory under H002 / Pressure Coring / Combined Datasets. See the readme file located there for more direction.

3.3.3 Pressure Core Acquisition

The PCTB-CS was deployed 8 times at H002. Only one core, UT-GOM2-1-H002-04CS, maintained pressure within the methane hydrate stability zone back to the vessel. The remaining 7 cores failed due to circumstances described in Table 3.3.4.

Core runs	Top (fbrf)	Bottom (fbrf)	Cored interval (ft)	Recovery length (ft)	Set boost pressure (psi)	Recovery pressure (psi)	Mud weight (ppg)	Comments
Core UT-GOM2-1-H002-01CS	8062	8072	10	2.26	4030	0	10.5	Ball valve closed; no pressure boost; pawls not engaged; middle section under residual pressure. Hydraulic lock and pressure buildup due to metal-on-metal seal.
Core UT-GOM2-1-H002-02CS	8072	8082	10	5.33	4040	0	10.5	Broken core liner remained in ball valve and valve could not close due to jamming.
Core UT-GOM2-1-H002-03CS	8082	8092	10	1.08	3900	0	10.5	Inner barrel jammed in BHA. Used emergency tool to release.
Core UT-GOM2-1-H002-04CS	8092	8102	10	4.6	4019	3372	10.5	No boost, although a slight pressure jump when tool was pulled. Loose, fluidized sediment above rabbit.
Core UT-GOM2-1-H002-05CS	8102	8112	10	3.1	3953	0	10.5	Ball valve only partially closed. Seal jammed in ball valve.
Core UT-GOM2-1-H002-06CS	8112	8122	10	5.2	3958	0	10.5	Ball valve closed. Seal at top end of plug failed.
Core UT-GOM2-1-H002-07CS	8122	8132	10	1.5	4020	0	10.5	Displaced ball valve seal. Fluidized sediment above rabbit.
Core UT-GOM2-1-H002-08CS	8132	8142	10	4.6	4058	0	10.5	The ball valve was open due to release sleeve failure by sliding over the stop position.

Table 3.3.4 Summary of pressure coring runs in H002.

Core UT-GOM2-1-H002-01CS

Depth: 8062-8072 fbrf (409.96-413.00 mbsf)
Recovery: 2.3 ft (0.69 m), 23%

Pressure status: 0 psi

The deployment of UT-GOM2-1-H002-01CS is described in detail while the remaining deployments are just summarized.

Deployment and recovery data for PCTB UT-GOM2-1-H002-01CS are shown in Figure 3.3.5, Figure 3.3.6, and Figure 3.3.7. The tool was initially lowered on the run-in tool and latched into the BHA (event 1, Figure 3.3.5A). The lowering of PCTB was indicated by the increase in slickline depth (Figure 3.3.5A) and the increase in pressure measured in the PCTB (Figure 3.3.5B). Temperature decreased as the tool was lowered through the water column to below the thermocline and into deeper water (Figure 3.3.5B). Pumping of drilling fluid occurred periodically in this interval (Figure 3.3.5C). After lowering the PCTB, the running tool was retrieved (between event 1 and 2) and the pulling tool was lowered to just above the BHA (between event 2 and 3). Lowering of the pulling tool was indicated by slickline depth increase (Figure 3.3.5A) and increase in pressure recorded at pulling tool (Figure 3.3.5B). Coring began (event 3) at a constant pump rate and a fairly constant rate of penetration (Figure 3.3.5C). When the full coring stroke was achieved, the bit was lifted and the weight on bit (WOB) decreased to zero (Figure 3.3.5C) bringing the coring to an end (event 4). The pulling tool was then latched onto the inner barrel (event 5) and the inner barrel was pulled out of the BHA and retrieved (Figure 3.3.5A).

In this case, as the PCTB was retrieved, the pressure dropped to atmospheric pressure when the tool reached the surface (event 6) because the PCTB did not seal (Figure 3.3.5B). An expanded view of the pullout and retrieval is shown in Figure 3.3.6. Figure 3.3.7 tracks the pressure and temperature measured at the top of the core, with a comparison to the methane hydrate stability boundary. As the inner barrel was lowered, it passed into the methane hydrate stability zone (event 1 through event 5) (Figure 3.3.7). When the inner barrel was retrieved, because the tool did not seal, the PCTB passed back out of the methane hydrate stability zone (event 5 through event 6).

The pressure decreased as UT-GOM2-1-H002-01CS was pulled up through the water column indicating that the core barrel was not sealed. On recovery of core UT-GOM2-1-H002-01CS, it was determined that the ball valve had activated and closed. The pawls were not engaged and the middle section was under residual pressure. The initial analysis of the tool suggested the PolyPak flow diverter seal might have sealed on a surface which it was not designed to seal. Such inadvertent sealing could have created a hydraulic lock and pressure buildup, preventing the complete retraction of the inner tube plug and inner liner into the autoclave. This in turn would have prevented the pawls from locating correctly and not allowed the top of the plug to seal. During the coring of UT-GOM2-1-H002-02CS this initial interpretation was revised (see Core UT-GOM2-1-H002-02CS below).

Core UT-GOM2-1-H002-01CS was removed from the autoclave manually. A curated length of 0.79 m was processed by the science party. The basket core catcher had been inverted and then crushed, with partial twist breakage of 1 or 2 fingers.

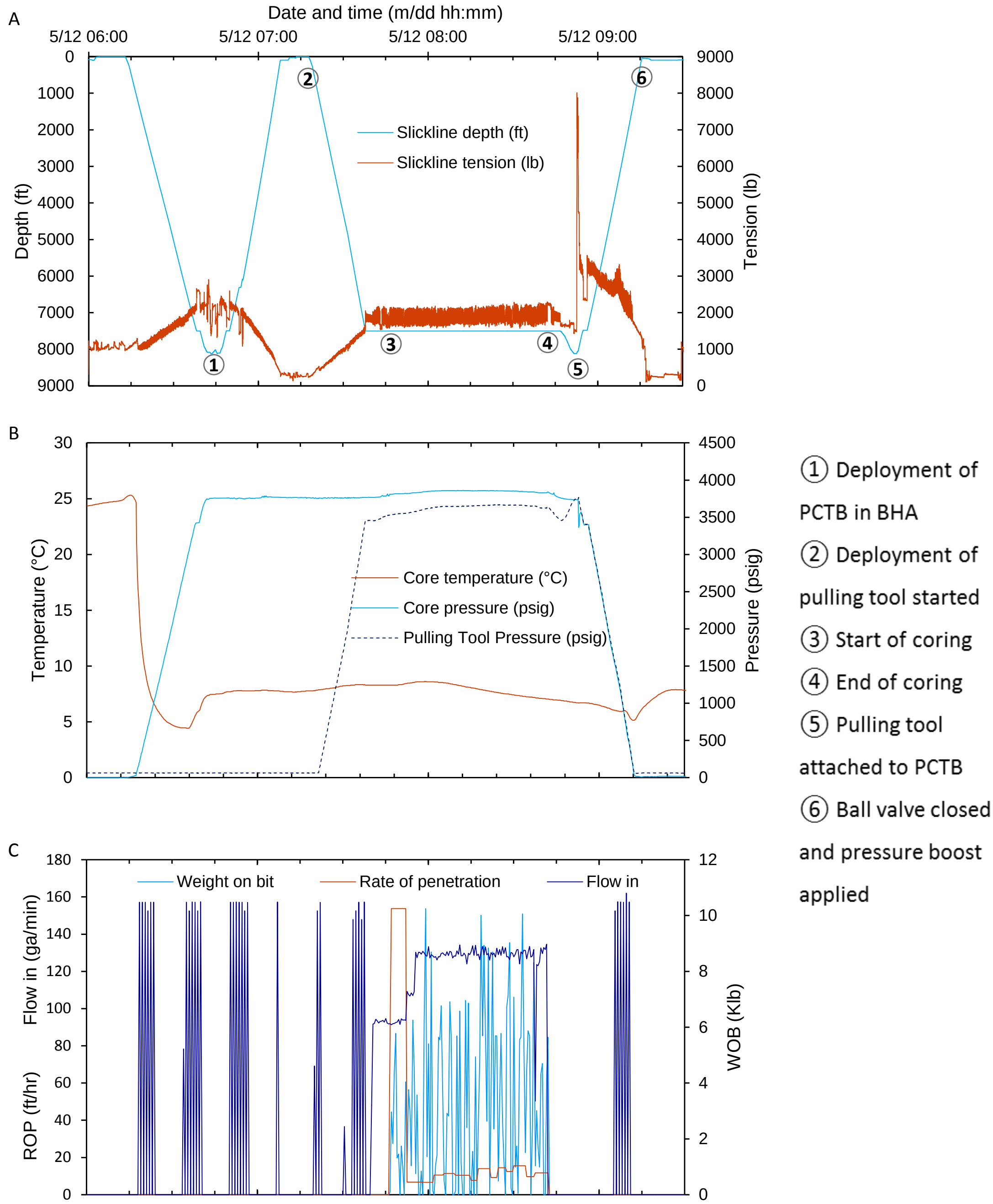

Figure 3.3.5 UT-GOM2-1-H002-01CS coring data.A) slickline tension and depth, B) pressure and temperature as measured in gauge pressure by the Data Storage Tag (DST) inside the rabbit, the cap that contacts the top of the core in the PCTB, and C) WOB, ROP, and pump flow rate. WOB = weight on bit. ROP = rate of penetration. Flow in is the sum of all pump flows. All H002 pressure coring combined Weatherford, Schlumberger, and DST data can be found in the expedition data directory under H002 / Pressure Coring / Combined Datasets. See the readme file located there for more direction.

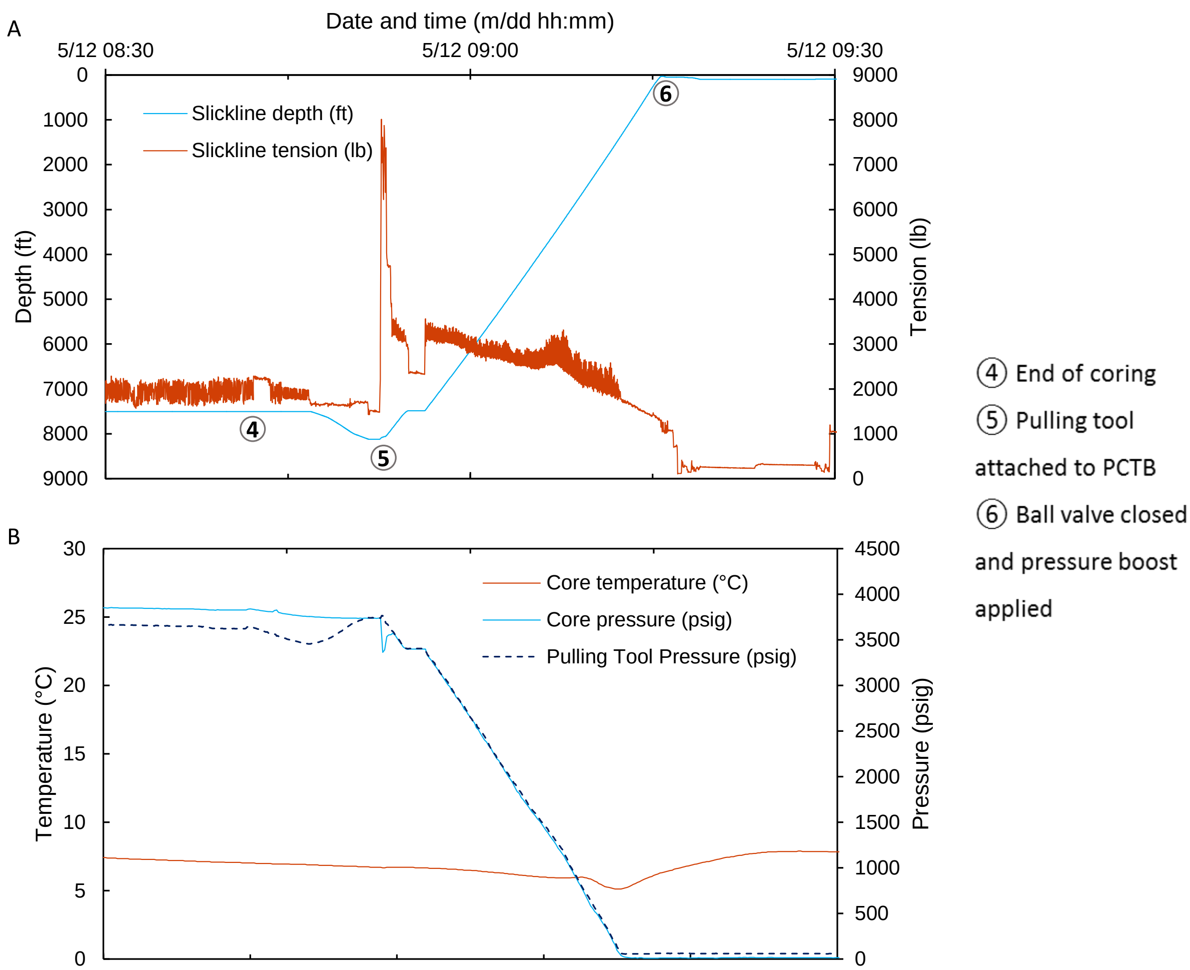

Figure 3.3.6 UT-GOM2-1-H002-01CS core retrieval details. A zoomed in section of Figure 3.3.5 showing the completion of coring and the pressure temperature conditions as the PCTB tool was pulled to the surface.

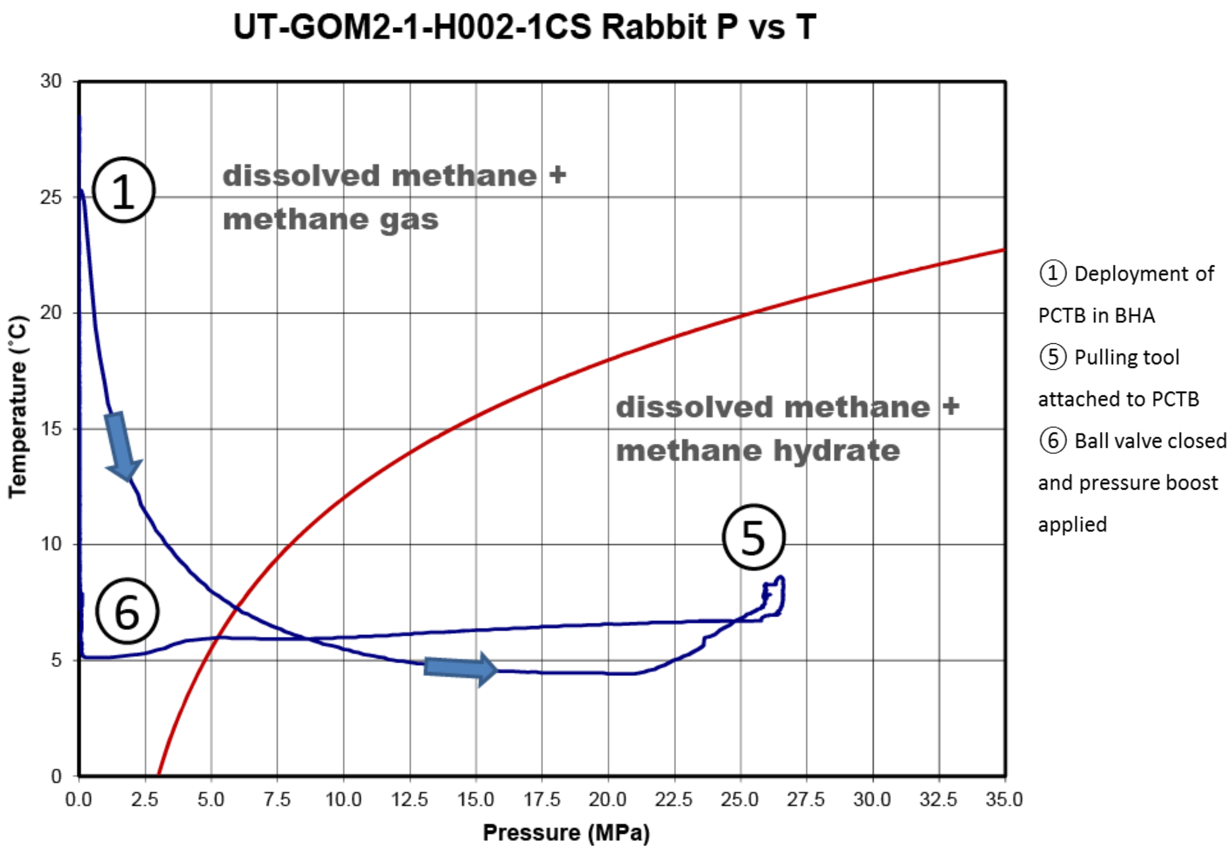

Figure 3.3.7 UT-GOM2-1-H002-01CS pressure and temperature versus calculated hydrate stability. Arrows on the P-T DST data, in blue, indicate the direction of increasing time. The methane hydrate stability boundary, in red, assumes methane in the presence of brine at seawater salinity.

Core UT-GOM2-1-H002-02CS

Depth: 8072-8082 fbrf (413.00-416.05 mbsf)
Recovery: 5.3 ft (1.63 m), 53%
Pressure status: 0 psi

The deployment of the tool is described in Figure 3.3.8, Figure 3.3.9, and Figure 3.3.10. The pump rate during this coring run was only 1/3 of that during core UT-GOM2-1-H002-01CS. The rate of penetration (ROP) remained relatively constant during coring. UT-GOM2-1-H002-02CS did not seal, allowing all pressure to dissipate (Figure 3.3.10). Core recovery was ~50% and no hydrate was recovered.

UT-GOM2-1-H002-02CS was run without any seal in the flow diverter. While the tool was being assembled, however, another possible cause for the hydraulic lock became apparent when the possibility of a metal to metal seal between moving parts in the middle section was noted. These parts, while of old design, were newly machined and highly polished. To remove any possibility of these parts creating a hydraulic lock, after coring run UT-GOM2-1-H002-02CS, small flats were ground onto the part surfaces to ensure they could no longer form a seal. Ultimately it was determined that the metal to metal seal, rather than the flow diverter (See Core UT-GOM2-1-H002-01CS), was the cause of the hydraulic lock.

Recovery of core UT-GOM2-1-H002-02CS, revealed that the core liner had broken at the top threaded joint with the lower five-inch spacer. Consequently, when pulling the inner assembly, the bottom end of the liner was not lifted and remained in the ball valve, preventing the ball valve from closing. Sand-to-silt sized sediments were found jammed tight inside the cutting shoe. The retraction of the plug was complete and the pressure boost had fired but the autoclave had not sealed.

The failure of this core to hold pressure was attributed to core jamming which led to an over-torque on the core liner. This can occur when the core is not cut cleanly and the waste material is not removed fast enough by the pumped mud. Core jamming resulting in broken liners have been seen on previous expeditions, including NGHP-02. This failure was not related to the previous failures in UT-GOM2-1-H002-01CS or the Full Function Tests (see above) and had nothing to do with the removal of the flow diverter seal. To avoid core jamming, it was proposed to cut the next core more slowly and with a higher pump rate.

The core was removed from the autoclave manually. Large voids in the sediment core were indicative of gas expansion in the core, though it is unknown whether the gas was produced from exsolution of dissolved gas or from dissociation of gas hydrate.

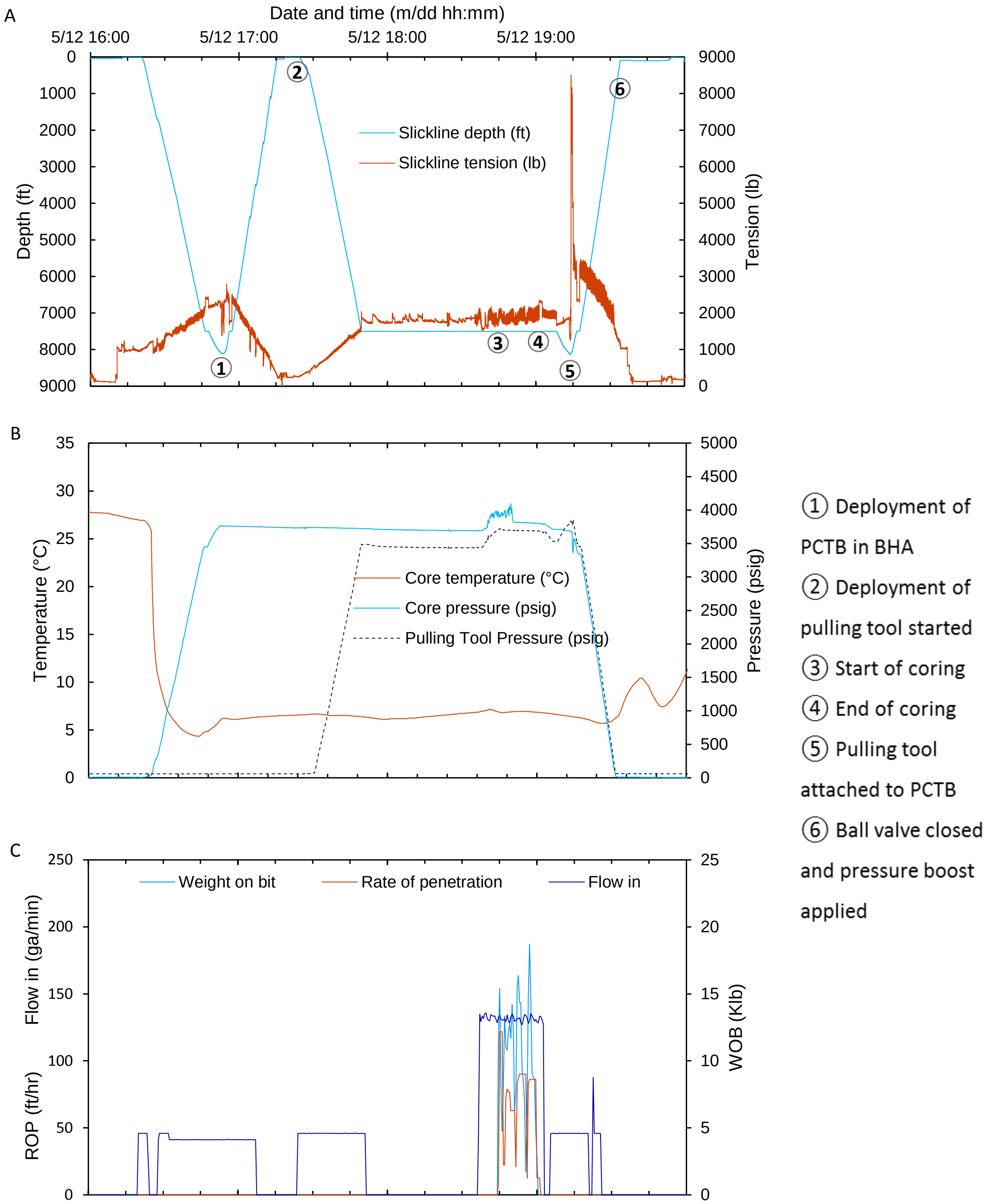

Figure 3.3.8 UT-GOM2-1-H002-02CS coring data. A) slickline tension and depth, B) pressure and temperature as measured in gauge pressure by the Data Storage Tag (DST) inside the rabbit, the cap that contacts the top of the core in the PCTB, and C) WOB, ROP, and pump flow rate. WOB = weight on bit. ROP = rate of penetration. Flow in is the sum of all pump flows. All H002 pressure coring combined Weatherford, Schlumberger, and DST data can be found in the expedition data directory under H002 / Pressure Coring / Combined Datasets. See the readme file located there for more direction.

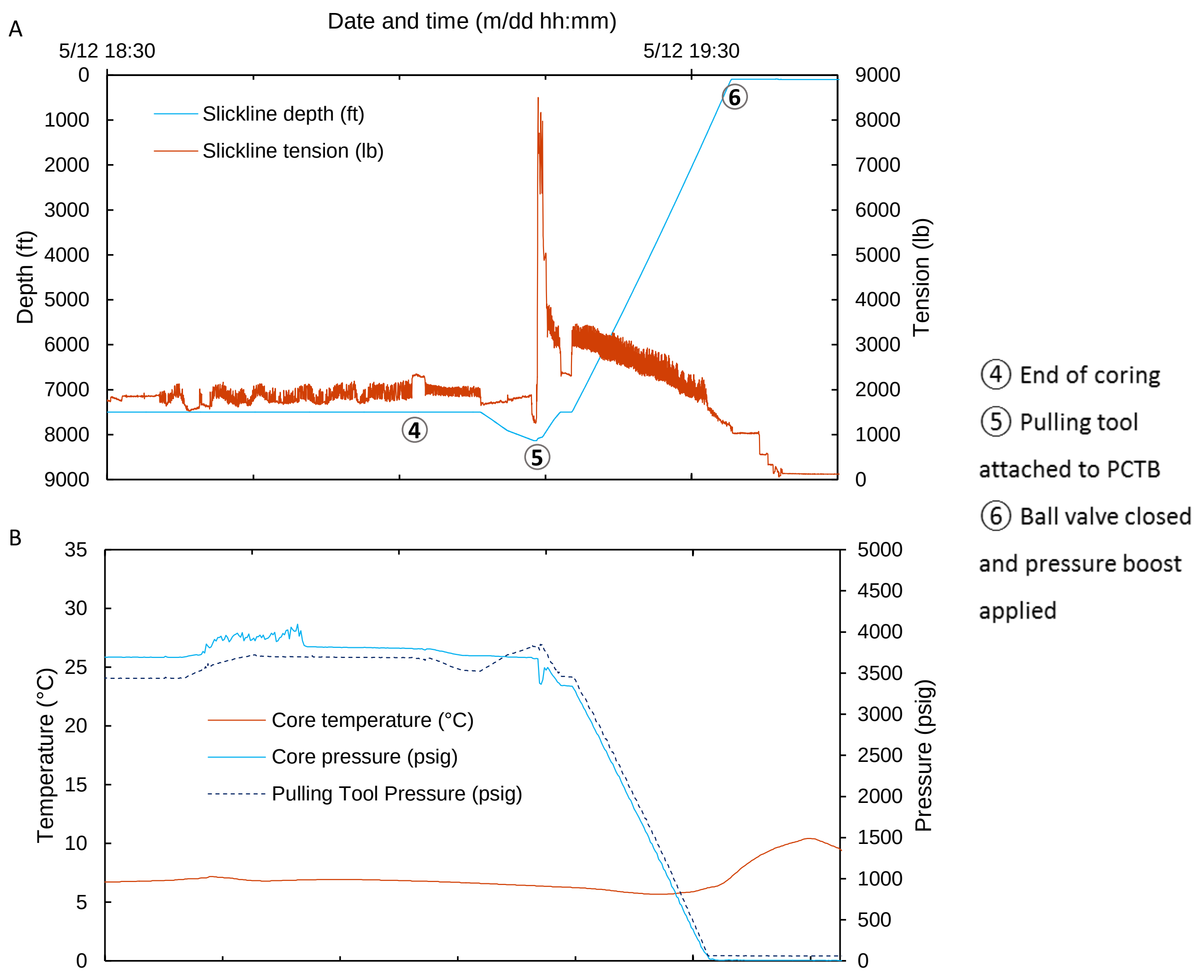

Figure 3.3.9 UT-GOM2-1-H002-02CS core retrieval details. A zoomed in section of Figure 3.3.8 showing the completion of coring and the pressure temperature conditions as the PCTB tool was pulled to the surface.

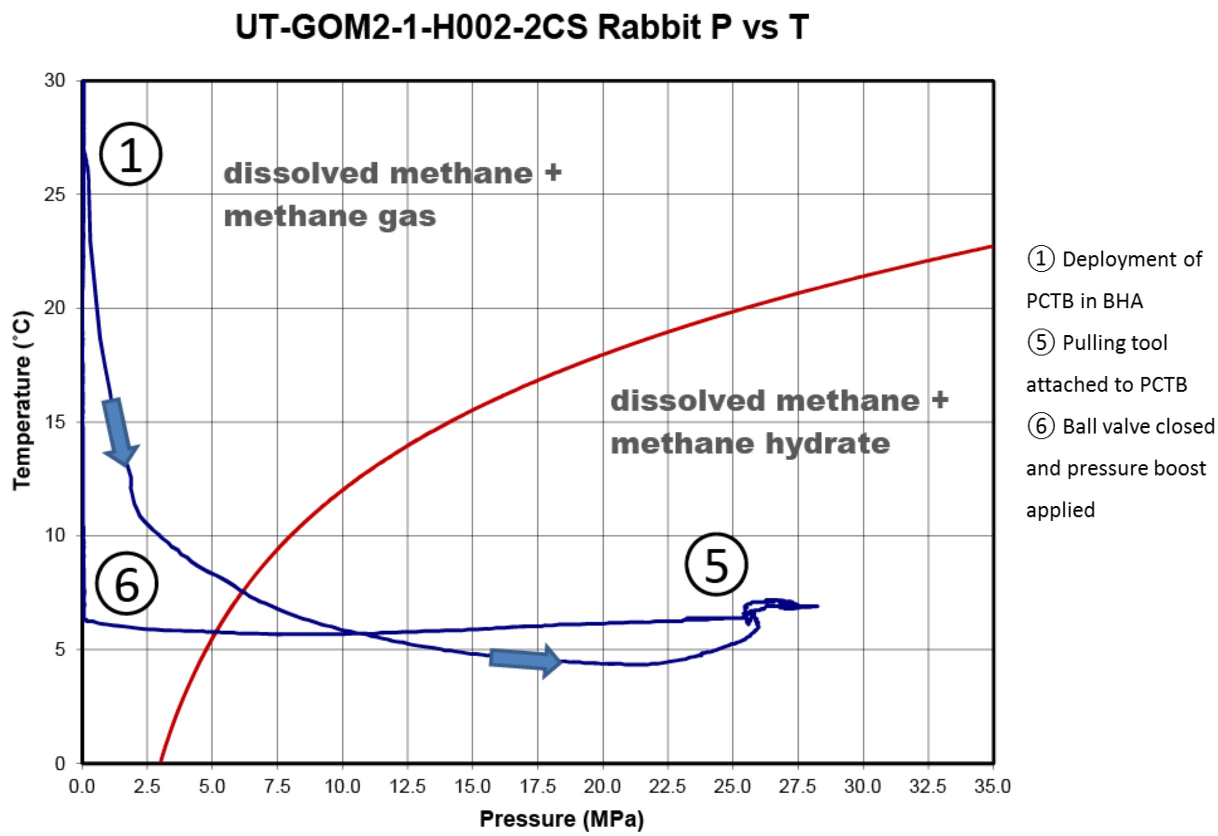

Figure 3.3.10 UT-GOM2-1-H002-02CS pressure and temperature versus calculated hydrate stability. Arrows on the P-T DST data, in blue, indicate the direction of increasing time. The hydrate stability boundary, in red, assumes methane in the presence of brine at seawater salinity.

Core UT-GOM2-1-H002-03CS

Depth: 8082-8092 fbrf (416.05-419.10 mbsf)
Recovery: 1.1 ft (0.33 m), 11%
Pressure status: 0 psi

The deployment of the PCTB during the collection of UT-GOM2-1-H002-03CS is described in Figure 3.3.11, Figure 3.3.12, and Figure 3.3.13. Due to a networking error, no pump data were collected during this run. UT-GOM2-1-H002-03CS was run with the same configuration as UT-GOM2-1-H002-2CS (no seal in the flow diverter), but the tool became firmly lodged in the BHA during coring. Because the pulling tool could not release the PCTB from the BHA after 2.5 hours of pulling, the emergency pulling tool was deployed. After multiple attempts at pulling and jarring with the emergency tool, a final pull freed the tool from the BHA and it was brought to the surface. The emergency pulling tool prevents closing of the ball valve, thus recovery of pressure core within the methane hydrate stability zone was not possible. The cutting shoe was again jammed with silt and sand despite the increased flow rate. There was no pressure in the core and core recovery was poor (33 cm).

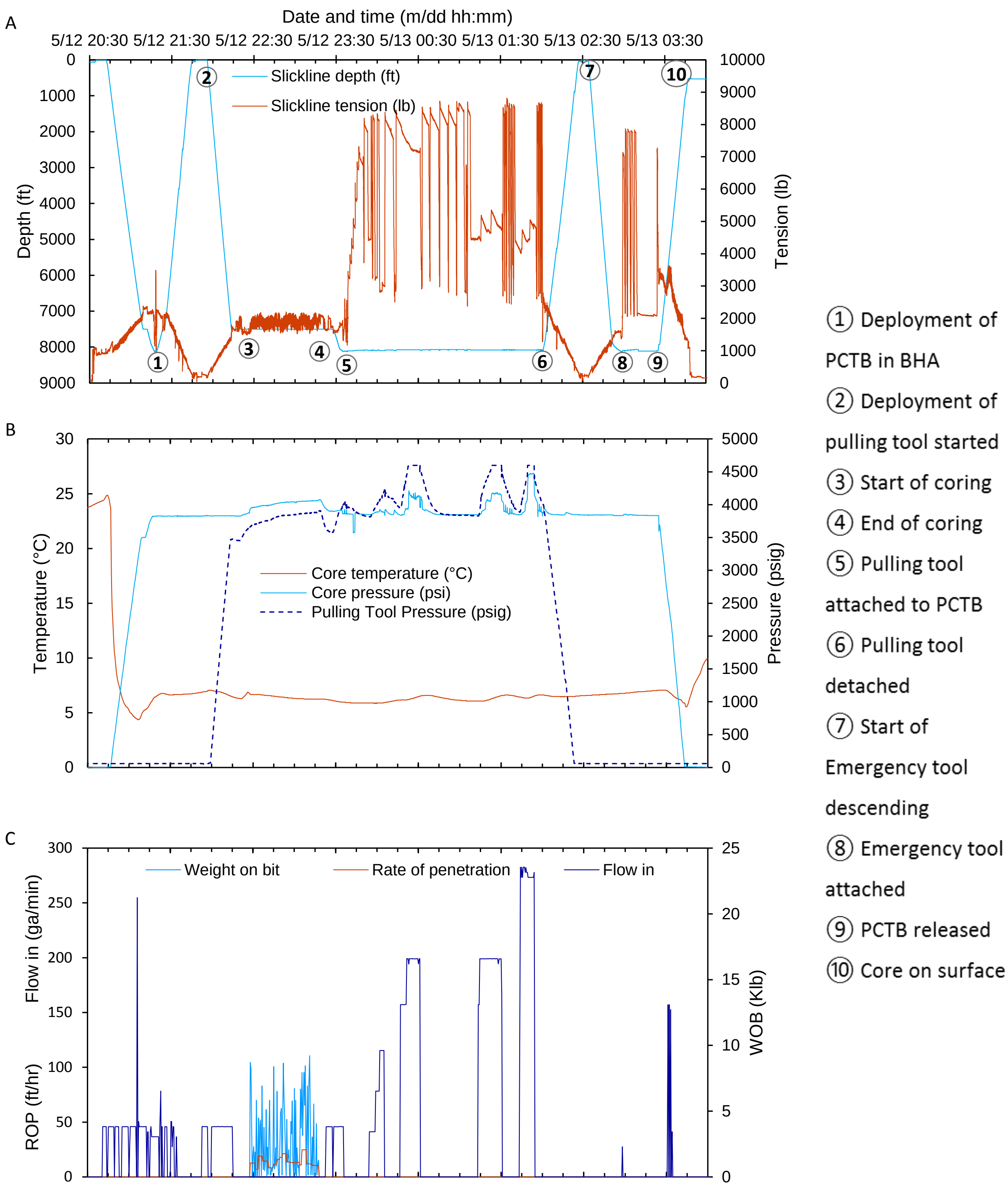

Figure 3.3.11 UT-GOM2-1-H002-3CS coring data. A) slickline tension and depth, B) pressure and temperature as measured in gauge pressure by the Data Storage Tag (DST) inside the rabbit, the cap that contacts the top of the core in the PCTB, and C) WOB, ROP, and pump flow rate. WOB = weight on bit. ROP = rate of penetration. Flow in is the sum of all pump flows. All H002 pressure coring combined Weatherford, Schlumberger, and DST data can be found in the expedition data directory under H002 / Pressure Coring / Combined Datasets. See the readme file located there for more direction.

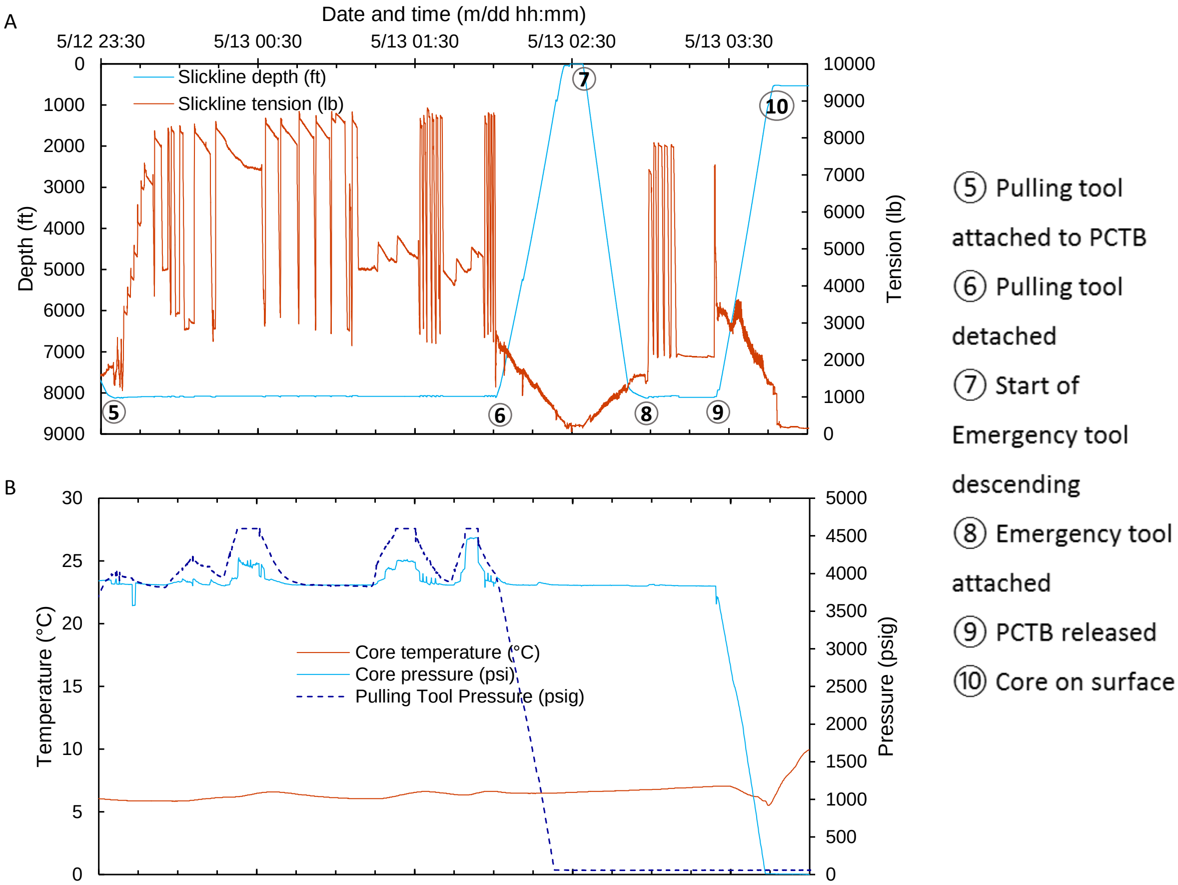

Figure 3.3.12 UT-GOM2-1-H002-03CS core retrieval details. A zoomed in section of Figure 3.3.11 showing the completion of coring and the pressure temperature conditions as the PCTB tool was pulled to the surface.

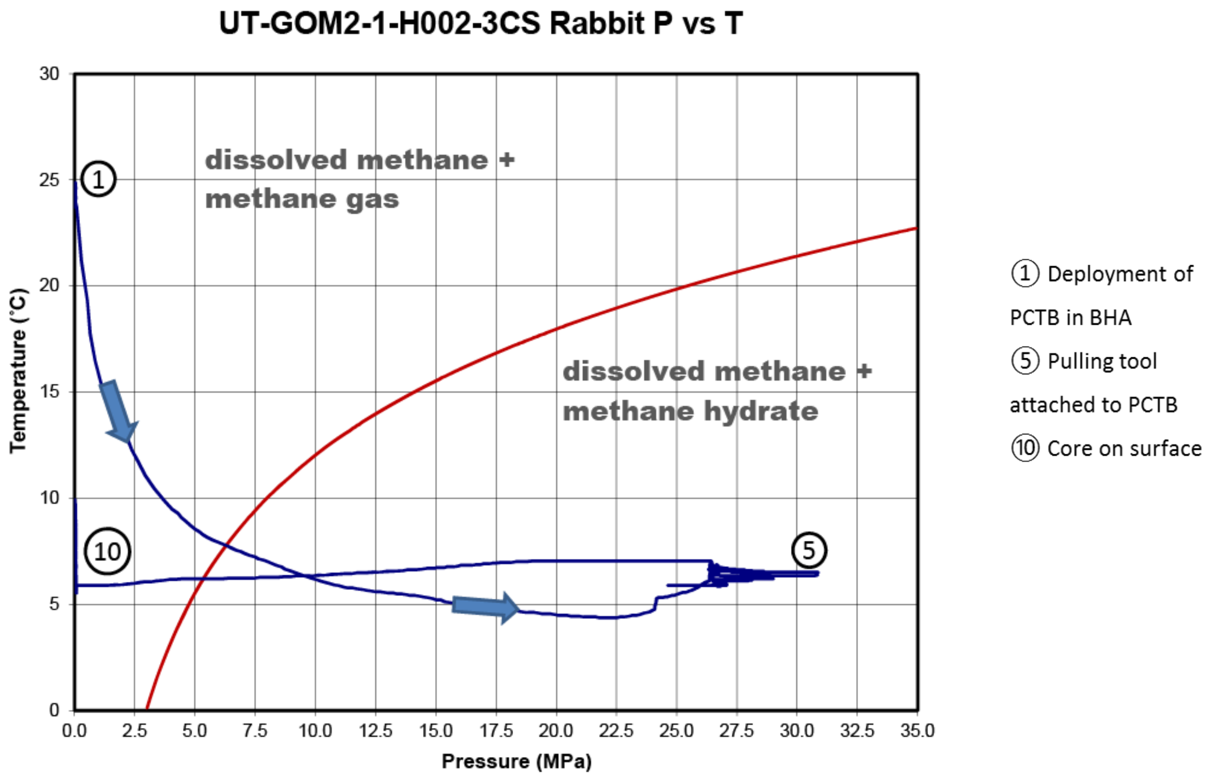

Figure 3.3.13 UT-GOM2-1-H002-3CS pressure and temperature versus calculated hydrate stability. Arrows on the P-T DST data, in blue, indicate the direction of increasing time. The hydrate stability boundary, in red, assumes methane in the presence of brine at seawater salinity.

Core UT-GOM2-1-H002-04CS

Depth: 8092-8102 fbrf (419.10-422.15 mbsf)
Recovery: 4.5 ft (1.37 m), 45%
Pressure status: 3372 psi

A total of 4.5 ft of core was brought to the surface under about 3400 psi of pressure, and Core UT-GOM2-1-H002-04CS remained within the methane hydrate stability zone throughout recovery.

Prior to the coring run UT-GOM2-1-H002-04CS as recorded in Figure 3.3.14, Figure 3.3.15 and Figure 3.3.16, the coring tool detached from the wireline and fell around 500 ft into the BHA. The coring tool was recovered from the BHA with the emergency pulling tool. An analysis of the slickline and pump records during the lowering of the tool showed that a sudden stop and restart of the slickline winch caused the tool to float and become detached. After this deployment, the slickline winch was more closely monitored. Once the coring tool was recovered with the emergency pulling tool, the coring tool was completely reset prior to a second attempt at coring run UT-GOM2-1-H002-04CS.

Prior to redeploying UT-GOM2-1-H002-04CS, another full function test was requested, however, a miscommunication resulted in a coring run (UT-GOM2-1-H002-04CS) being performed instead of a full function test.

On recovery, the ball valve was closed and the plug had moved up to the correct position, indicating that the pressure boost had fired and the autoclave was under pressure. After half an hour in the vertical cold shuck, the core was transferred to the PCTB van, where the pressure was measured at 3372 psi. Transfer from the autoclave to the pressure core analysis and transfer system (PCATS) revealed a full core as well as a large amount of silty sand (> 1.5 m) that had washed up above the rabbit to the top of the liner.

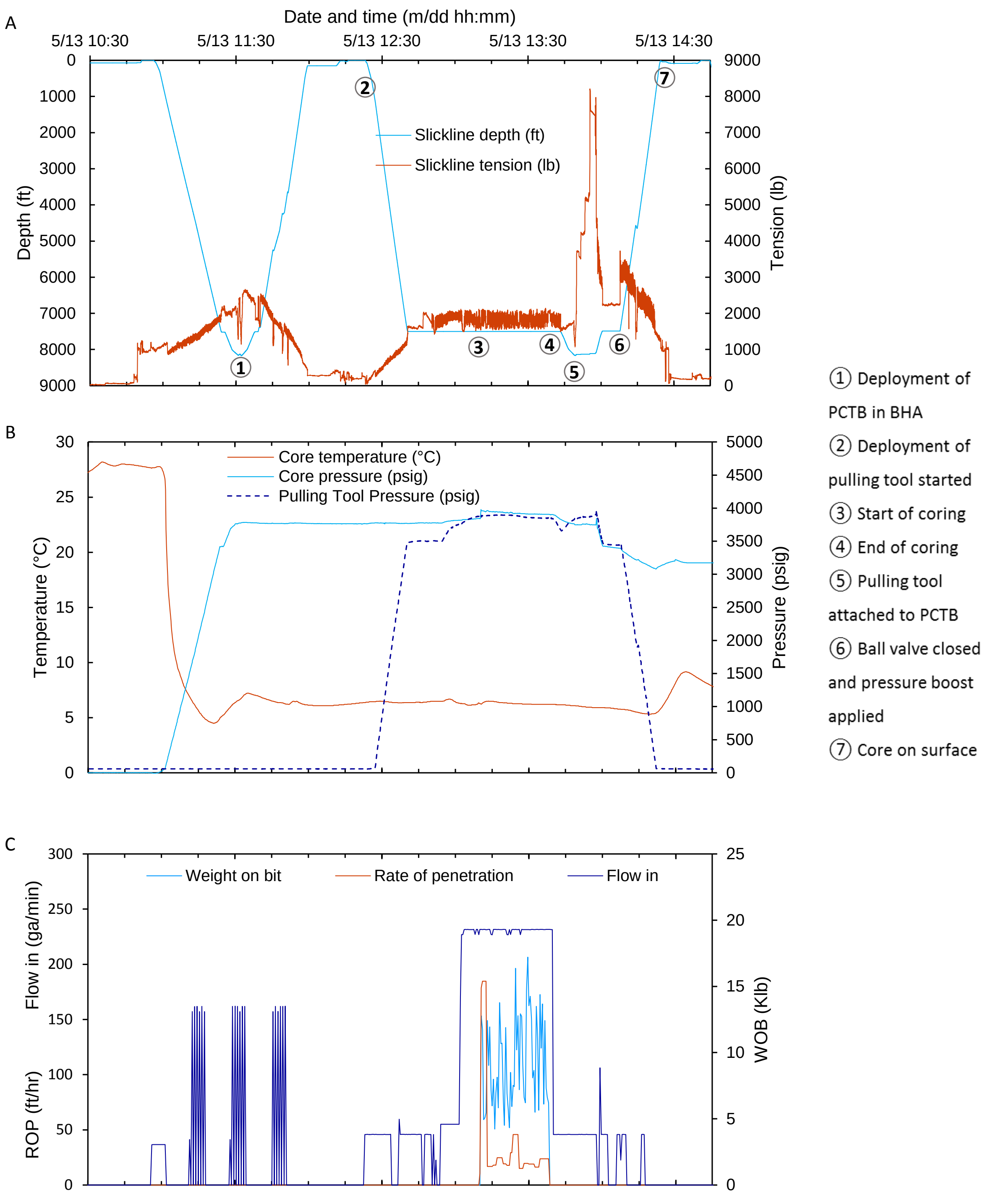

Figure 3.3.14 UT-GOM2-1-H002-4CS coring data. A) slickline tension and depth, B) pressure and temperature as measured in gauge pressure by the Data Storage Tag (DST) inside the rabbit, the cap that contacts the top of the core in the PCTB, and C) WOB, ROP, and pump flow rate. WOB = weight on bit. ROP = rate of penetration. Flow in is the sum of all pump flows. All H002 pressure coring combined Weatherford, Schlumberger, and DST data can be found in the expedition data directory under H002 / Pressure Coring / Combined Datasets. See the readme file located there for more direction.

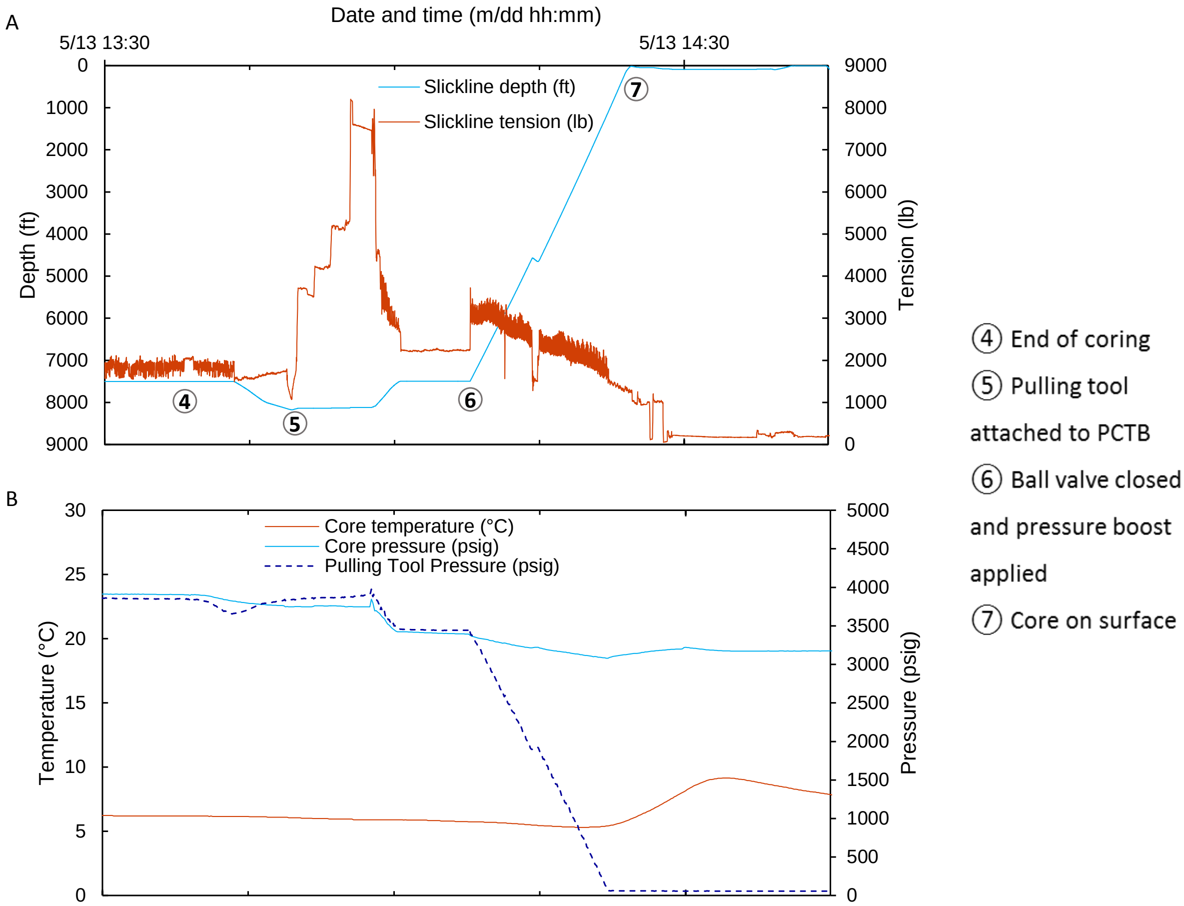

Figure 3.3.15 UT-GOM2-1-H002-4CS core retrieval details. A zoomed in section of Figure 3.3.14 showing the completion of coring and the pressure temperature conditions as the PCTB tool was pulled to the surface.

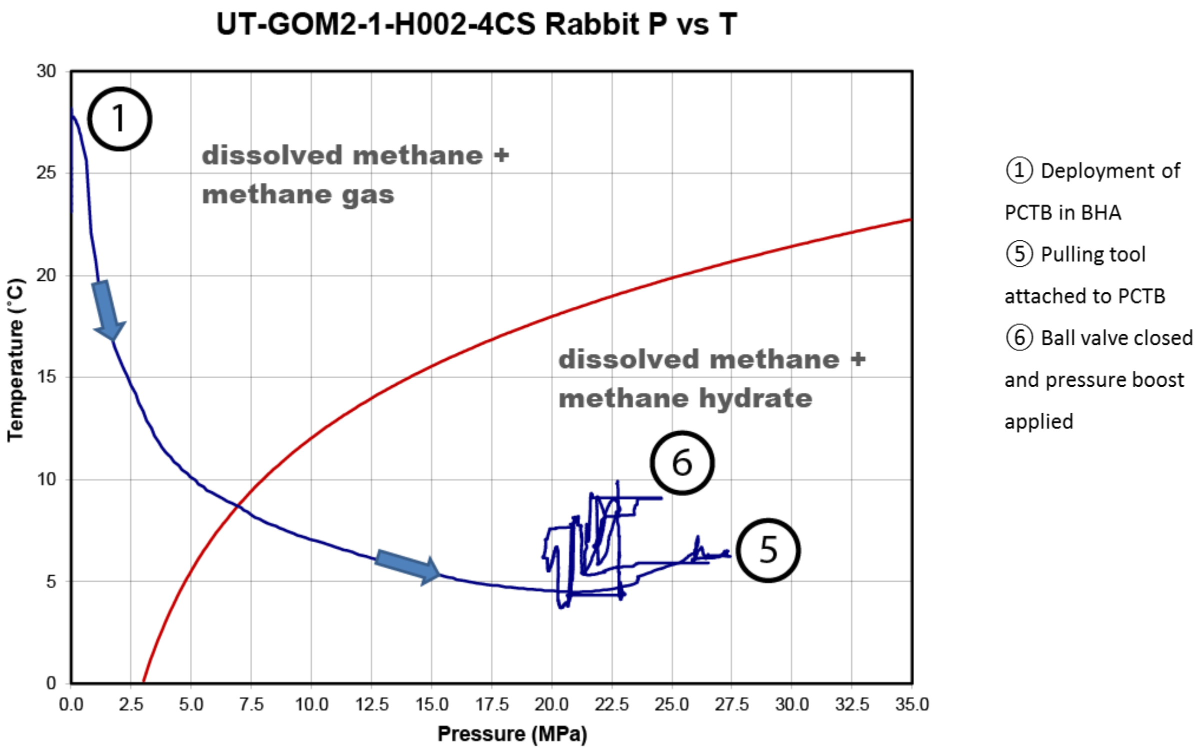

Figure 3.3.16 UT-GOM2-1-H002-4CS pressure and temperature versus calculated hydrate stability. Arrows on the P-T DST data, in blue, indicate the direction of increasing time. The hydrate stability boundary, in red, assumes methane in the presence of brine at seawater salinity.

Core UT-GOM2-1-H002-05CS

Depth: 8102-8112 fbrf (422.15-425.20 mbsf)
Recovery: 3.1 ft (0.93 m), 31%
Pressure status: 0 psi

Deployment and recovery data for PCTB UT-GOM2-1-H002-05CS are shown in Figure 3.3.17, Figure 3.3.18 and Figure 3.3.19. The pump rate was lowered stepwise throughout the coring run.
The ball valve was only partially closed due to a misplaced seal. The core left the methane hydrate stability zone (Figure 3.3.19) and was returned to the rig floor at atmospheric pressure. About ~90 cm of core was recovered. There was no sand in the liner above rabbit DST sensor.

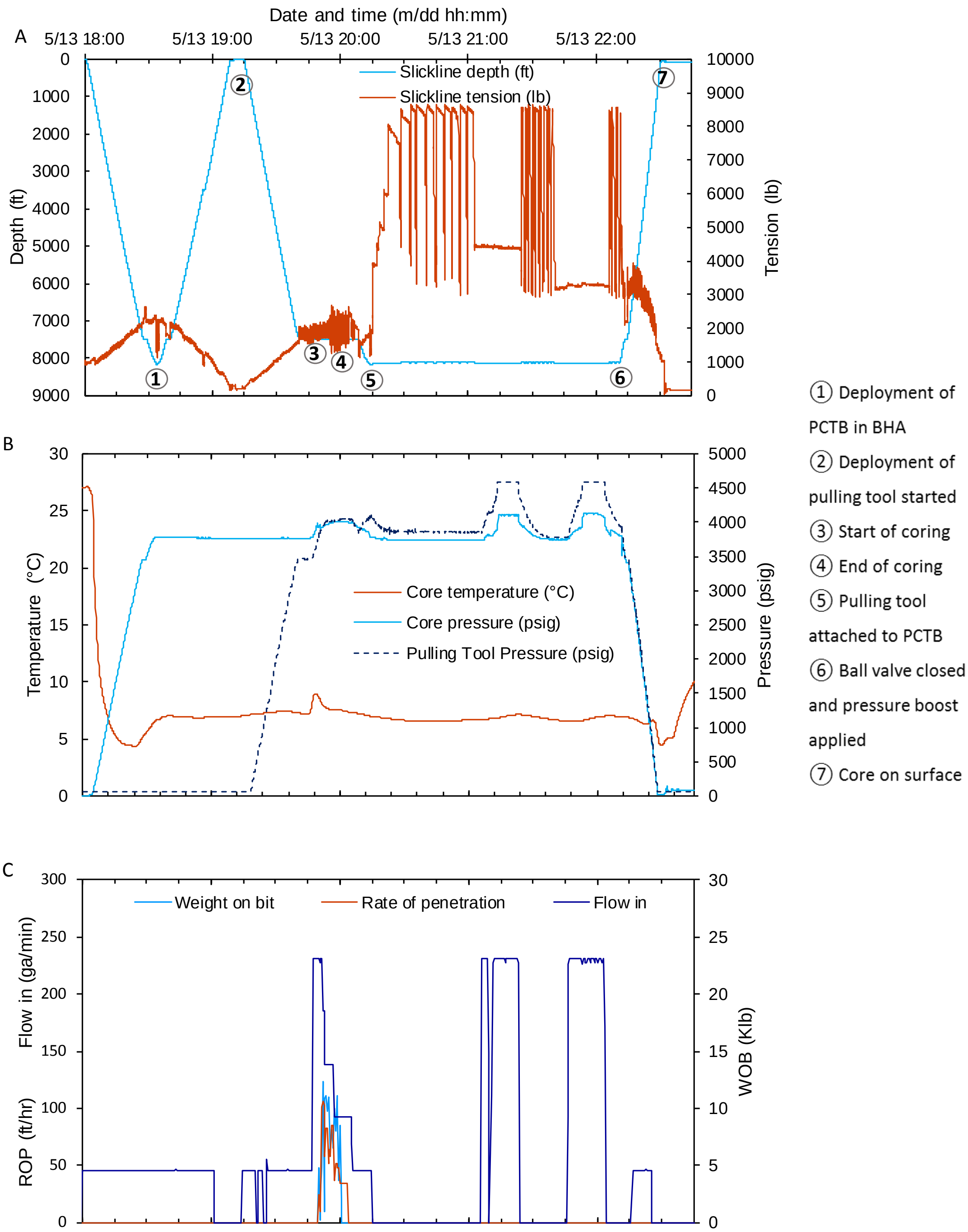

Figure 3.3.17 UT-GOM2-1-H002-5CS coring data. A) slickline tension and depth, B) pressure and temperature as measured in gauge pressure by the Data Storage Tag (DST) inside the rabbit, the cap that contacts the top of the core in the PCTB, and C) WOB, ROP, and pump flow rate. WOB = weight on bit. ROP = rate of penetration. Flow in is the sum of all pump flows. All H002 pressure coring combined Weatherford, Schlumberger, and DST data can be found in the expedition data directory under H002 / Pressure Coring / Combined Datasets. See the readme file located there for more direction.

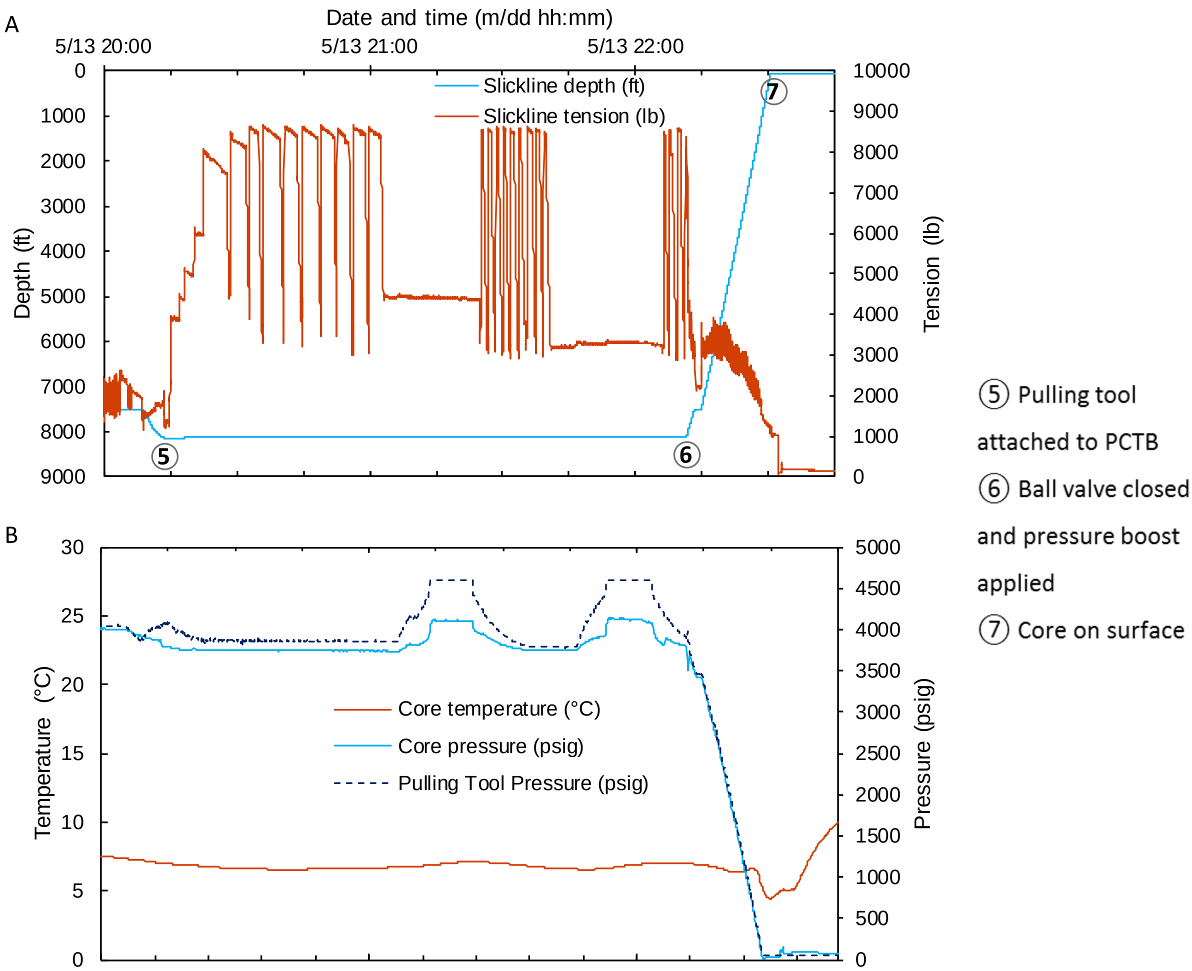

Figure 3.3.18 UT-GOM2-1-H002-5CS core retrieval details. A zoomed in section of Figure 3.3.17 showing the completion of coring and the pressure temperature conditions as the PCTB tool was pulled to the surface.

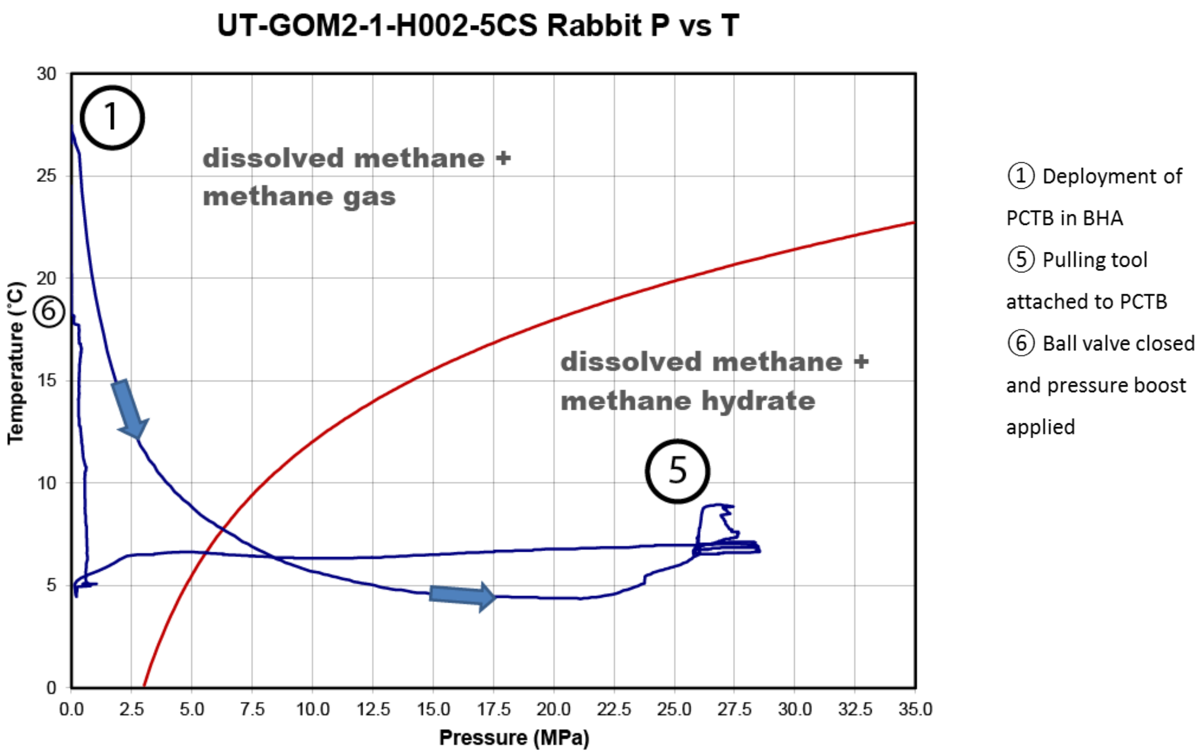

Figure 3.3.19 UT-GOM2-1-H002-5CS pressure and temperature versus calculated hydrate stability. Arrows on the P-T DST data, in blue, indicate the direction of increasing time. The hydrate stability boundary, in red, assumes methane in the presence of brine at seawater salinity.

Core UT-GOM2-1-H002-06CS

Depth: 8102-8112 fbrf (425.20-428.24mbsf)
Recovery: 3.1 ft (0.93 m), 31%
Pressure status: 0 psi

Deployment and recovery data for PCTB UT-GOM2-1-H006 are shown in Figure 3.3.20, Figure 3.3.21 and Figure 3.3.22. The tool did not seal during recovery (events 5 to 6), allowing the tool and core to pass out of the methane hydrate stability zone. The ball valve closed during recovery, but the seal at the top end of the plug failed. Core recovery was 159 cm. Unlike UT-GOM2-1-H002-04CS, there was no sand above the rabbit, which indicated that the pump rates during coring were appropriate for this formation.

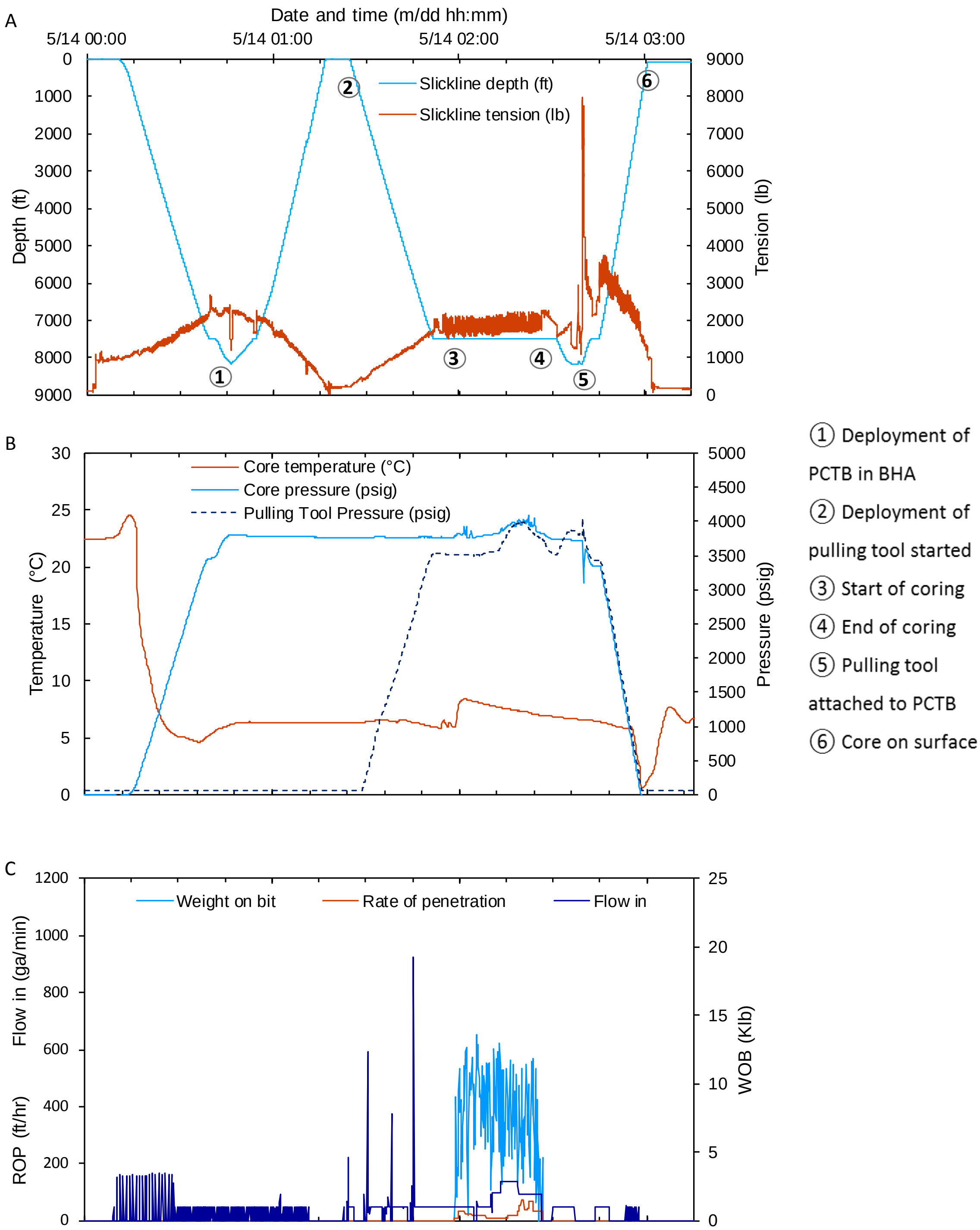

Figure 3.3.20 UT-GOM2-1-H002-6CS coring data. A) slickline tension and depth, B) pressure and temperature as measured in gauge pressure by the Data Storage Tag (DST) inside the rabbit, the cap that contacts the top of the core in the PCTB, and C) WOB, ROP, and pump flow rate. WOB = weight on bit. ROP = rate of penetration. Flow in is the sum of all pump flows. All H002 pressure coring combined Weatherford, Schlumberger, and DST data can be found in the expedition data directory under H002 / Pressure Coring / Combined Datasets. See the readme file located there for more direction.

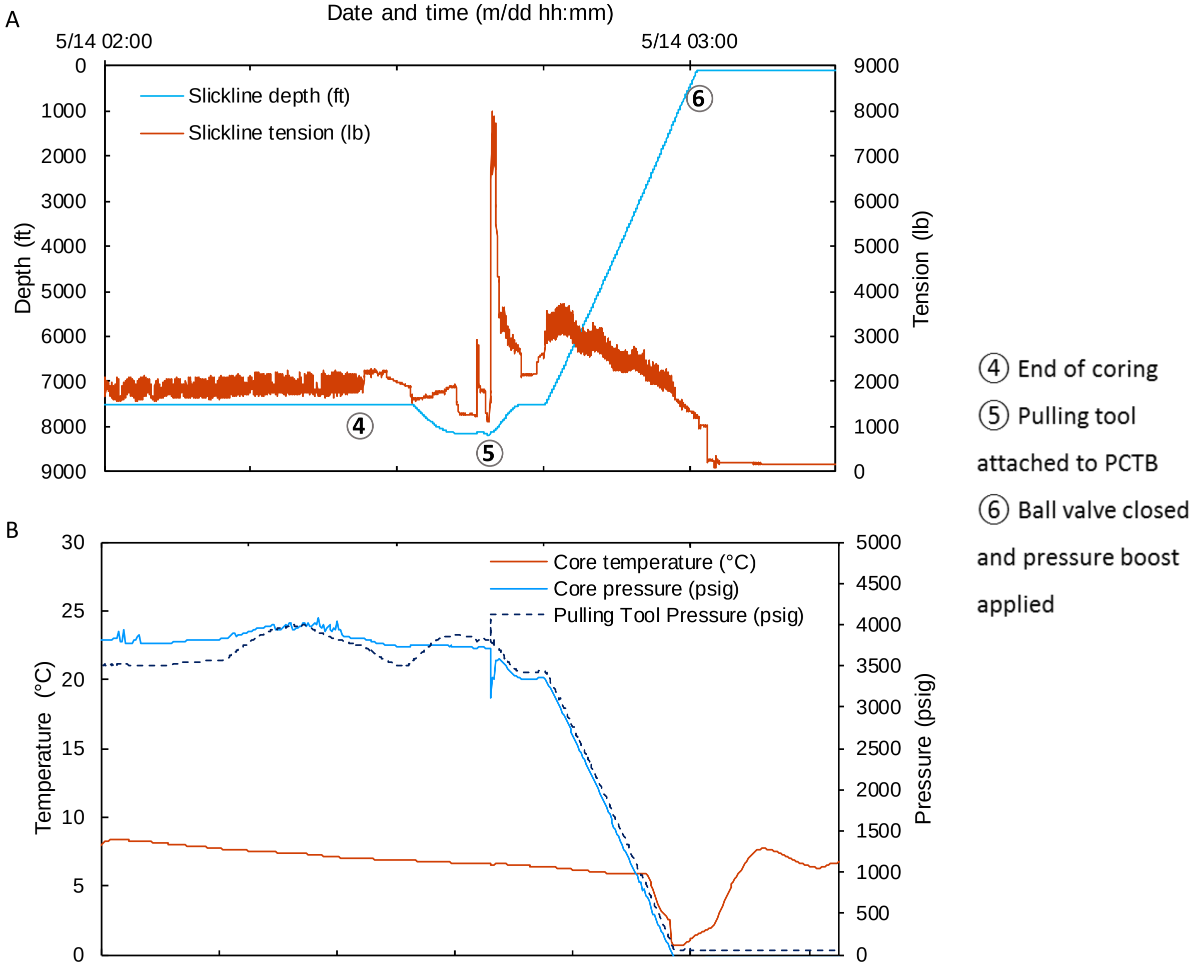

Figure 3.3.21 UT-GOM2-1-H002-6CS core retrieval details. A zoomed in section of Figure 3.3.20 showing the completion of coring and the pressure temperature conditions as the PCTB tool was pulled to the surface.

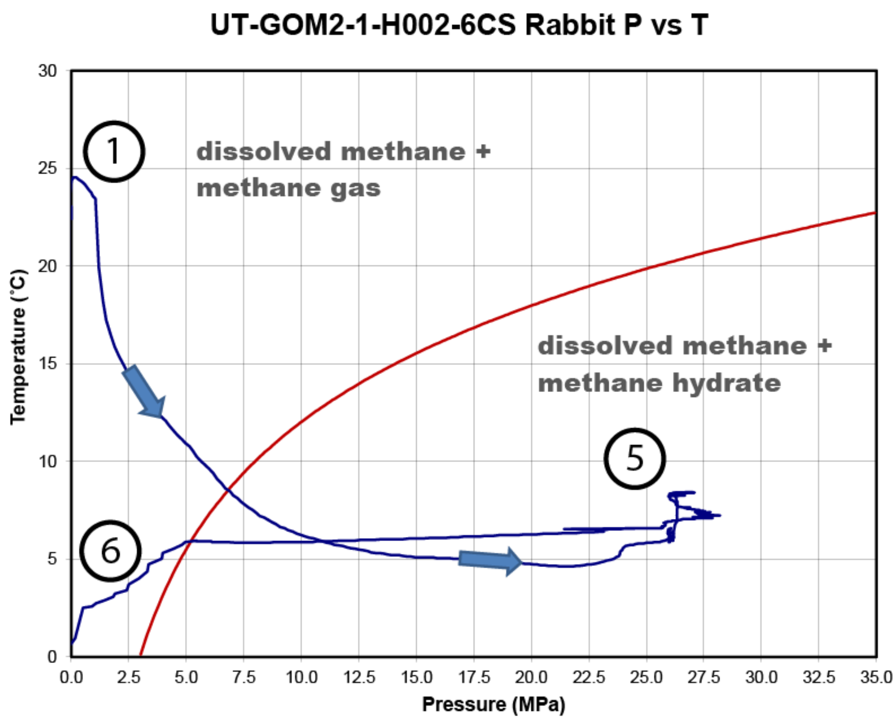

① Deployment of PCTB in BHA
⑤ Pulling tool attached to PCTB
⑥ Ball valve closed and pressure boost applied

Figure 3.3.22 UT-GOM2-1-H002-6CS pressure and temperature versus calculated hydrate stability. Arrows on the P-T DST data, in blue, indicate the direction of increasing time. The hydrate stability boundary, in red, assumes methane in the presence of brine at seawater salinity.

Core UT-GOM2-1-H002-07CS

Depth: 8102-8112 fbrf (428.24-431.29mbsf)
Recovery: 3.1 ft (0.93 m), 31%
Pressure status: 0 psi

Deployment and recovery data for PCTB UT-GOM2-1-H002-07CS are shown in Figure 3.3.23, Figure 3.3.24 and Figure 3.3.25. Core UT-GOM2-1-H002-07CS was recovered at 0 psi. The ball valve was not fully closed upon recovery due to the displacement of the valve seal. Fluidized sediment accumulated above the rabbit during this coring run.

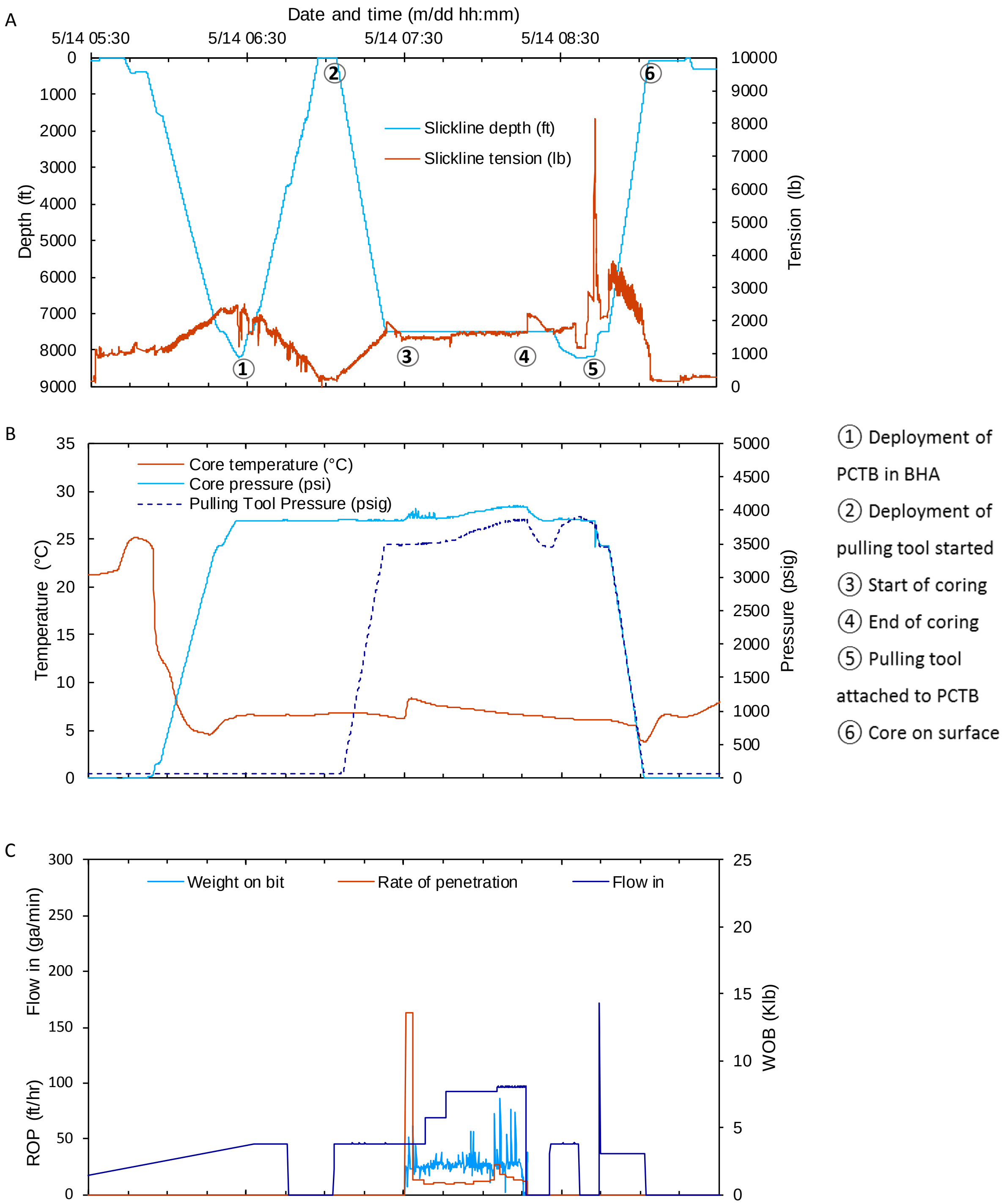

Figure 3.3.23 UT-GOM2-1-H002-7CS coring data. A) slickline tension and depth, B) pressure and temperature as measured in gauge pressure by the Data Storage Tag (DST) inside the rabbit, the cap that contacts the top of the core in the PCTB, and C) WOB, ROP, and pump flow rate. WOB = weight on bit. ROP = rate of penetration. Flow in is the sum of all pump flows. All H002 pressure coring combined Weatherford, Schlumberger, and DST data can be found in the expedition data directory under H002 / Pressure Coring / Combined Datasets. See the readme file located there for more direction.

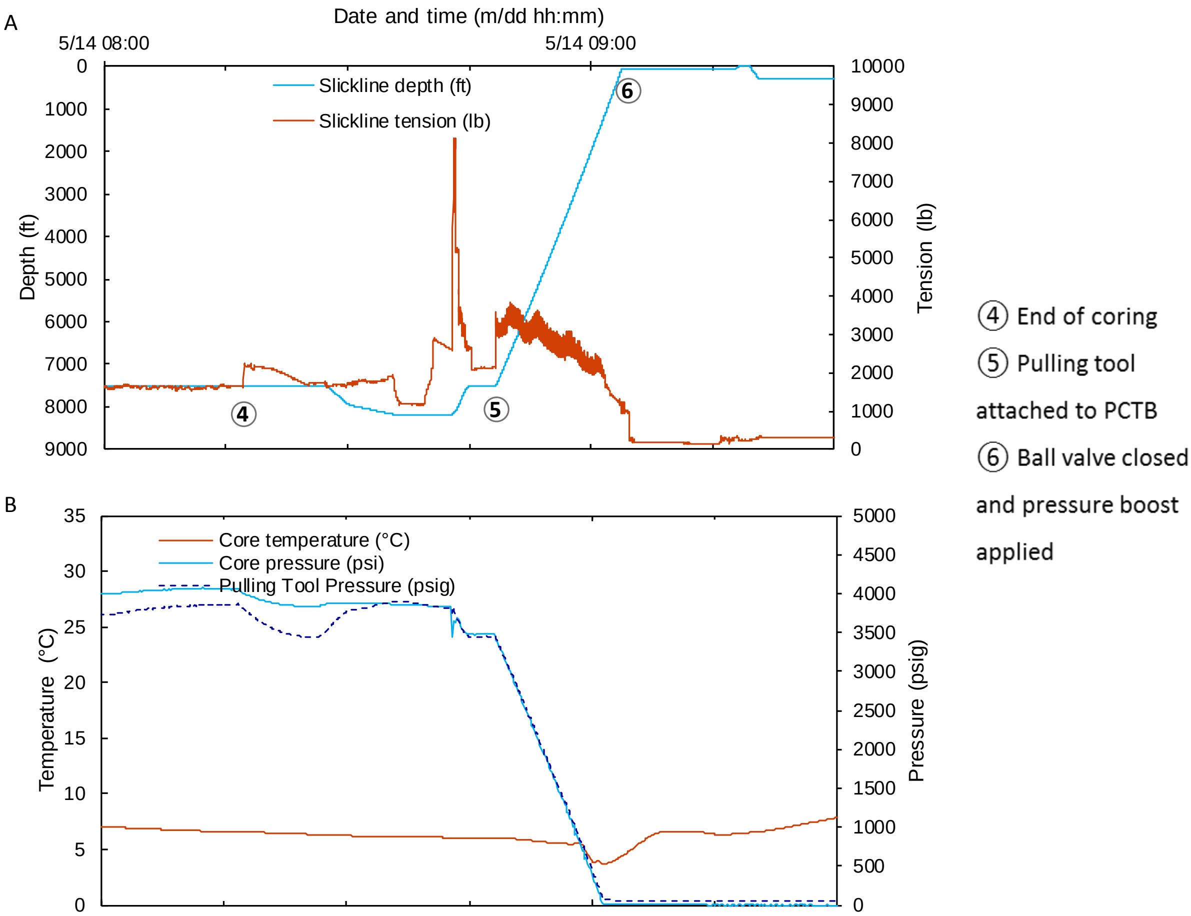

Figure 3.3.24 UT-GOM2-1-H002-7CS core retrieval details. A zoomed in section of Figure 3.3.23 showing the completion of coring and the pressure temperature conditions as the PCTB tool was pulled to the surface.

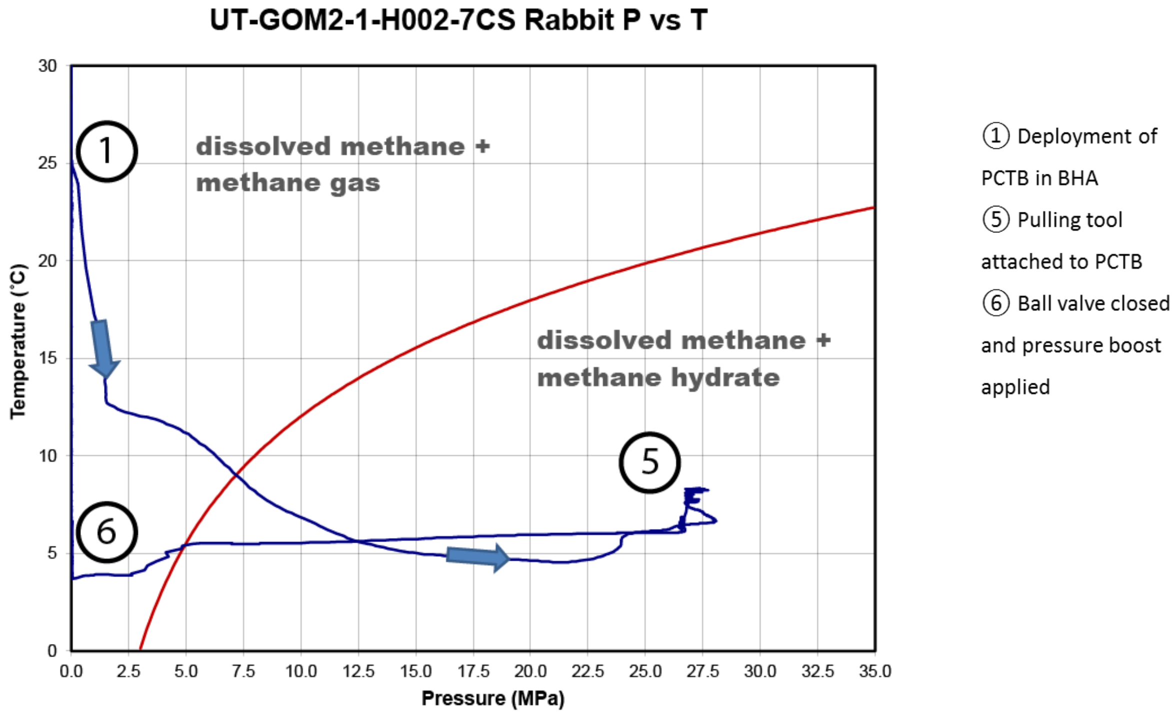

Figure 3.3.25 UT-GOM2-1-H002-7CS pressure and temperature versus calculated hydrate stability. Arrows on the P-T DST data, in blue, indicate the direction of increasing time. The hydrate stability boundary, in red, assumes methane in the presence of brine at seawater salinity.

Core UT-GOM2-1-H002-08CS

Depth: 8102-8112 fbrf (431.29-434.34 mbsf)
Recovery: 3.1 ft (0.93 m), 31%
Pressure status: 0 psi

Deployment and recovery data for PCTB UT-GOM2-1-H005-08CS are shown in Figure 3.3.26, Figure 3.3.27 and Figure 3.3.28. Core UT-GOM2-1-H002-08CS recovered 197 cm of sediment. However, when the core was recovered, the ball valve was open and the autoclave was at atmospheric pressure. The ball valve release sleeve failed by sliding over the stop position.

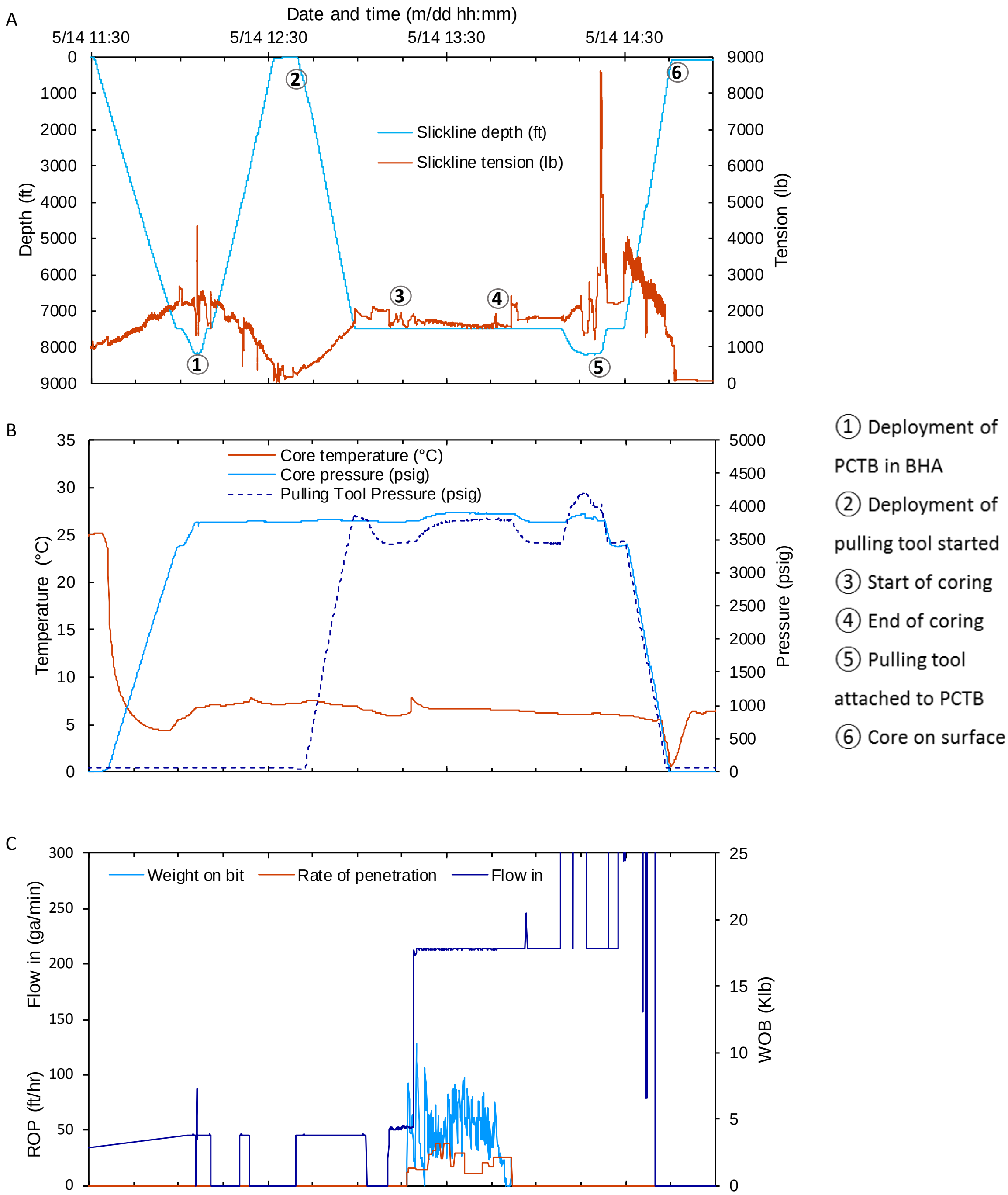

Figure 3.3.26 UT-GOM2-1-H002-8CS coring data. A) slickline tension and depth, B) pressure and temperature as measured in gauge pressure by the Data Storage Tag (DST) inside the rabbit, the cap that contacts the top of the core in the PCTB, and C) WOB, ROP, and pump flow rate. WOB = weight on bit. ROP = rate of penetration. Flow in is the sum of all pump flows. All H002 pressure coring combined Weatherford, Schlumberger, and DST data can be found in the expedition data directory under H002 / Pressure Coring / Combined Datasets. See the readme file located there for more direction.

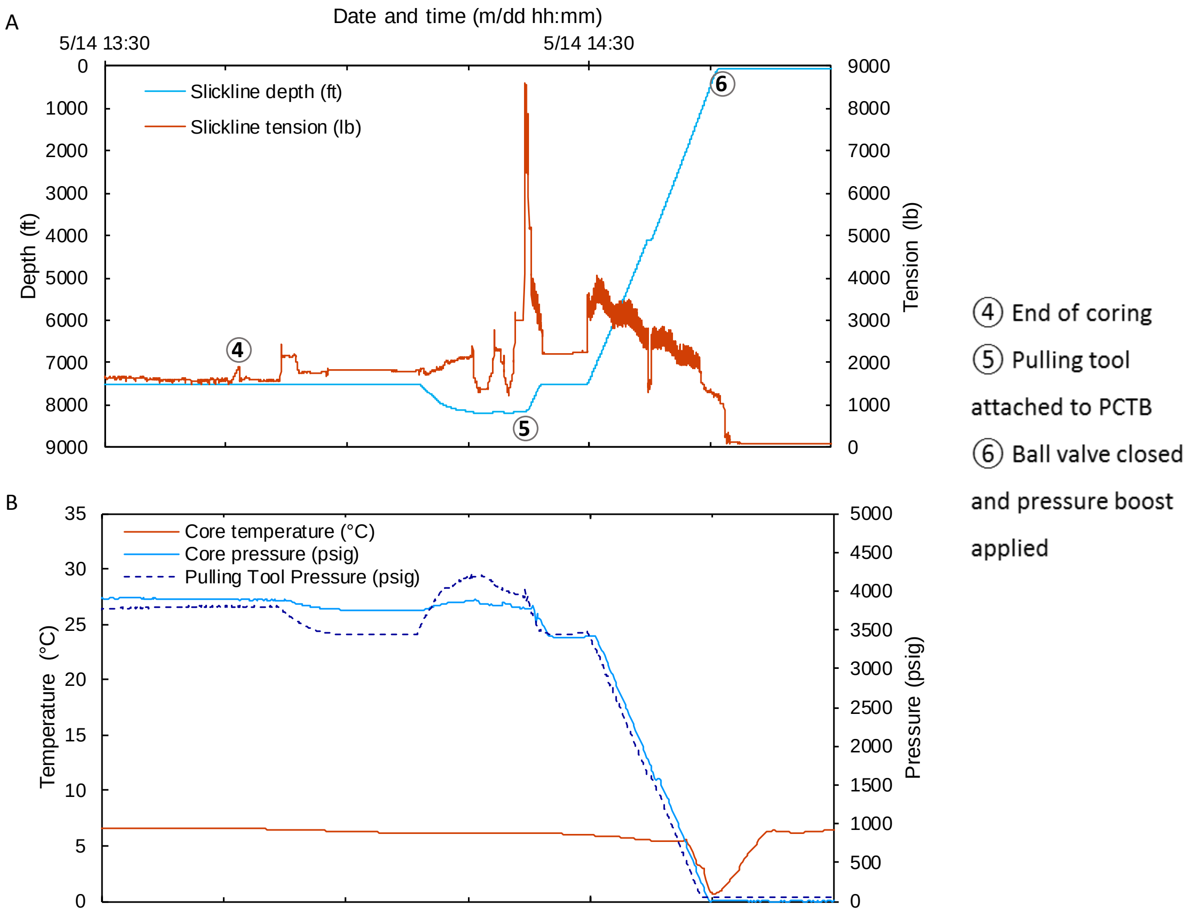

Figure 3.3.27 UT-GOM2-1-H002-8CS core retrieval details. A zoomed in section of Figure 3.3.26 showing the completion of coring and the pressure temperature conditions as the PCTB tool was pulled to the surface.

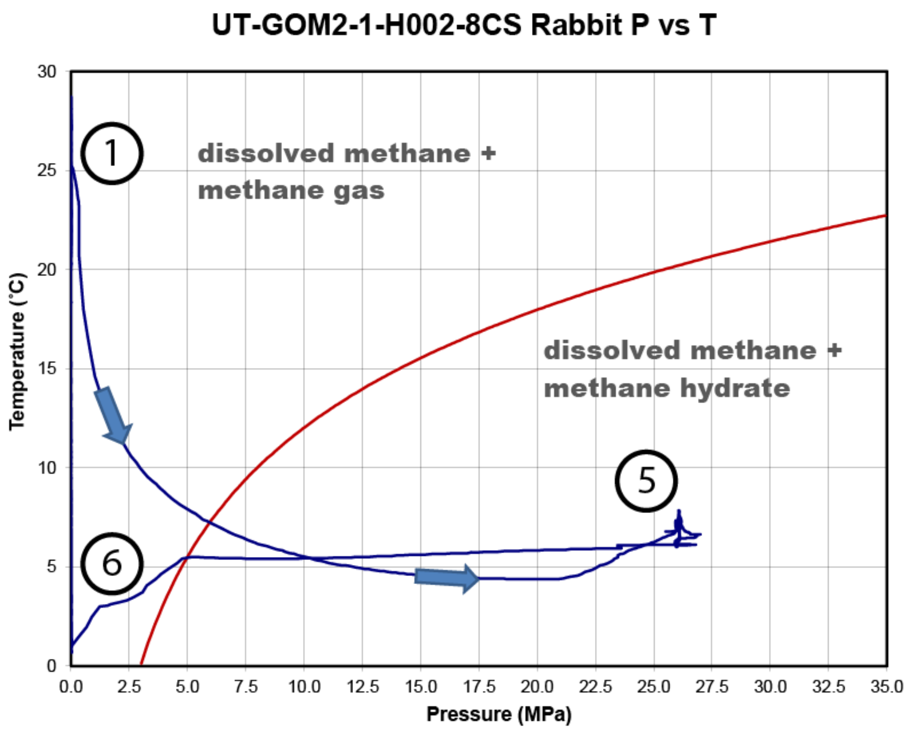

① Deployment of PCTB in BHA
⑤ Pulling tool attached to PCTB
⑥ Ball valve closed and pressure boost applied

Figure 3.3.28 UT-GOM2-1-H002-8CS pressure and temperature versus calculated hydrate stability. Arrows on the P-T DST data, in blue, indicate the direction of increasing time. The hydrate stability boundary, in red, assumes methane in the presence of brine at seawater salinity.

3.3.4 PCTB Performance Review

Only one pressure core H002-4CS was recovered at a pressure and temperature within the methane hydrate stability zone. During this run, the ball valve closed while the PCTB was 600 ft above the coring point, but still below the seafloor (Figure 3.3.29; Table 3.3.5). This core was recovered with the PCTB-CS after the flow diverter was removed and the PolyPak seal was replaced with an O-ring. However, other runs in this configuration failed to hold pressure due to problems with seal displacement (Figure 3.3.29). Cores UT-GOM2-1-H002-01CS and – 06CS were recovered with the ball valve closed. However, the depth/pressure of closure was not identified due to the loss of pressure elsewhere in the tool.

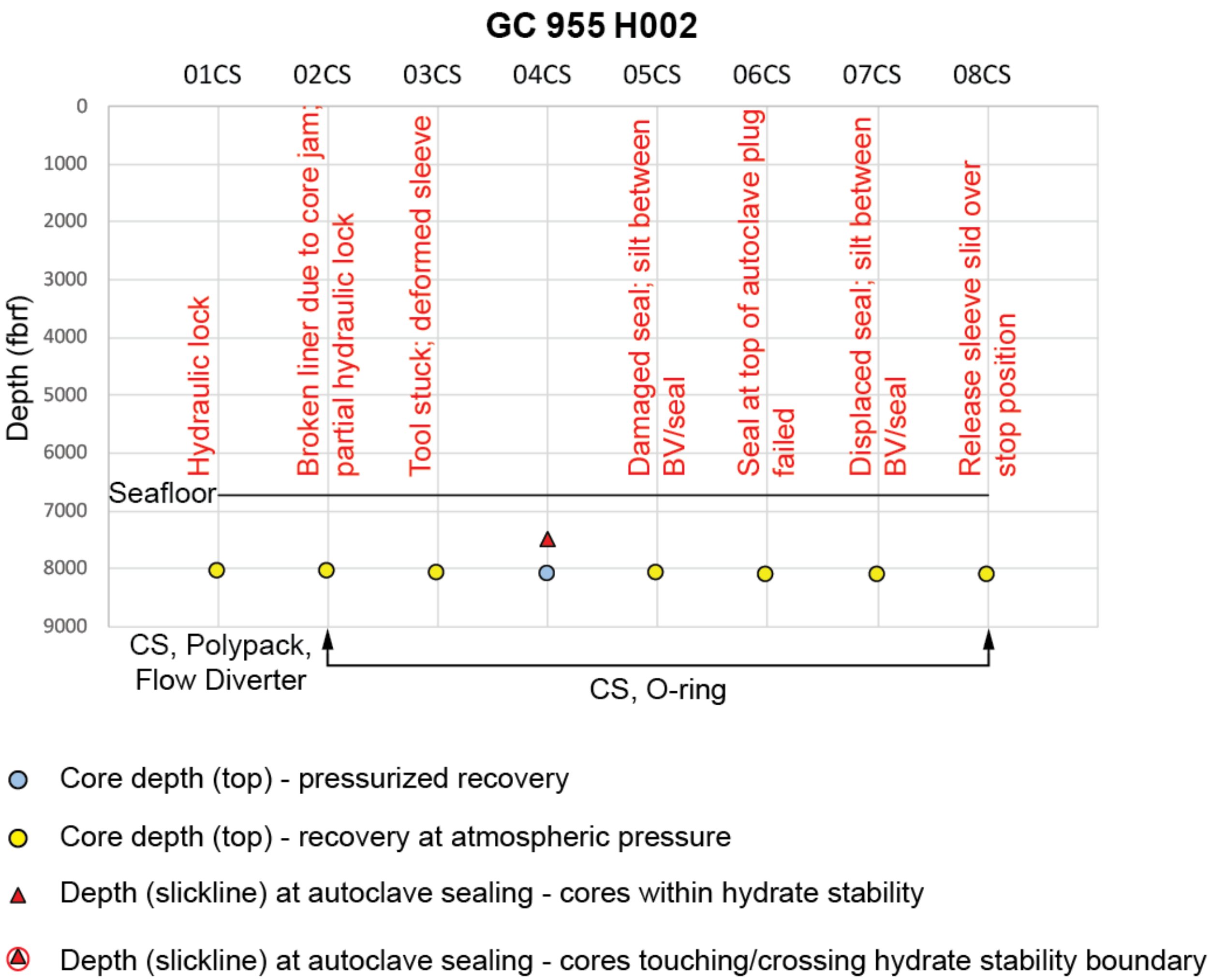

Figure 3.3.29 Depth of PCTB ball autoclave sealing for each of the 8 coring runs. All cores cross out of the methane hydrate stability zone except 4CS before the ball valve closed (1CS and 6CS) or the ball valve failed to close (2CS, 3CS, 5CS, 7CS, and 8CS).

Core	Top of core depth (fbrf)	Ball valve closure slickline depth (fbrf)	Pressure when the autoclave sealed (psi)
01CS	8062	Unknown	Unknown
02CS	8072	NA	NA
03CS	8082	NA	NA
04CS	8092	7491.6	3393
05CS	8102	NA	NA
06CS	8112	Unknown	Unknown
07CS	8122	NA	NA
08CS	8132	NA	NA

Table 3.3.5 Depth of coring with the depth and pressure when the autoclave sealed.

PCTB Failure Analysis

Following the disappointing performance of the pressure coring in H002, the Geotek coring team conducted a thorough failure mode analysis. The following main failure modes were identified to have either occurred or were likely to have contributed to the failures:

- Core jamming/broken liner - this occurs when the drill cuttings are not adequately removed from the immediate cutting shoe area during coring (2CS, 3CS).
- Hydraulic lock caused by flow diverter in middle section, which resulted in a pressure build up in the middle section and an incomplete pulling action (1CS, Full Function Test 1).
- Ball valve seal unseating that caused the ball to not fully close if the seal is caught by the ball and the autoclave to leak pressure (5CS, 7CS).
- The DST record from the successful core did not record a pressure boost pressure at the time of release from the BHA. Boost pressure timing can adversely affect ball valve sealing.

The failure modes are summarized in Table 3.3.6.

The critical dimensions of the tool's major moving parts were measured to ensure that there were no differences between the 4 PCTB tools. Key findings/remedies from the failure analysis were as follows:

- There was a design oversight which could cause a hydraulic lock to occur as a result of a metal to metal seal. To remedy this oversight, simple flow paths were ground into the offending part to prevent locking occurring.
- The removal of the flow diverter may have aggravated other failure modes, including the ball valve seal unseating. The flow diverter was re-activated in the next hole.
- There was a design oversight in the ball valve release sleeve. It transpired that the collets on the sleeve can jump over the reaction lip if it is hit too hard, which prevents the ball valve from being triggered. To remedy this, welded buttons were attached to each collet finger to prevent this from happening.
- At the start of the coring operation, setting down on the bottom of the hole with the right mud pump flow rate is important to clear any debris and prevent initial jamming. However, the flow

rates must not be high enough to cause remobilized sediment to flow up the liner and above the rabbit.

- Initial retraction speed of the inner barrel with the pulling tool at the end of the coring run may be a critical step to allow the ball valve to close prior to firing the pressure boost.
- The speed of the ball valve closure is likely to be affected by both the viscous drilling mud being used during the coring and fine silt that can be found around the ball. To mitigate against this drag, a tighter fitting ball valve seal can be used and no lubricant should be used around the ball because it can aggravate the build-up of sand around the ball.
- To confirm that these changes have no negative effects, Geotek proposed to conduct a number of Full Function Tests in the face bit BHA at about 1000 fbrf prior to drilling the next hole (H005).

Failure Mode	Affected Runs	solution
Hydraulic Lock (Flow Diverter Assembly)	1CS	- Removed flow diverter - Grinded relieving flats on offending parts
BV Jamming/Broken Liner	2CS	Optimized flow rate and WOB
BV Seal Dislodging as BV closes (BV release sleeve jumped over reaction lip preventing BV from triggering)	5CS, 6CS, 7CS,	Remedied in H005 by fitting a tighter seal and not lubing the ball as to avoid attracting sediment (occurred in-between H002 and H005)

Table 3.3.6 Failure modes for the unsuccessful coring runs and the measures implemented.

3.3.5 Core Recovery

As described above, eight pressure cores were attempted at H002 between 8081-8193 fbrf (Table 3.3.7). Seven of these cores did not maintain pressure during recovery, and as a result the core liner contained material filled with voids and expansion cracks. Recovery was calculated based on actual length of sediment contained in the liner. The intervals with intact sediment were sampled for time sensitive analyses (see 3.7 Geochemistry and Microbiology) and the remaining sections were split and described (see 3.4 Physical Properties and Core Transfer and 3.6 Lithostratigraphy). Core recovery averaged 34%, with no discernable pattern of yield with respect to depth or interval (Figure 3.3.30). Cores UT-GOM2-1-H002-02CS and -06CS had the highest core recoveries, (52% and 53%, respectively). Core UT-GOM2-1-H002-04CS did hold pressure during recovery therefore PCATS analysis and quantitative degassing were performed (see 3.4 Physical Properties and Core Transfer and 3.5 Quantitative Degassing).

Core	Interval from (fbrf)	Interval to (fbrf)	Interval from (msbf)	Interval to (mbsf)	Recovery (ft)	Recovery (m)	% Recovery
UT-GOM2-1-H002-1CS	8062	8072	409.35	412.35	2.3	0.70	23
UT-GOM2-1-H002-2CS	8072	8082	412.35	415.45	5.3	1.62	53
UT-GOM2-1-H002-3CS	8082	8092	415.45	418.45	1.1	0.34	11
UT-GOM2-1-H002-4CS	8092	8102	418.45	421.55	4.5	1.37	45
UT-GOM2-1-H002-5CS	8102	8112	421.55	424.55	3.1	0.94	31
UT-GOM2-1-H002-6CS	8112	8122	424.55	427.65	5.2	1.58	52
UT-GOM2-1-H002-7CS	8122	8132	427.65	430.65	1.5	0.46	15
UT-GOM2-1-H002-8CS	8132	8142	430.65	433.75	4.6	1.40	46
Totals					27.5	8.38	34

Table 3.3.7 Core intervals and recovered length.

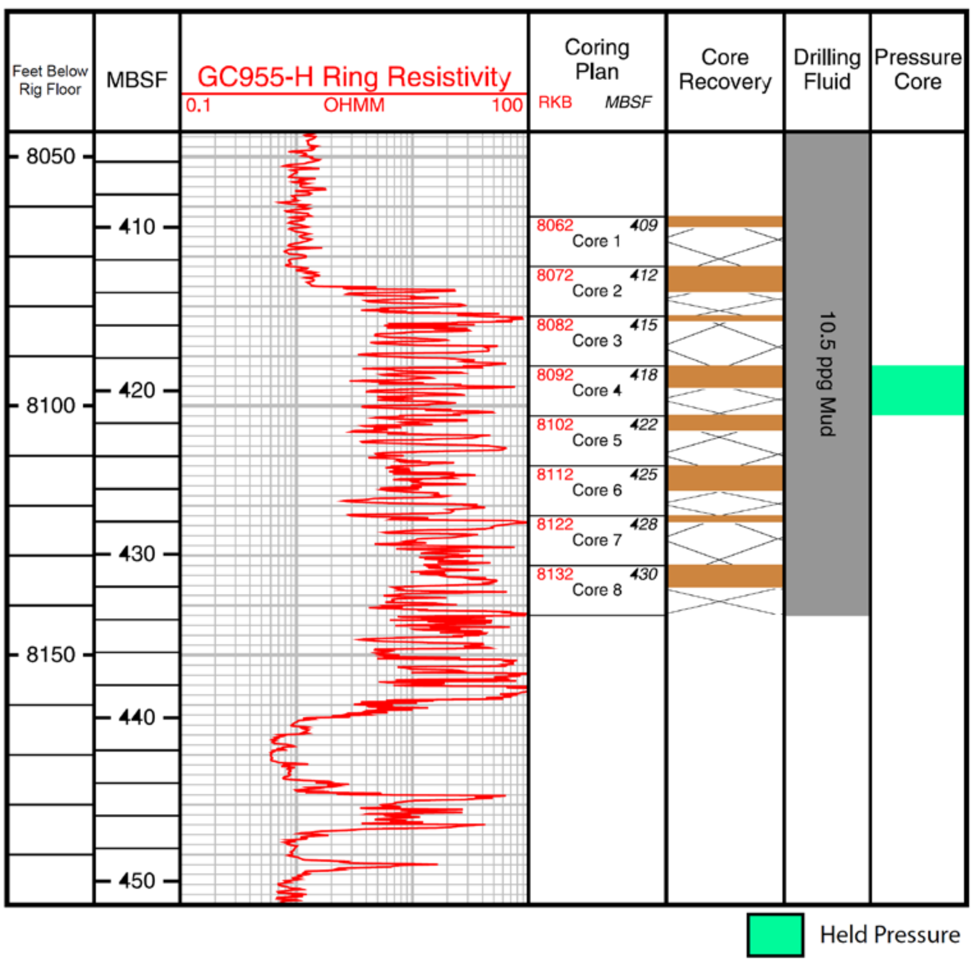

Figure 3.3.30 Planned and actual core recovery for H002 versus H001 LWD data. Brown boxes delineating the amount of core recovered from each interval. Core UT-GOM2-H002-4CS was the only interval to hold pressure upon reaching the surface.

3.4. Physical Properties and Core Transfer

This section of the expedition report will discuss the X-ray imaging, gamma density, P-wave velocity of pressure and depressurized core, and core cutting.

3.4.1 Pressurized Whole Core

Core UT-GOM2-1-H002-4CS (Figure 3.4.1) was the only core recovered at pressure and processed in PCATS (see 3.3 Pressure Coring). A total of 1.38 m was scanned in PCATS including X-ray (2D and 3D CT), gamma density, and P-wave velocity. PCATS logging from this core, along with pressure cores from H005, suggest two main sediment lithofacies interbedded within the hydrate-bearing interval.

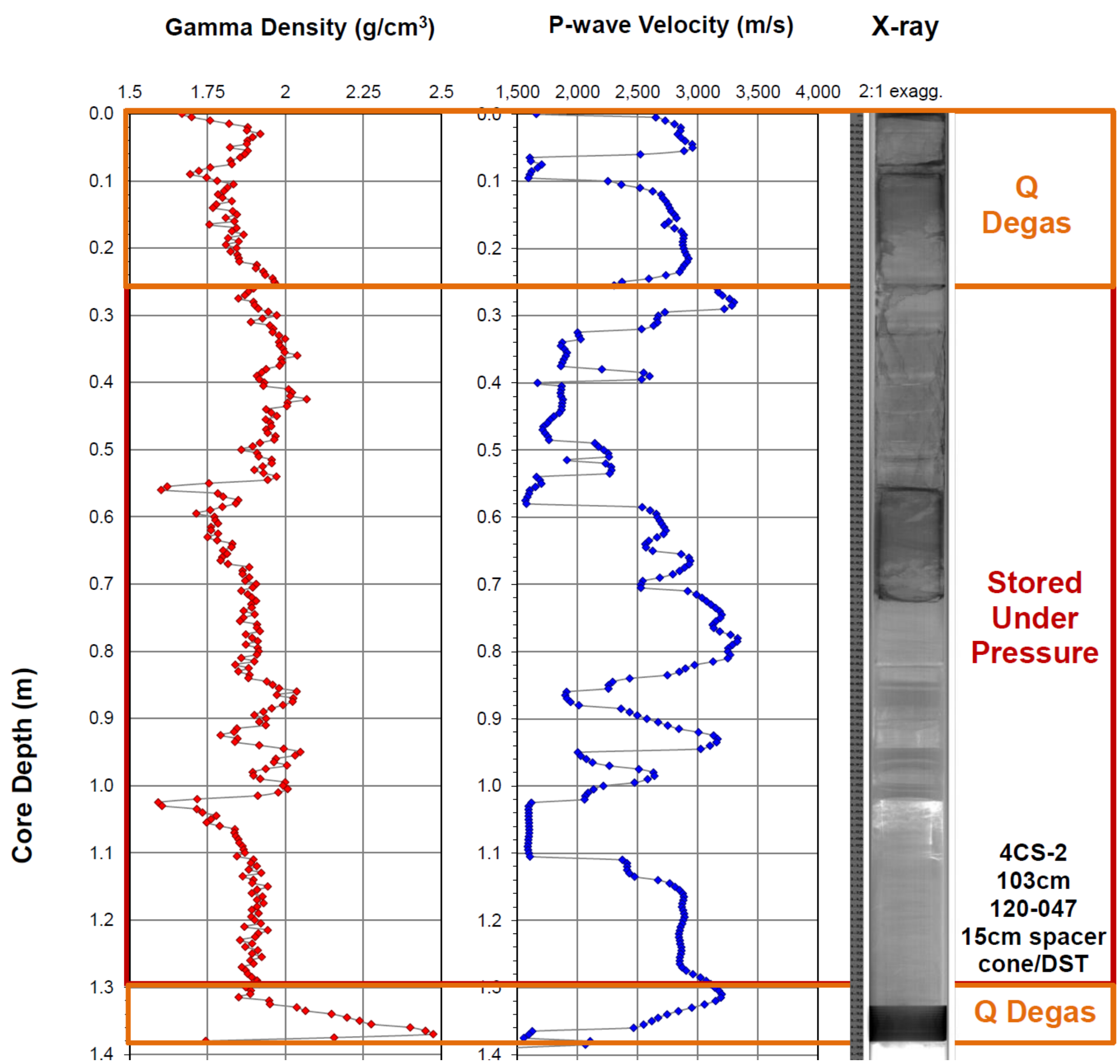

Figure 3.4.1 UT-GOM2-1-H002-4CS PCATS data and section cuts. All H002 Physical property and CT data can be found in the expedition data directory under H002 / Physical Properties.

PCATS density and velocity

Gamma density measurements for Core UT-GOM2-1-H002-4CS reflected a combination of sedimentological features and core disturbance. Sections of core containing lithofacies 3 that filled the liner had densities near 2.0 g/cm^3. Lithofacies 2 sediments had maximum apparent densities near 1.9 g/cm^3, though the harder lithofacies 2 sediments did not fill the core liner and the densities will require correction. Down core variation in density can be influenced by variation in core diameter.

P-wave velocities showed an obvious distinction between lithofacies 2 and 3 sediments (Figure 3.4.1). Lithofacies 2 sediments had recorded velocities of ~2500-3300 m/s, consistent with the presence of pore-filling gas hydrate, while lithofacies 3 sediments had velocities which varied from 1550-2000 m/s. As with the density, the sediment velocities in lithofacies 2 will require correction for diameter variations and will increase when corrected. The variation in lithofacies 3 velocities cannot be explained by variations in core diameter, as these sediments fill the liner. These sediments should be examined carefully for core disturbance to understand their true variation in velocity, and whether such a variation might be related to the presence of gas hydrate.

PCATS 2D and 3D X-ray

X-ray 2D linear images and X-ray 3D CT data sets were collected for Core UT-GOM2-1-H002-4CS. The X-ray images showed that the core contained at least two basic lithologies, an X-ray-dark (dense) lithology (likely more clay-rich) and an X-ray-light lithology. These correspond to lithofacies 3 and 2, respectively, as described in section 3.6 Lithostratigraphy. Interbedding of these two facies can be clearly seen (Figure 3.4.2), as well as subhorizontal density variations within lithofacies 2. A sedimentological description of the core from the X-rays can be found in section 3.6 Lithostratigraphy.

Very low-density features in the X-ray CT (bright white, e.g., Core UT-GOM2-1-H002-4CS, 12-18 cm in the XZ slab, Figure 3.4.3) are either water-filled cracks or gas hydrate. Cracks that propagate to the outside of the core might be expected to be filled with mud and appear dense in the X-ray; however, these cracks or veins still appeared as low density. It is not possible to tell from the X-ray data whether these thin features were definitively gas hydrate.

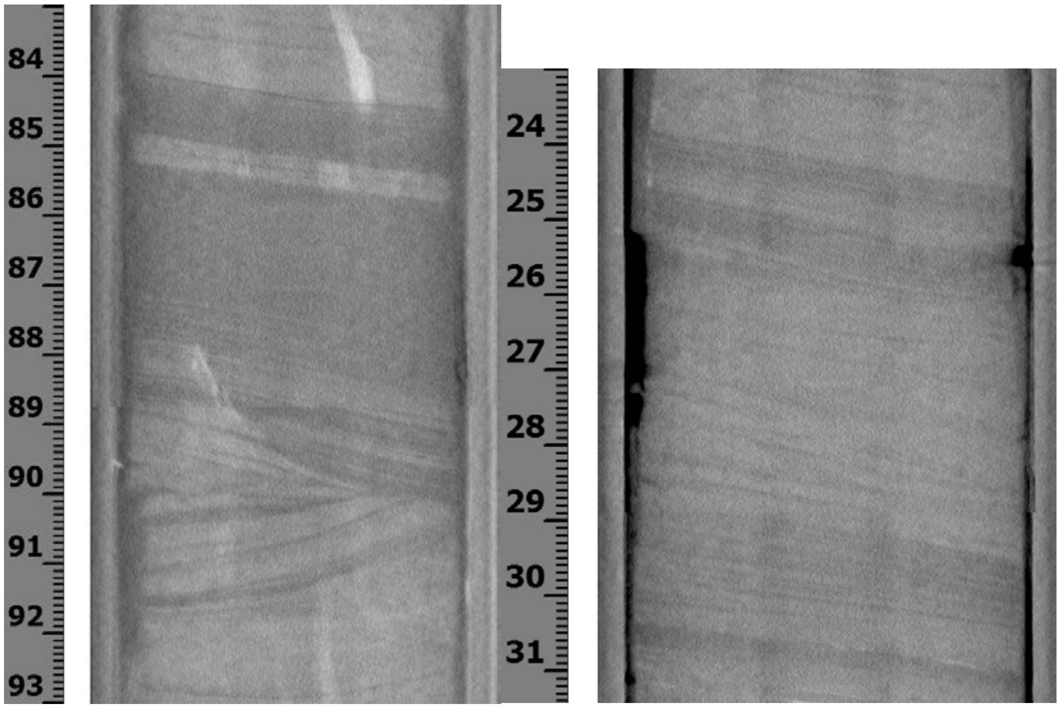

Figure 3.4.2 UT-GOM2-1-H002-4CS X-ray CT XZ slab portions. Lithofacies 2 (light) and Lithofacies 3 (dark), along with subhorizontal density variations in Lithofacies 2. All H002 Physical property and CT data can be found in the expedition data directory under H002 / Physical Properties.

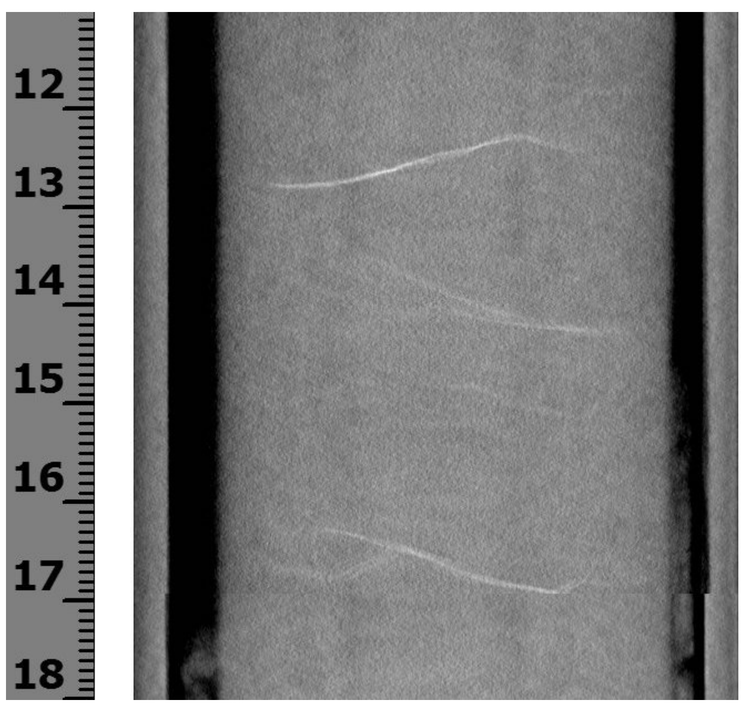

Figure 3.4.3 UT-GOM2-1-H002-4CS Low-density (light) features in the X-ray CT XZ slab. All H002 Physical property and CT data can be found in the expedition data directory under H002 / Physical Properties.

Core quality from nondestructive data

Rotary coring creates characteristic core disturbance features. In harder material, core collected via rotary coring tools breaks periodically. Between these breaks, the pieces of core rotate relative to each other, and the top portion of the bottom piece may be ground into a conical point (e.g., Core UT-GOM2-1-H002-4CS, 98 cm, Figure 3.4.4). Drilling mud (e.g., Core UT-GOM2-1-H002-4CS, 56 cm, Figure 3.4.4) or softer parts of the formation (e.g., Core UT-GOM2-1-H002-4CS, 97 cm, Figure 3.4.4) may fill in the gap between pieces of core, complicating the interpretation of density and velocity. Soft material cored in a rotary fashion may be compressed to fill the whole liner, regardless of the actual clearance ratio between the cutting shoe or bit and the inner diameter of the liner. There is also the potential for soft material to be compressed prior to entry into the PCTB and lost. Material retained may be sheared and twisted (e.g., Core UT-GOM2-1-H002-4CS, 51-52 cm, Figure 3.4.4).

This core was cut with drilling mud, which can be seen as darker masses at the edges of the top half of the core. There was little evidence of mud invasion into the sediment other than between pieces of core. Low-density, thin layers (Figure 3.4.3) may be drilling-induced cracks, filled with low-density fluid or reformed hydrate, or they may represent real in situ layers of gas hydrate.

The core diameter in Core UT-GOM2-1-H002-4CS varied down the core in three blocks, starting near 10 cm, 55 cm, and 103 cm core depth, with core diameters narrow near the top of the block and gradually widening. The narrow core may be due to precession of the drill bit during core cutting. This variation in core diameter has strongly affected the gamma density as well as the P-wave velocity.

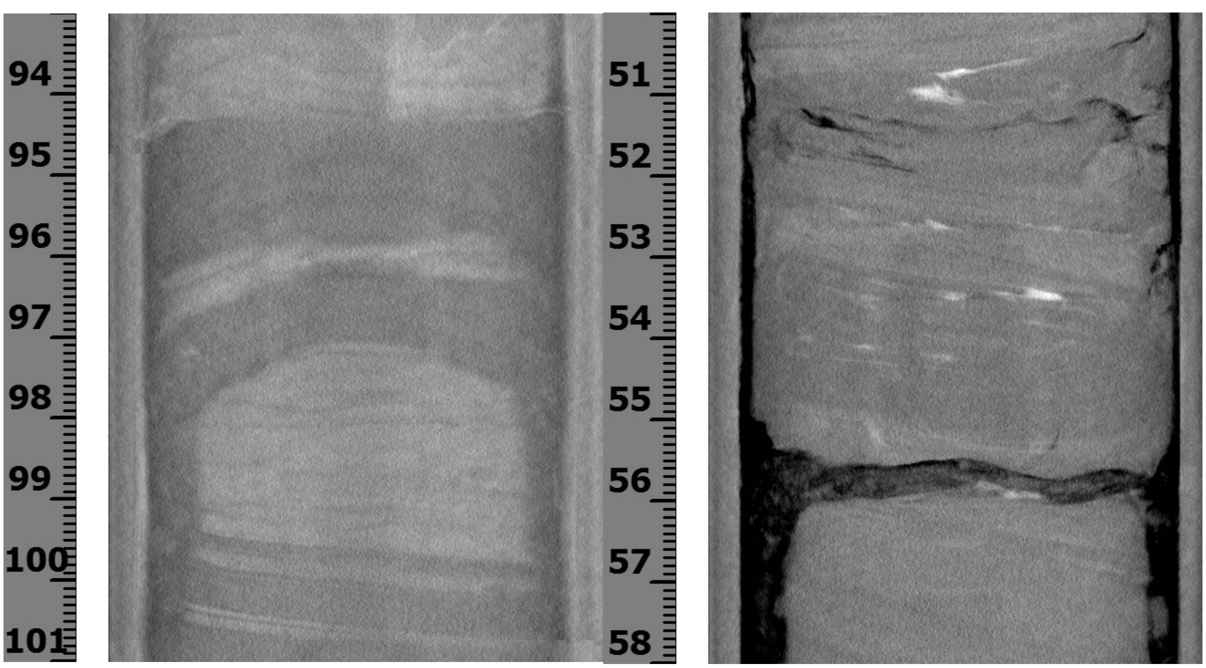

Figure 3.4.4 UT-GOM2-1-H002-4CS Examples of gaps between pieces of core material. Note the pointed conical feature to the left at 97-98 cm, and how it has impinged on the softer layer above it. Soft layers to the right near 51 cm have deformed, entraining mud, and the gap at 56 cm is filled with high-barite

drilling mud. All H002 Physical property and CT data can be found in the expedition data directory under H002 / Physical Properties.

Pressure Core Section Cut and Transfer

Core UT-GOM2-1-H002-4CS was cut into three sections using PCATS. Sections 1 and 3 (0-26.8 cm and 129.5-139 cm) were cut for quantitative degassing (see 3.5 Quantitative Degassing). Section 2 (26.8 to 129.5 cm) was transferred to a storage vessel for transport to UT.

Core	Recovered (cm)	fbrf	Section	Core Depth (cm)	Length (cm)	Allocation
UT-GOM2-1-H002-04CS	139	8092	4CS-1	0-26.8	26.8	Quantitative Degassing
UT-GOM2-1-H002-04CS	139	8092	4CS-2	26.8-129.5	103	UT
UT-GOM2-1-H002-04CS	139	8092	4CS-3	129.5-139	10	Quantitative Degassing

Table 3.4.1 Pressure Core distribution. Pressure Cores were transferred to Quantitative degassing (pink) and to UT (blue). All H002 Core distribution data can be found in the expedition data directory under H002 / Curation.

3.4.2 Depressurized Whole Core

Depressurized Core Section Cut and Transfer

As mentioned above, intervals of the core not recovered under pressure but with intact sediment were sampled for time sensitive analyses (see 3.7 Geochemistry and Microbiology). The remaining sections were split into 1 m sections or smaller, avoiding voids to maximize the length of the intact core. These sections were sent to Ohio State University and are described here and in 3.6 Lithostratigraphy.

Core	Recovered (cm)	fbrf	Section	Core Depth (cm)	Length (cm)	Depressurization	Allocation
UT-GOM2-1-H002-01CS	68.9	8062-8072	01CS-1	0-5	100	Failed pressure core	MAD
UT-GOM2-1-H002-01CS	68.9	8062-8072	01CS-1	5-20	15	Failed pressure core	Pore Water
UT-GOM2-1-H002-01CS	68.9	8062-8072	01CS-1	20-35	15	Failed pressure core	Microbiology
UT-GOM2-1-H002-01CS	68.9	8062-8072	01CS-1	37-79	44	Failed pressure core	XCT
UT-GOM2-1-H002-01CS	68.9	8062-8072	01CS-1	79	0	Failed pressure core	Headspace gas
UT-GOM2-1-H002-01CS	68.9	8062-8072	01CS-1	409		Failed pressure core	Grain Size -Laser Geotek
UT-GOM2-1-H002-02CS	162.5	8072-8082	02CS-1	0-45	45	Failed pressure core	XCT
UT-GOM2-1-H002-02CS	162.5	8072-8082	02CS-2	45	0	Failed pressure core	Headspace gas
UT-GOM2-1-H002-02CS	162.5	8072-8082	02CS-2	45-60	15	Failed pressure core	Pore Water
UT-GOM2-1-H002-02CS	162.5	8072-8082	02CS-1	60-75	15	Failed pressure core	Microbiology
UT-GOM2-1-H002-02CS	162.5	8072-8082	02CS-2	45-91	46	Failed pressure core	XCT
UT-GOM2-1-H002-02CS	162.5	8072-8082	02CS-2	75-80	78	Failed pressure core	MAD
UT-GOM2-1-H002-02CS	162.5	8072-8082	02CS-3	125-225	100	Failed pressure core	XCT
UT-GOM2-1-H002-02CS	162.5	8072-8082	02CS-4	93	0	Failed pressure core	Headspace gas
UT-GOM2-1-H002-02CS	162.5	8072-8082	02CS-4	225-217	97	Failed pressure core	XCT
UT-GOM2-1-H002-02CS	162.5	8072-8082	02CS-4	93-98	43	Failed pressure core	MAD
UT-GOM2-1-H002-03CS	32.9	8082-8092	03CS-1	0-27	27	Failed pressure core	XCT
UT-GOM2-1-H002-03CS	32.9	8082-8092	03CS-1	27-33	36	Failed pressure core	MAD
UT-GOM2-1-H002-04CS	140.2	8092-8102	04CS-1A	0-26.8	26.8	Q degas	Grain Size -Laser Geotek
UT-GOM2-1-H002-04CS	140.2	8092-8102	04CS-1B	0-26.8	26.8	Q degas	Grain Size -Laser Geotek
UT-GOM2-1-H002-04CS	140.2	8092-8102	04CS-3A	129.5-139	9.5	Q degas	Grain Size -Laser Geotek
UT-GOM2-1-H002-04CS	140.2	8092-8102	04CS-3B	129.5-139	9.5	Q degas	Grain Size -Laser Geotek
UT-GOM2-1-H002-05CS	94.5	8102-8112	05CS-1	5	0	Failed pressure core	Headspace gas
UT-GOM2-1-H002-05CS	94.5	8102-8112	05CS-1	0-95	95	Failed pressure core	XCT
UT-GOM2-1-H002-05CS	94.5	8102-8112	05CS-1	0-5	5	Failed pressure core	MAD
UT-GOM2-1-H002-05CS	94.5	8102-8112	05CS-CC	422		Failed pressure core	Grain Size -Laser Geotek
UT-GOM2-1-H002-06CS	158.5	8112-8122	06CS-1	0-19	19	Failed pressure core	XCT
UT-GOM2-1-H002-06CS	158.5	8112-8122	06CS-2	19-119	100	Failed pressure core	XCT
UT-GOM2-1-H002-06CS	158.5	8112-8122	06CS-3	119-219	100	Failed pressure core	XCT
UT-GOM2-1-H002-06CS	158.5	8112-8122	06CS-4	72-81	9	Failed pressure core	Pore Water
UT-GOM2-1-H002-06CS	158.5	8112-8122	06CS-4	62-72	10	Failed pressure core	Microbiology
UT-GOM2-1-H002-06CS	158.5	8112-8122	06CS-4	219-281	62	Failed pressure core	XCT
UT-GOM2-1-H002-06CS	158.5	8112-8122	06CS-4	95-100	5	Failed pressure core	MAD
UT-GOM2-1-H002-06CS	158.5	8112-8122	06CS-5	19	0	Failed pressure core	Headspace gas
UT-GOM2-1-H002-06CS	158.5	8112-8122	06CS-5	319-338	19	Failed pressure core	XCT
UT-GOM2-1-H002-06CS	158.5	8112-8122	06CS-5	19-24	5	Failed pressure core	MAD
UT-GOM2-1-H002-07CS	45.7	8122-8132	07CS-1	6	0	Failed pressure core	Headspace gas
UT-GOM2-1-H002-07CS	45.7	8122-8132	07CS-1	6-72	66	Failed pressure core	XCT
UT-GOM2-1-H002-07CS	45.7	8122-8132	07CS-1	0-6	6	Failed pressure core	MAD
UT-GOM2-1-H002-08CS	140.2	8132-8142	08CS-1	28	0	Failed pressure core	Headspace gas
UT-GOM2-1-H002-08CS	140.2	8132-8142	08CS-1	31-57	26	Failed pressure core	Pore Water
UT-GOM2-1-H002-08CS	140.2	8132-8142	08CS-1	31-57	26	Failed pressure core	Microbiology
UT-GOM2-1-H002-08CS	140.2	8132-8142	08CS-4	37	0	Failed pressure core	Headspace gas
UT-GOM2-1-H002-08CS	140.2	8132-8142	08CS-4	25-37	12	Failed pressure core	Pore Water
UT-GOM2-1-H002-08CS	140.2	8132-8142	08CS-4	9-25	16	Failed pressure core	Microbiology
UT-GOM2-1-H002-08CS	140.2	8132-8142	08CS-4	0-9	9	Failed pressure core	MAD
UT-GOM2-1-H002-08CS	140.2	8132-8142	08CS-CC	430		Failed pressure core	Grain Size -Laser Geotek

Table 3.4.2 Depressurized Core distribution. Depressurized cores were transferred to Geochemistry, Microbiology, Grain Size, and Conventional Core Analyses. All H002 Core distribution data can be found in the expedition data directory under H002 / Curation.

Linear X-ray

Some of the depressurized core sections were imaged through the liner in PCATS at atmospheric pressure on-board between the coring of H002 and H005. PCATS X-ray images can be found in the H002 data directory under Physical Properties / Depressurized Core.

XCT

The depressurized core sections shipped to Ohio State and scanned using a CereTom XCT. Table 3.4.3 lists all of the depressurized cores and core sections that were scanned in H002.

The XCT illustrates that core recovery in the depressurized core sections was poor (Figure 3.4.5). Unlike Core UT-GOM2-1-H002-4CS, sedimentary layering and cross-laminations were observed in only a few in small, cm-thick sections. Most of the cores were not intact and are highly disturbed, containing soupy mixture, air-bubble rich sections or broken fragments. Drilling mud was visible in some intact sections, often concentrating on the edges of the core barrel or between layers of core (Figure 3.4.5 and Figure 3.4.6).

			Depth in section (cm)				
Core	Type	Section	From	To	Length (cm)*	Depth, top of core (mbsf)	Depth, top of core (fbrf)
1	CS	1	37	79	44	409	8062
2	CS	1	0	45	45	412	8072
2	CS	2	45	91	46	412	8072
2	CS	3	125	225	100	412	8072
2	CS	4	225	317	97	412	8072
3	CS	1	0	27	27	415	8082
5	CS	1	0	95	95	422	8102
6	CS	1	0	19	19	425	8112
6	CS	2	19	119	100	425	8112
6	CS	3	119	219	100	425	8112
6	CS	4	219	281	62	425	8112
6	CS	5	319	338	19	425	8112
7	CS	1	6	72	66	428	8122
8	CS	2	57	157	100	430	8132
8	CS	3	157	235	78	430	8132
8	CS	4	272	315	43	430	8132
8	CS	5	315	351	36	430	8132

*Note: Length does not imply core recovery, only the length (in cm) of the core barrel scanned. Some core barrels contained large empty sections.

Table 3.4.3 Depressurized cores scanned on XCT. All H002 XCT data can be found in the expedition data directory under H002 / Physical Properties / XCT.

Because the core samples were depressurized during core recovery and could not be scanned while still in the methane hydrate stability zone, it is not possible to definitively identify lithofacies, or determine if the core previously contained gas hydrate. In some cases, core description observations were made that supplement lithofacies type (see 3.6 Lithostratigraphy).

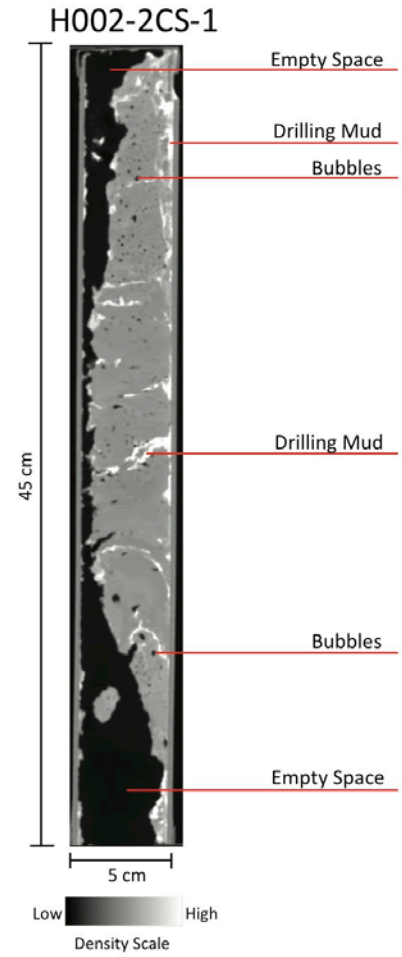

A.

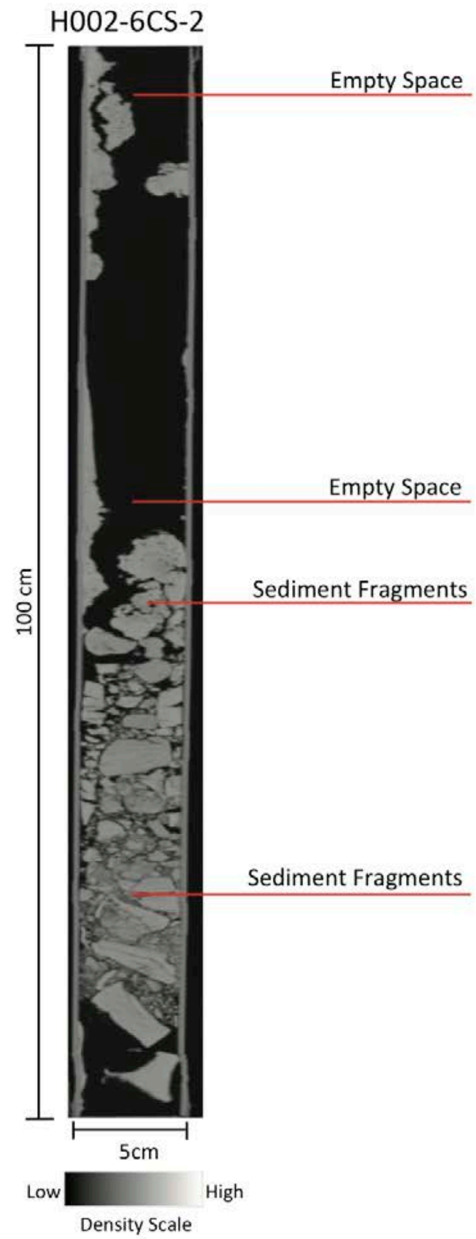

B.

Figure 3.4.5 XCT slices showing artifacts of poor recovery. A. UT-GOM2-01-H002-2CS-1 (Left) and B. UT-GOM2-01-H002-6CS-2 (Right). All H002 XCT data can be found in the expedition data directory under H002 / Physical Properties / XCT.

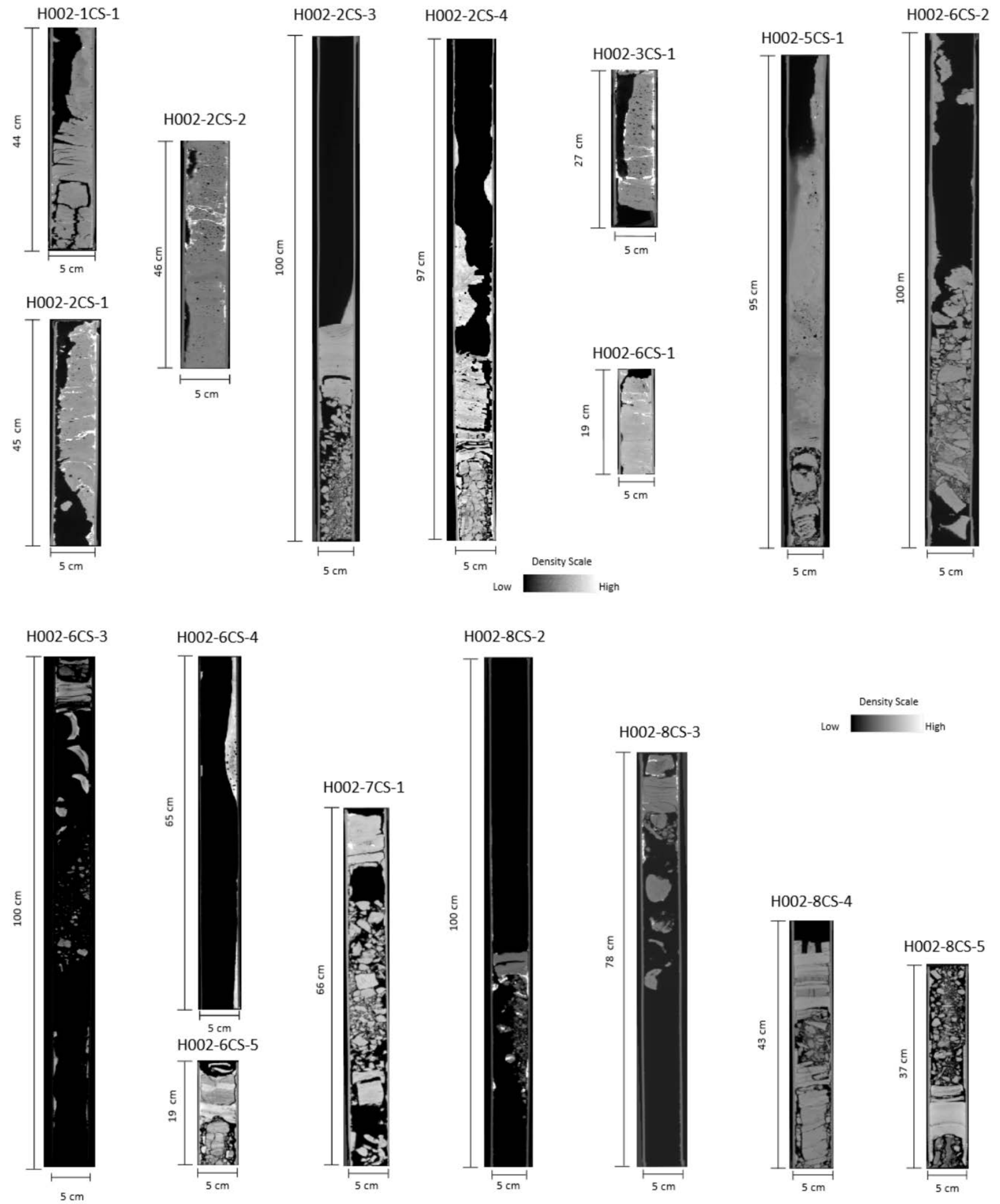

Figure 3.4.6 An XCT slice of each depressurized core. All H002 XCT data can be found in the expedition data directory under H002 / Physical Properties / XCT.

3.5. Quantitative Degassing

This section of the expedition report describes the results of quantitative degassing experiments of the core samples from H002 (Core UT-GOM2-H002-04CS), including pressure-volume relationships, total methane, and hydrate saturation.

3.5.1 Overview

Two sections cut from UT-GOM2-H002-04CS in PCATS and transferred to small storage vessels were subjected to quantitative degassing. Section UT-GOM2-1-H002-04CS-1 (0 to 26.8 cm depth in core) at the top of the core, and Section 3 (129.5 to 139 cm depth in core) at the bottom of the core including the core catcher. The sections degassed from H002 each contain both lithofacies 2 (high P-wave velocity, low density) and lithofacies 3 (low P-wave velocity, high density (see Section 3.4 Physical Properties and Core Transfer and Section 3.6 Lithostratigraphy).

Hole	Core	Section	Depth in core - top (cm)	Depth in core - bottom (cm)	Depth - top (mbsf)	Depth - bottom (mbsf)	Length (cm)	Section volume (L)	Lithofacies	Total methane (L)	Hydrate saturation (%)	Degassing duration (hr)
H002	04CS	1	0	26.8	418.49	418.76	26.8	0.54	2 and 3	23.56	66	71.5
H002	04CS	3	129.5	139	419.79	419.88	10.0	0.19	2 and 3	11.24	87	27.1

Table 3.5.1 UT-GOM2-1-H002-4CS quantitatively degassed core section properties. Lithofacies, total gas evolved and average hydrate saturation are listed

The length of sections degassed ranged from 10.0 to 26.8 cm and the volume of gas produced ranged from 11.24 to 23.56 L (Table 3.5.2). Average hydrate saturations of each section were calculated based on volume estimates from the length and diameter of each core section and an assumed porosity of 0.4, with the calculated saturations estimated at 66 to 87% (Table 3.5.1 and Figure 3.5.1; Also see Methods Section 2.5 Quantitative Degassing).

All 15 gas samples collected during degassing have >92.4% methane by volume of total gas and less than 7.6 % nitrogen and oxygen contamination (see Chapter 4.0, Section 4.7 Geochemistry and Microbiology). Quantifiable ethane (140 to 177 ppmv) and detectable propane was also present in the composition of gases evolved from the degassing of the two core sections.

			Hydrate saturation	
Lithofacies	# of Cores	Length range	Range	Mean
Multiple/uncertain	2	10 - 26.8	66 - 87	76.5

Table 3.5.2 UT-GOM2-1-H002-4CS total gas released and average hydrate saturation.

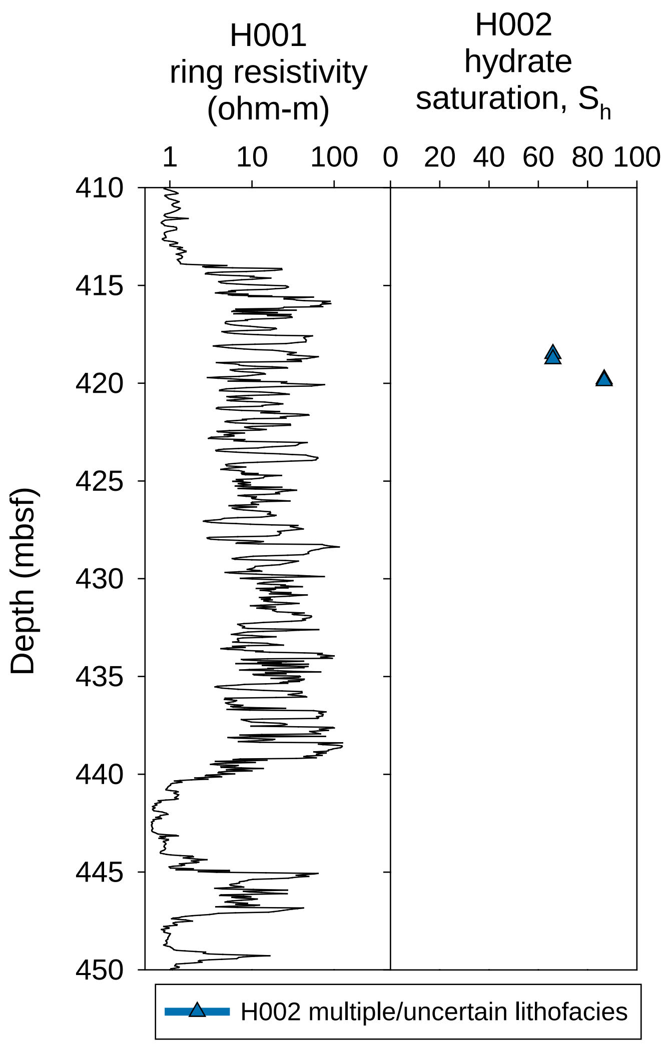

Figure 3.5.1 Hydrate saturation with depth versus H001 LWD resistivity. All H002 Quantitative Degassing data can be found in the expedition data directory under H002 / Quantitative Degassing.

3.5.2 Test Results

UT-GOM2-H002-04CS-1

Multiple lithofacies are present in UT-GOM2-H002-04CS-1 and released a total of 23.56 L of methane (Figure 3.5.2) from a 27 cm section from the top of the core. Nine gas samples were collected and analyzed indicating the hydrate gas is composed of 93 to 98.5% methane with 1.5 to 7.0% nitrogen and oxygen contamination (see Section 3.7 Geochemistry and Microbiology). An additional seven gas samples were collected in copper tubes and four gas samples in stainless steel gas canisters for additional shore-based analysis. Rebounds in pressure after fluid release began at approximately 7.4 MPa indicating hydrate dissociation had initiated. Based on the assumptions described in the methods chapter, the average hydrate saturation was calculated to be 66%. This section was degassed over a period of 71.5 hr.

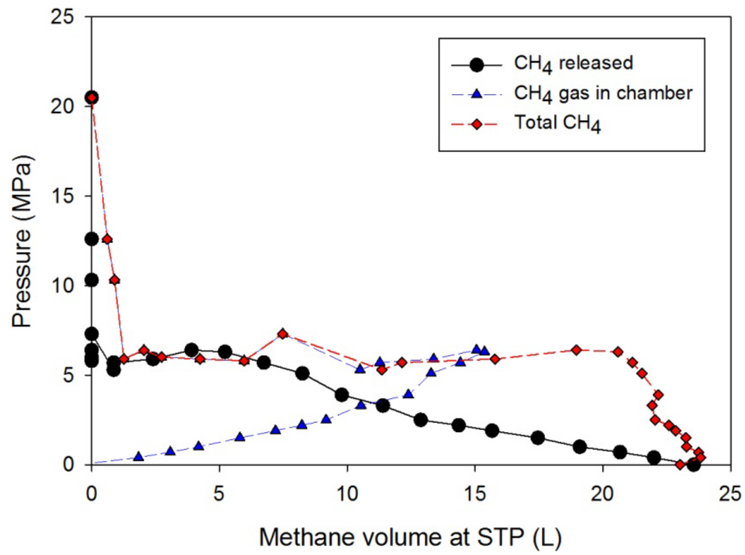

Figure 3.5.2 UT-GOM2-1-04CS-1 pressure versus cumulative volume released. All H002 Quantitative Degassing data can be found in the expedition data directory under H002 / Quantitative Degassing.

UT-GOM2-H002-04CS-3

Multiple/uncertain lithofacies are present in UT-GOM2-H002-04CS-3 and released a total of 11.24 L of methane (Figure 3.5.3) from a 9.5 cm long section from the bottom of the core, including the core catcher. Five gas samples were collected and analyzed indicating the hydrate gas is composed of 92.4 to 98.0% methane with 1.5 to 7.6% nitrogen and oxygen contamination with 2.0 to 7.6% nitrogen and oxygen contamination (see 3.7 Geochemistry and Microbiology). An additional three gas samples were collected in copper tubes for further shore-based analysis. Hydrate dissociation was observed starting at 7.8 MPa as indicated by rebounds in pressure after each fluid release. Based on the assumptions described in the methods chapter, the average hydrate saturation was calculated to be 87%. This section was degassed over a period of 27.1 hr.

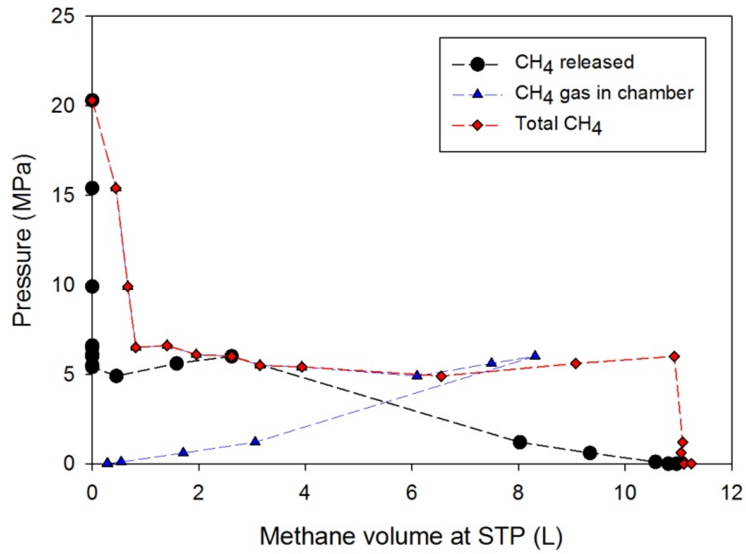

Figure 3.5.3 UT-GOM2-1-04CS-3 Pressure versus cumulative volume released. All H002 Quantitative Degassing data can be found in the expedition data directory under H002 / Quantitative Degassing.

3.6. Lithostratigraphy

This section of the expedition report describes the Lithostratigraphic Units and lithofacies observed in H002. The results of visual core description, smear slide description, laser particle size analysis, and minerology are reported. The recovered strata is categorized in one Lithostratigraphic Unit (Unit II) that is composed of smaller-scale lithofacies. These lithofacies are defined by characteristics described below (Table 3.6.1).

		Lithostratigraphic Unit I	Lithostratigraphic Unit II	
		Lithofacies 1	Lithofacies 2	Lithofacies 3
PCATS physical properties analysis	Density	~2.0 g/cm3	~1.9 g/cm3	2.0-2.1 g/cm3
	P-wave velocity	1700 m/s	2500-3250 m/s	1700-2000 m/s
	X-ray Ct scan	Dark, with cm-scale bedding and steeply dipping fractures.	Light, with ripple-laminated sets up to 2 cm thick.	Dark and massive, with some lighter layers. No crossbedding.
Laser-particle size analysis	Dominant lithology	silty clay	sandy silt	clayey silt with sand

Table 3.6.1 Defining characteristics of the lithologic units within the recovered H002 pressure core. Smear slide and visual descriptions are not included due to the effects of depressurization obscuring the lithofacies as defined by PCATS physical properties measured while under pressure.

3.6.1 Lithostratigraphic Units

Two Lithostratigraphic Units were recognized at this location from the original H001 LWD data acquired by the Chevron JIP (Boswell et al., 2012; Collett et al., 2010). As shown in Figure 3.6.1, Lithostratigraphic Unit I extends from the seafloor to ~391 mbsf, had a low gamma ray value and is interpreted to be hemipelagic mud (upper grey zone). H002 was drilled to 433 mbsf, with 3 m pressure coring runs from 409-433 mbsf. Due to the depth that coring was initiated, only one lithostratigraphic unit (Lithostratigraphic Unit II) was identified within H002. This unit is composed of smaller, repeating lithofacies described below. The shallower Lithostratigraphic Unit I, which was cored in Hole GC 955 H005, was not investigated within this hole (See Chapter 4, Section 4.6 Lithostratigraphy for information on Lithostratigraphic Unit I).

Lithostratigraphic Unit II

Cores UT-GOM2-1-H002-01CS through UT-GOM2-1-H002-08CS
8062-8142 fbrf (409 – 430 mbsf)

Lithostratigraphic Unit II is captured by UT-GOM2-1-H002-01CS through UT-GOM2-1-H002-08CS, from depths of 8062-8142 fbrf (409 – 430 mbsf). Lithostratigraphic Unit II contains the main hydrate reservoir within the study area.

Lithofacies

Within the one pressurized core of Lithostratigraphic Unit II (UT-GOM2-1-H002-04CS), two distinct, repeating facies of varying thickness were identified by relative differences of gamma density, P-wave velocity, and X-ray imaging. Grain size analyses distinguished these facies by sand-silt-mud fraction. These lithofacies within Lithostratigraphic Unit II have been termed lithofacies 2 and lithofacies 3. Lithofacies 2 was the dominant facies in Core UT-GOM2-1-H002-04CS.

Lithofacies 2

Lithofacies 2 is interspersed throughout UT-GOM2-1-H002-4CS (Figure 3.6.1). This unit is composed of low density (2.05-2.1 g/cc) and high velocity (3000-3250 m/s) beds. Rippled lamination and/or cross-lamination can be observed in X-ray images (Figure 3.6.1). Individual sets of climbing ripple lamination measure up to 1.5 cm in relief. Larger sets feature convex-up cross-stratification, while smaller sets feature parallel cross-stratification. Planar lamination, with individual laminae measuring 0.1-2 cm in thickness is also present. Contacts between planar laminae vary between sharp and gradational. Truncation surfaces between cross-stratified sets and planar laminae are sharp. Results from initial laser diffraction grain size analyses are shown in Table 3.6.2. The mean grain size (d 0.5) of lithofacies 2 is 49.7 um (Figure 3.6.2 and Figure 3.6.5). No signs of bioturbation are observed within lithofacies 2.

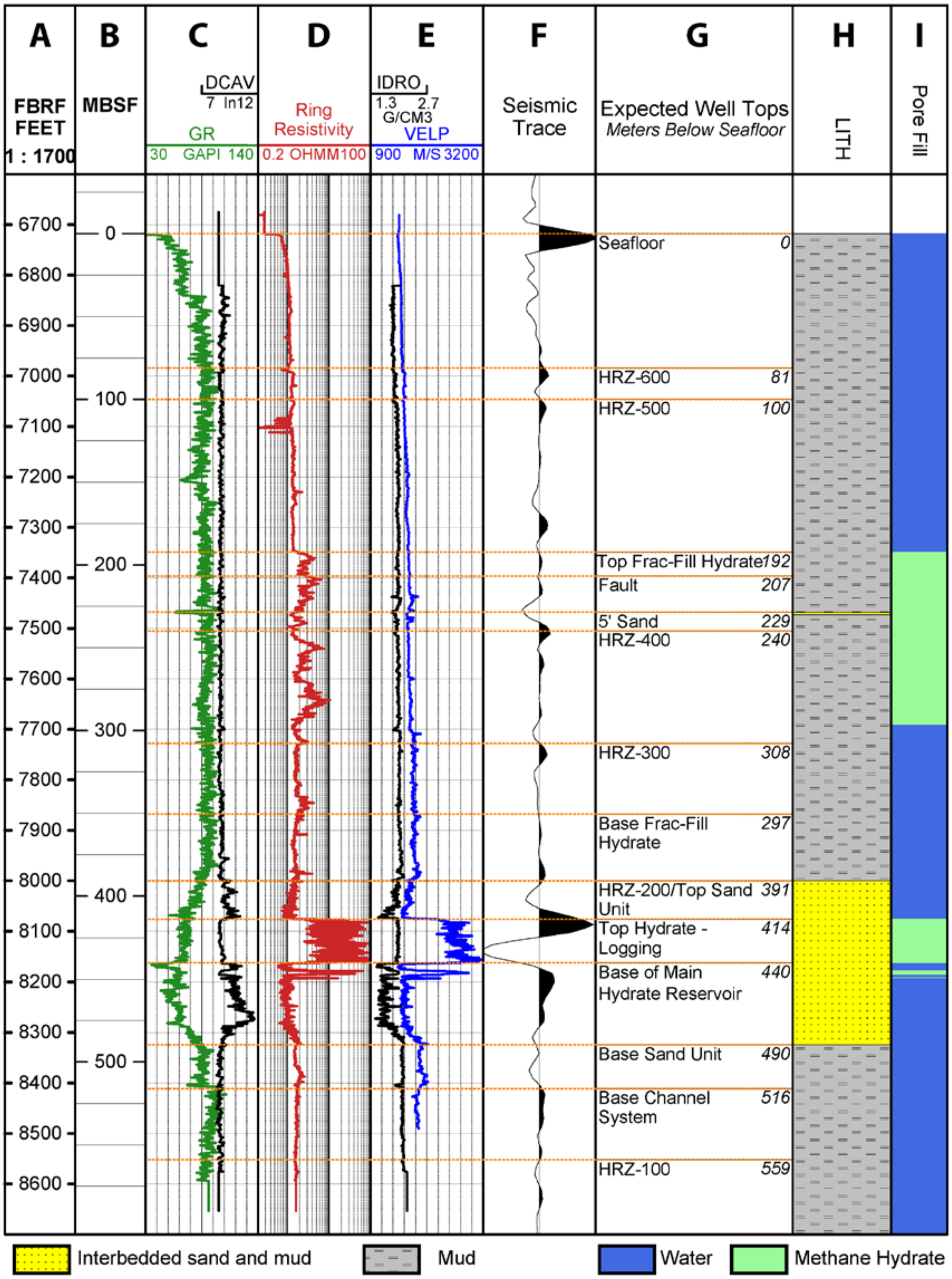

Figure 3.6.1 H001 interpreted stratigraphic surfaces, Lithology, and Pore Fill. Columns C, D, and E illustrate H001 LWD data. GR-Gamma Ray, DCAV-calipers, IDRHO-bulk density, VELP-compressional velocity. F) Seismic trace at the GC 955 location (courtesy of Western Geco). G) Interpreted stratigraphic surfaces. H) Interpreted Lithology. I) Pore Fill documents whether the rock is 100% water saturated (blue) or contains hydrate (green). H001 results have been discussed in detail (Boswell et al., 2012; Collett and Boswell, 2012; Collett et al., 2010).

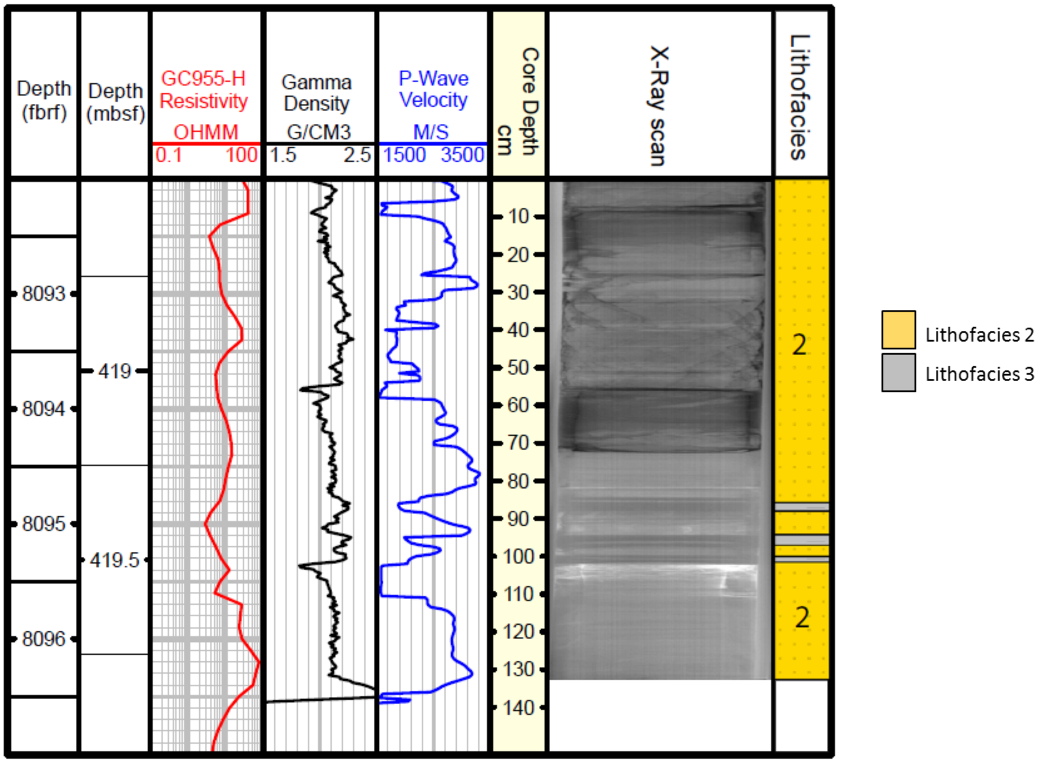

Figure 3.6.2 UT-GOM2-1-H002-4CS log and Lithofacies identification versus H001 LWD resistivity. UT-GOM2-H002-4CS is within Lithostratigraphic Unit II. All H002 Physical property and CT data can be found in the expedition data directory under H002 / Physical Properties.

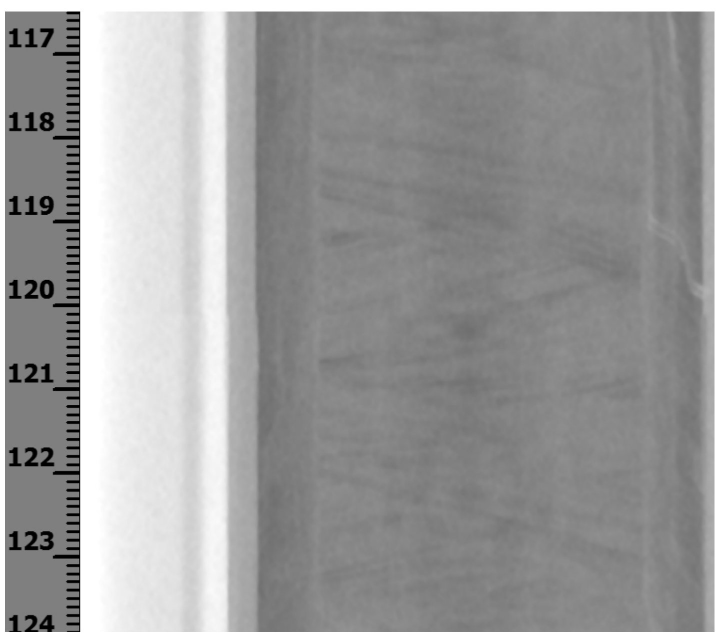

Figure 3.6.3 UT-GOM2-1-H002-4CS wispy, mm-scale, convex-up ripple lamination within Lithofacies 2. All H002 Physical property and CT data can be found in the expedition data directory under H002 / Physical Properties.

Lithofacies 3

Lithofacies 3 is interbedded with lithofacies 2 (Figure 3.6.4). This lithofacies is composed of high density (2.2-2.3 g/cc) and low velocity (~1700 m/s) beds. In X-ray images, lithofacies 3 is generally massive and more deformed than lithofacies 2 (Figure 3.6.1). There is no ripple lamination within lithofacies 3. Lithofacies 3 is dominated by dark, higher density layers several centimeters thick with thin, mm-scale laminations of lighter, less dense material. No signs of bioturbation are observed within Lithofacies 3. No samples of lithofacies 3 from H002 have been analyzed for grain size.

Visual Descriptions

The sediments in the depressurized pressure cores are dominated by silt beds with occasional silty clay intervals. Descriptions of split depressurized cores UT-GOM2-1-H002-01CS to -03CS, and -05CS to -08CS show interbedded silt and clay beds (Figure 3.6.3) ranging from thin laminations (mm-scale) to medium beds (tens of cm). Some sections contained bubbles, which record the depressurization process (Figure below). The silt beds were clean, unconsolidated, and uniform in texture (see sand-silt-clay estimates) and composition. The color of the sediments varies from olive gray to light olive gray (5Y 3/2 to 5Y 5/2 on the Munsell Soil Color Chart (Munsell Color Company, 1994)). Cross-laminations and rip up clasts were observed in many intervals.

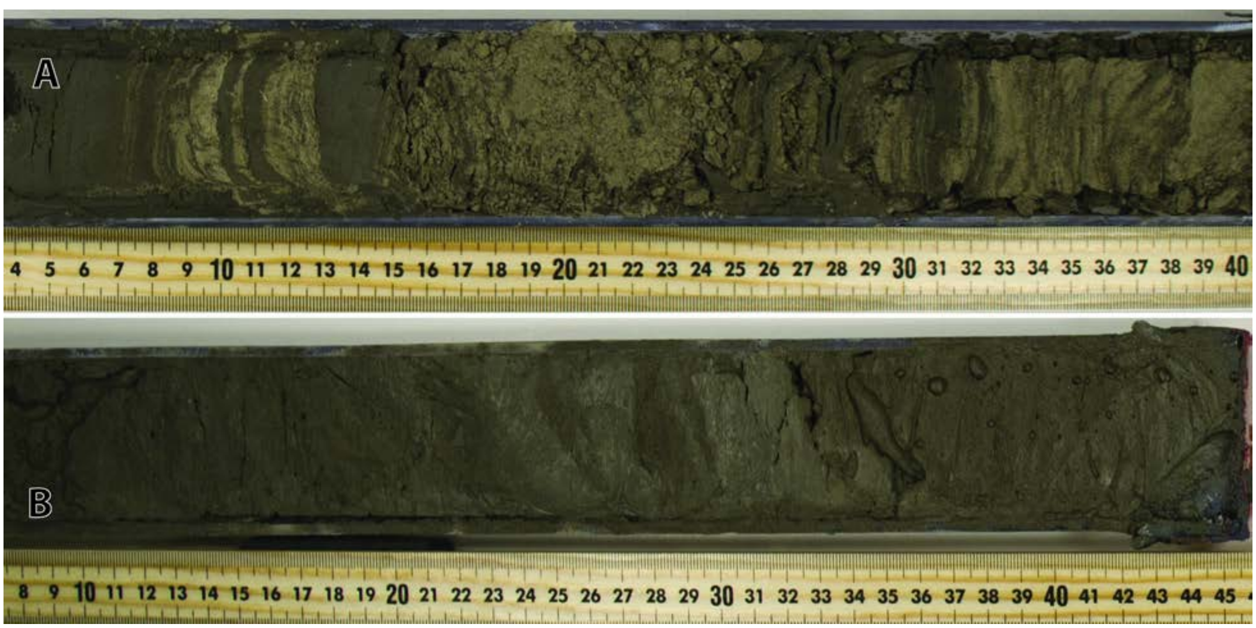

Figure 3.6.4 H002 depressurized core photos. A. Interbedded silt and clay layers within Core 8CS-4. B. Clay-dominated section of 2CS-2, with depressurization bubbles at 34-45 cm. All H002 Core Photos can be found in the expedition data directory under H002 / Lithostratigraphy / Core Photos.

Smear Slide Analysis

Based on smear slide observations, grains in the silt-dominated samples were dominated by quartz (~50%), 3 types of feldspar (microcline>plagioclase>K-spar) (5%), and notable amphibole (up to 3%)

(Figure 3.6.4). Opaque and heavy minerals such as zircon were present in trace amounts. Volcanic glass and plant debris are rare, but observed in some samples. A significant fraction of the silt (20-50%) is rock fragments that are dominated by detrital carbonate and igneous/volcanic lithics, with occasional chert grains (Figure 3.6.4). Slightly subrounded dolomite rhombs were observed in trace amounts. Trace foraminifera were present, often containing framboidal pyrite. Mineral fragments were notably angular compared to rock fragments that were subrounded.

The sediments in the clay intervals are dominated by clay sized mineral (75-95%) with rock fragments and with a notable lack of biogenic grains. Calcareous nannofossils are present only in trace amounts in most samples and foraminifera were not observed (Figure 3.6.4). Mineral grains visible in the silt fraction (up to 25%), were dominated by quartz (up to 12%), amphibole (up to 3%), microcline and plagioclase (up to 1%), and opaque minerals (up to 1%). Rock fragments (up to 10%) visible in the silt fraction were dominated by detrital carbonates with only trace chert and igneous lithics. Slightly subrounded dolomite rhombs were observed in trace amounts.

Physical property scans from PCATS confirm the interbedded nature and highlight two lithofacies that repeat in variable thickness and frequency throughout the unit (Chapter 4, Figure 4.6.5).

Core-section	**Depth in section (cm)**	**Depth (mbsf)**	**Visual description**
01CS-1	38	409.73	Silt
02CS-2	13	412.97	Silt
02CS-3	61	414.25	Clay
02CS-3	95	414.59	Silt
02CS-4	75	415.39	Clay
02CS-4	81	415.45	Silt
05CS-1	30	421.81	Silt
05CS-1	75	422.29	Clay
06CS-1	10	424.69	Silt
06CS-4	16	426.94	Silt
06CS-5	7	427.85	Silt
08CS-2	57	431.82	Clay
08CS-5	27	434.1	Clay
08CS-5	32.5	434.155	Silt

Table 3.6.2 Smear slide samples described from H002. Samples collected from clay and silt intervals observed during visual description. All H002 Smear Slide data can be found in the expedition data directory under H002 / Lithostratigraphy / Smear Slides.

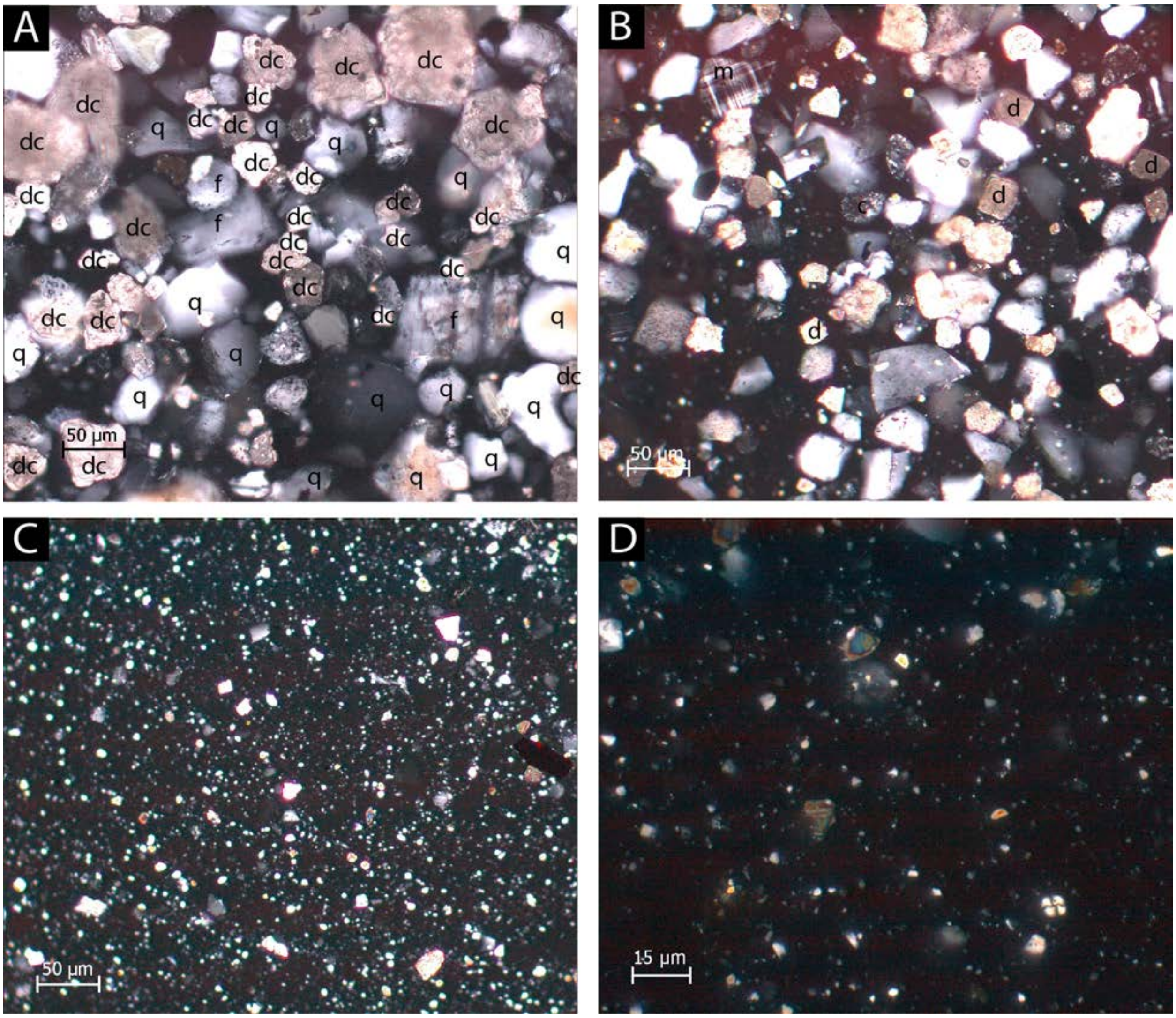

Figure 3.6.5 Photomicrographs of smear slides from the dominant lithologies observed. Photomicrographs were taken using cross-polarized light. (A) Section H002-2CS-3, 125-225 cm, 95 cm down section in silt bed-200x magnification. Notice the abundance subrounded detrital carbonate (dc) grains among angular quarts (q) and feldspar (f) grains. (B) Section H002-6CS-1, 0-19 cm, 10 cm down section in silt bed-200x magnification. Note the similar composition, with a microcline feldspar (m), dolomite rhombs (d), and chert lithic (c) grains labeled. (C) Section H002-2CS-3, 125-225 cm, 61 cm down section in clay bed-200x magnification. Note the dominance of lithogenic materials with the exception of the larger brown grain of organic matter on the right of the image. The composition of the visible grains in all the clay beds was similar to the silt beds. Biogenic grains were observed only in trace amounts in the clay beds. (D) Section H002-2CS-4m 225-317 cm, 75 cm down section in clay bed-630x magnification. Again, note the dominance of lithogenic materials in this clay sample viewed at higher magnification. A single calcareous nannofossil is present here as the small fan 4 blade-shaped pattern in the lower right of the image. All H002 Smear Slide data can be found in the expedition data directory under H002 / Lithostratigraphy / Smear Slides.

3.6.2 Laser diffraction particle size analysis

In Port Fourchon, seven samples were analyzed with a Malvern Mastersizer for particle size distribution (Table 3.6.2). All of these samples are from sediments that were slowly depressurized during degassing experiments either on-board or in Port Fourchon (see 3.5 Quantitative Degassing). Four of the samples were from intact, depressurized core in the liner, while three were from disaggregated sediments that fell from the core liner or core catcher after depressurization and were collected in bags. The length of sampling intervals ranges from 9.9 - 42 cm sections of core. In some cases (H002 4CS-1A and H002 4CS-1B, H002 4CS-3A and H002 4CS-3B), multiple samples were analyzed from the same core section.

Sample Name	Core Depth (cm)	Source	Facies	% Sand > 61.58 µm	% Silt 1.93-61.58 µm	% Clay < 1.93 µm	d (0.1)	d (0.5)	d (0.9)
H002 4CS-1A	0-26.8	Core	2	32.80	60.45	6.76	3.19	40.85	86.71
H002 4CS-1B	0-26.8	Core	2	38.61	56.45	4.94	6.14	46.34	91.09
H002 4CS-3A	129.5-139	Core	2	49.52	46.86	3.62	17.65	54.71	104.57
H002 4CS-3B	129.5-139	Core	2	52.33	45.23	2.44	24.79	56.87	106.36
H002 1CS-1	37-79	Disaggregated	unknown	9.29	68.13	22.43	0.95	5.94	53.08
H002 5CS-CC	core catcher	Disaggregated	unknown	40.66	54.50	4.85	5.93	47.58	95.30
H002 8CS-CC	core catcher	Disaggregated	unknown	47.86	49.18	2.95	21.76	53.55	97.90
Facies 2 Average			2	43.31	52.24	4.44	12.94	49.70	97.18

Table 3.6.3 Initial laser diffraction particle size analysis. All H002 Laser Diffraction Particle size data can be found in the expedition data directory under H002 / Lithostratigraphy / Grain size. See Chapter 2 Methods, Section 2.6 Lithostratigraphy for % sand/silt/clay calculations.

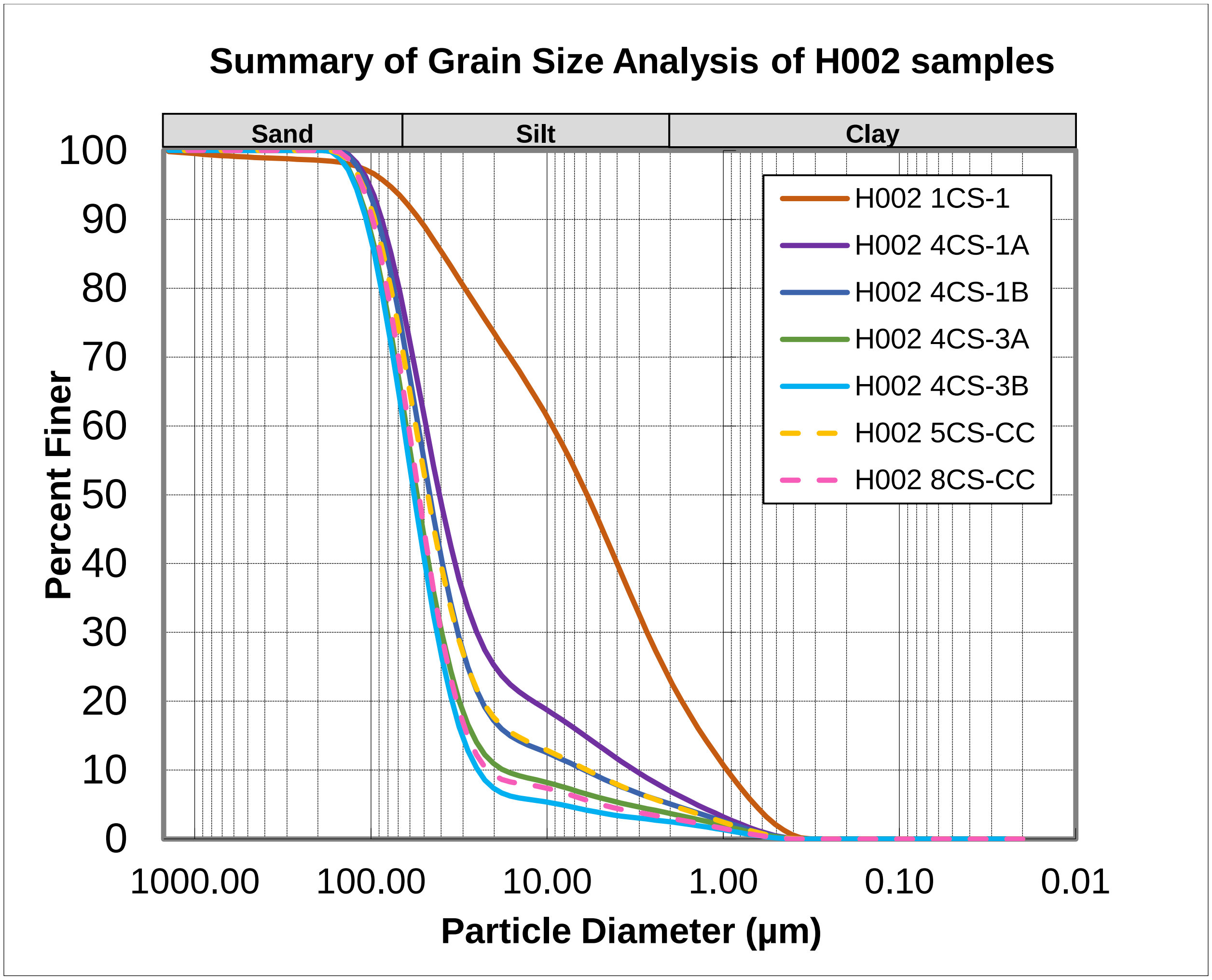

Figure 3.6.6 H002 average grain size distribution of Lithofacies 2. All H002 Laser Diffraction Particle size data can be found in the expedition data directory under H002 / Lithostratigraphy / Grain size.

The grain size distribution from all H002 samples is displayed in Figure 3.6.5. The mean grain size of analyzed sediments ranged from 5.94 to 56.87 µm (Table 3.6.2). Samples H002 4CS-1A, H002 4CS-1B, H002 4CS-3A, and H002 4CS-3B were from lithofacies 2 (Figure 3.6.1). On average, lithofacies 2 is sand-rich, with 44% sand, 3.89% clay, and a median grain size of 50.66 µm.

3.6.3 Mineralogy

Using X-ray diffraction (XRD) the bulk mineralogy of powdered 2 gram subsamples taken from H002 cores that were depressurized and sent to Ohio State were determined. Subsampling took place in silt intervals (likely Lithofacies 2), denoted XRD-S, drilling mud intruded intervals, denoted XRD-M (likely Lithofacies 2). Note that all cores in the initial XRD analysis were drilled with drilling mud, and may contain drilling mud whether identified or not.

XRD-S (Lithofacies 2) initial results show a composition of mainly quartz with minor amounts of albite, dolomite, calcite, muscovite, amphibole, chlorite and microcline (Figure 3.6.7). No specific clay mineralogical analyses (e.g. <2 µm, oriented samples) were performed. The identification of clay minerals from bulk powder XRD is limited due to slight differences in chemistry, polytype, and degree of order, which create many possible permutations of phyllosilicate structures.

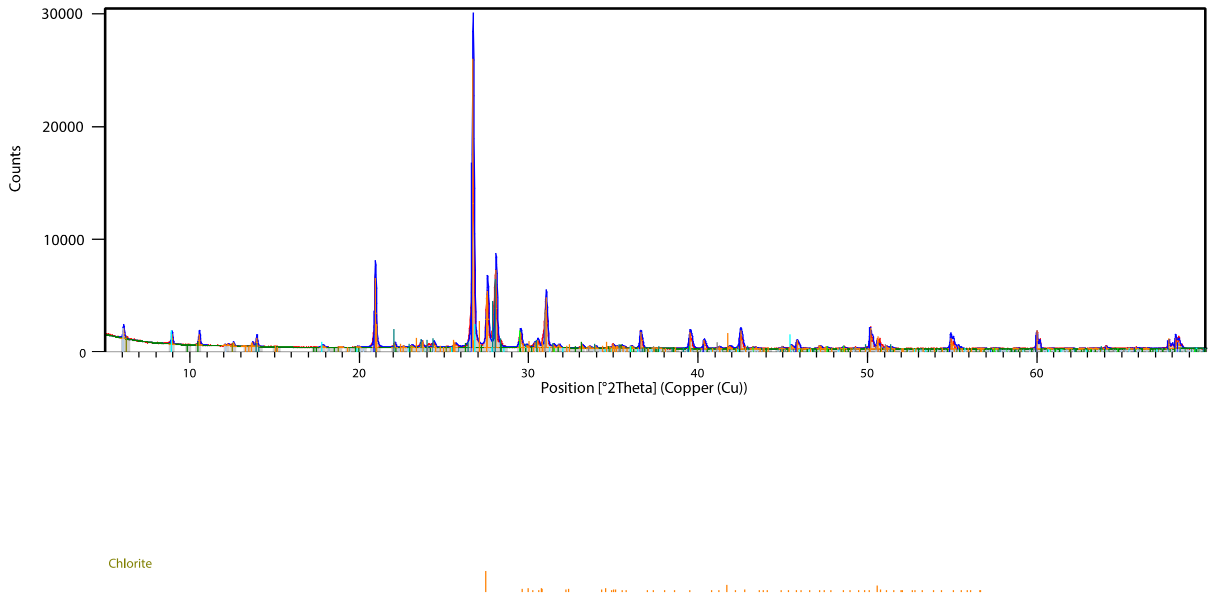

Figure 3.6.7 An example spectra from a subsample from Core H002-3CS-1, which is likely Lithofacies 2. Initial XRD results can be found in the H002 data directory under H002 / Lithostratigraphy / XRD.

Initial results of XRD-M show a similar composition including quartz, albite, amphibole, muscovite, dolomite, and calcite but with the addition of barite (a component used in drilling mud). Further analysis will be conducted in order to identify specific clay minerals, in addition to providing at least semi-quantitative estimates of mineral abundance.

3.6.4 Lithofacies Interpretation

Lithofacies 2 is composed of sandy-silts and silty-sands (Figure 3.6.6 and Figure 3.6.8). These coarse-grained beds were deposited in a high-energy environment. The high P-wave velocity and low density associated with this facies is interpreted to record the presence of methane hydrate, likely occupying and cementing the pore space between the coarse grains. Lithofacies 3 is interpreted to be a finer-grained, lower-energy facies based on its massive nature. The relatively low velocity and high density are interpreted to record lower hydrate saturation.

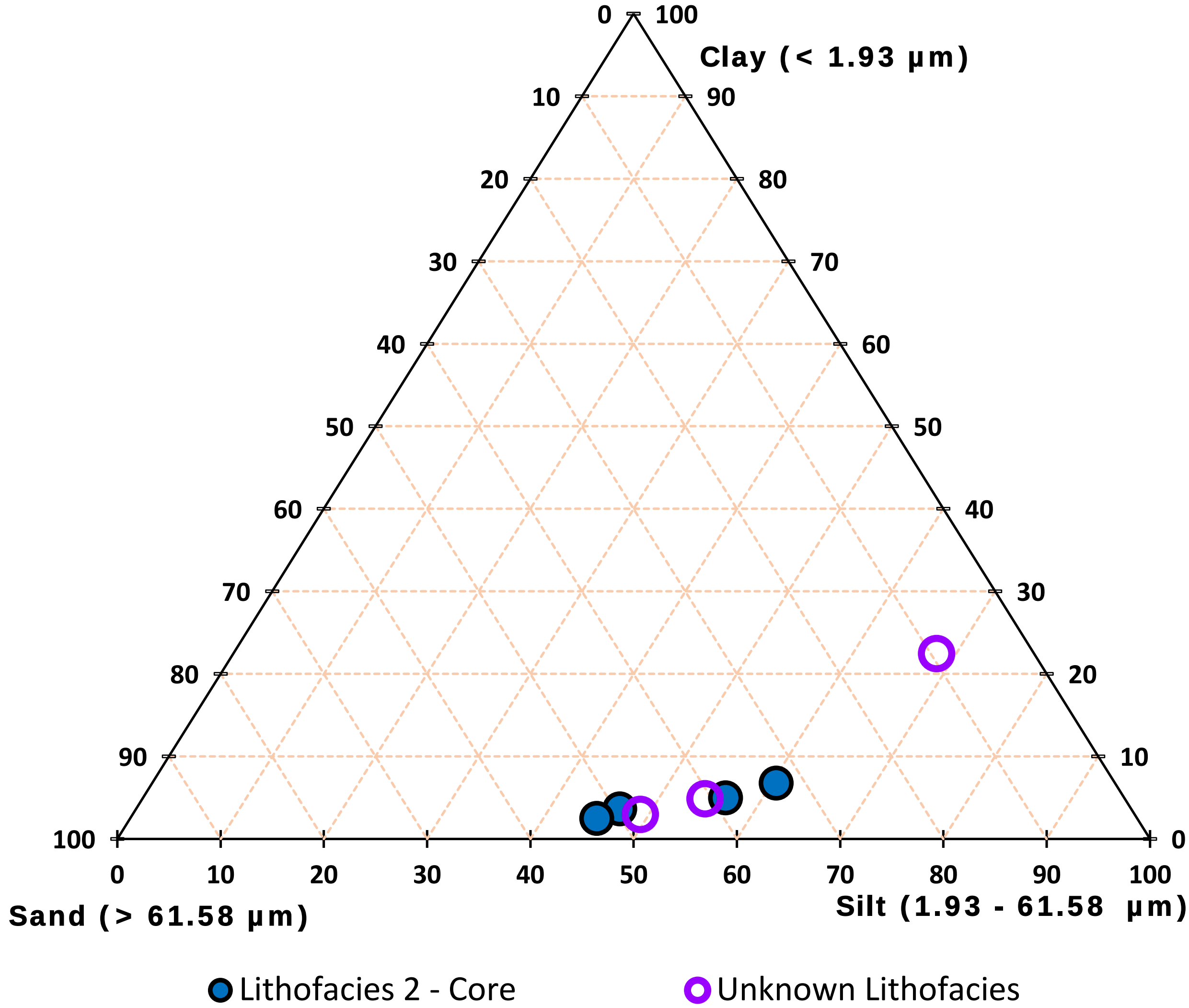

Figure 3.6.8 Ternary diagram of H002 sediments analyzed by laser diffraction. All H002 Laser Diffraction Particle size data can be found in the expedition data directory under H002 / Lithostratigraphy / Grain size.

3.7. Geochemistry and Microbiology

This section reports the analysis of pressure core gas and pore water as sampled from depressurized cores from H002. In addition, the samples collected for microbiological analyses and additional geochemical analyses are documented.

3.7.1 Pressure core gases

Field analyses

Two sections from Core UT-GOM2-1-H002-04CS were degassed onboard (see Section 3.5 Quantitative Degassing). Ten gas samples from section UT-GOM2-1- H002-04CS-1 were analyzed on-board and dockside on the gas chromatograph (Table 3.7.1). The composition of the gases is predominantly methane (93.0 to 98.5 %) with quantifiable ethane (105 to 191 ppmv) and detectable, but not quantifiable propane (Table 3.7.1). These samples contained 0.24 to 1.41% oxygen and 1.22 to 5.79% nitrogen likely from atmospheric gas in the tool (Table 3.7.1). Five samples from section UT-GOM2-1-H002-04CS-3 were run on the gas chromatograph (Table 3.7.1). The composition of the gases is predominantly methane (92.4 to 98.0% of total gas) with quantifiable ethane (140 to 177 ppmv) and detectable propane. These samples contained 0.28 to 1.32% oxygen and 1.73 to 2.63% nitrogen likely from atmospheric gas in the PCTB. The average methane to ethane ratio (C1/C2) is 6084 from UT-GOM2-1- H002-04CS-1 and 6026 from UT-GOM2-1- H002-04CS-3 (Figure 3.7.1).

Hole	Core	Section	Depth top	Depth bottom	Sample	Syringe	Oxygen	Nitrogen	Methane	Ethane	Propane
			mbsf	mbsf			%	%	%	ppm	presence
H002	04CS	1	418.49	418.76	1	1G	1.16	5.79	93.0	105	x
H002	04CS	1	418.49	418.76	2	2G	0.43	2.42	97.1	121	-
H002	04CS	1	418.49	418.76	3	3G	0.43	2.19	97.4	157	-
H002	04CS	1	418.49	418.76	4	4G	0.56	2.23	97.2	172	-
H002	04CS	1	418.49	418.76	5	5G	0.33	1.60	98.1	178	-
H002	04CS	1	418.49	418.76	6	6G	0.29	1.42	98.3	178	-
H002	04CS	1	418.49	418.76	7	7G	0.32	1.50	98.2	181	-
H002	04CS	1	418.49	418.76	8	8G	0.27	1.37	98.3	189	-
H002	04CS	1	418.49	418.76	9	9G	0.29	1.34	98.4	185	-
H002	04CS	1	418.49	418.76	10	10G	0.24	1.22	98.5	191	-
H002	04CS	3	419.79	419.88	1	1Y	1.32	6.27	92.4	140	x
H002	04CS	3	419.79	419.88	2	2Y	0.30	1.95	97.7	157	x
H002	04CS	3	419.79	419.88	3	3Y	0.28	1.73	98.0	158	-
H002	04CS	3	419.79	419.88	4	4Y	0.32	2.22	97.4	177	-
H002	04CS	3	419.79	419.88	5	5Y	0.36	2.63	97.0	173	-

Table 3.7.1 UT-GOM2-1-H002-04CS gas analyses. All H002 Gas Analysis data can be found in the expedition data directory under H002 / Geochemistry / Gas.

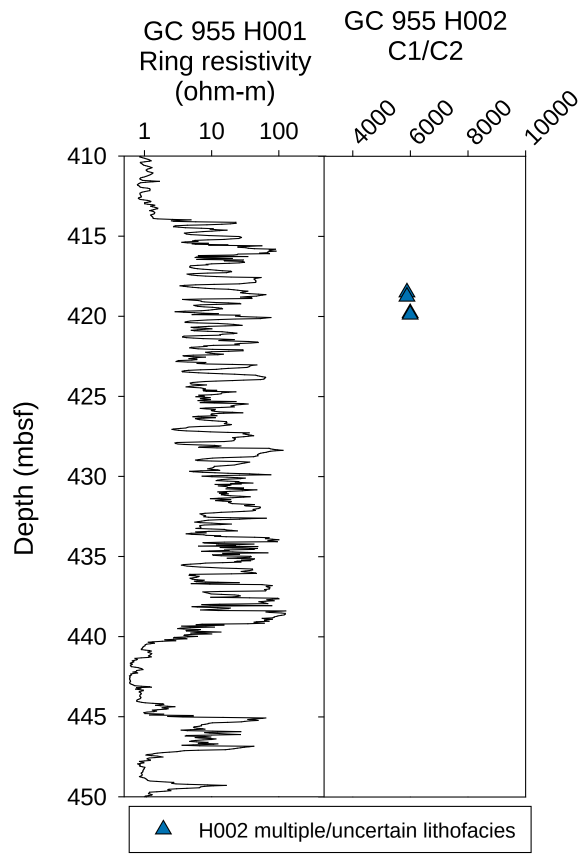

Figure 3.7.1 H002 Methane to ethane ratio (C1/C2) versus H001 LWD resistivity. See 3.6 Lithostratigraphy for a description of lithofacies. All H002 Gas Analysis data can be found in the expedition data directory under H002 / Geochemistry / Gas.

Field sampling

Nine gas samples were collected from section UT-GOM2-1-H002-04CS-1 and three samples were collected from UT-GOM2-1-04CS-3. These were stored in clamped copper tubes for shore-based analysis (Table 3.7.2). An additional subset of 4 samples was collected from UT-GOM2-1-H002-04CS-1 and stored in stainless steel gas cylinders for additional shore-based analyses.

Hole	Core	Section	Depth top (mbsf)	Depth bottom (mbsf)	Date	Time	Degassing P (bar)	Type	Sample #	Chamber
H002	04CS	3	419.79	419.88	5/16/2017	13:33	60	Copper	1	bubble
H002	04CS	3	419.79	419.88	5/16/2017	16:47	60 - 13	Copper	2	gas
H002	04CS	3	419.79	419.88	5/16/2017	20:14	13 - 6	Copper	3	bubble
H002	04CS	1	418.49	418.7584	5/17/2017	7:55	74	Copper	4	bubble
H002	04CS	1	418.49	418.7584	5/17/2017	7:55	-	Copper	5	-
H002	04CS	1	418.49	418.7584	5/17/2017	16:32	76-60	Copper	6	bubble
H002	04CS	1	418.49	418.7584	5/17/2017	16:32	76-60	Steel	A	bubble
H002	04CS	1	418.49	418.7584	5/17/2017	22:52	71-64	Copper	7	bubble
H002	04CS	1	418.49	418.7584	5/18/2017	7:18	69-63	Copper	8	bubble
H002	04CS	1	418.49	418.7584	5/18/2017	7:18	69-63	Steel	B	bubble
H002	04CS	1	418.49	418.7584	5/18/2017	17:50	64-57	Copper	9	bubble
H002	04CS	1	418.49	418.7584	5/18/2017	17:50	64-57	Steel	C	bubble
H002	04CS	1	418.49	418.7584	5/18/2017	22:30		Copper	10	bubble
H002	04CS	1	418.49	418.7584	5/18/2017	22:30		Steel	D	bubble
H002	04CS	1	418.49	418.7584	5/19/2017	2:20	7 to 4	Copper	11	bubble
H002	04CS	1	418.49	418.7584	5/19/2017	3:00	4 to 0	Copper	12	bubble

Table 3.7.2 UT-GOM2-1-H002-04CS gas samples collected during degassing. See the expedition data directory under H002 / Curation.

3.7.2 Sedimentary gases

Headspace gas sampling

A total of 7 samples were collected for shore-based headspace gas analysis from cores UT-GOM2-1-H002-01CS, -02CS, -05CS, -06CS, -07CS (Table 3.7.3).

Hole	Core	Section	Interval from (cm)	Interval to (cm)	Depth (mbsf)	Sample type	Date sampled	Time sampled
H002	01CS	1	79	79	410.14	Headspace gas	5/12/2017	13:45
H002	02CS	2	45	45	413.29	Headspace gas	5/12/2017	21:10
H002	02CS	4	93	93	415.57	Headspace gas	5/12/2017	21:10
H002	05CS	1	5	5	421.59	Headspace gas	5/14/2017	0:13
H002	06CS	5	19	19	427.97	Headspace gas	5/14/2017	8:40
H002	08CS	4	37	37	433.4	Headspace gas	5/14/2017	15:45
H002	08CS	1	28	28	430.96	Headspace gas	5/14/2017	17:18
H002	07CS	1	6	6	427.69	Headspace gas	5/14/2017	18:11

Table 3.7.3 H002 Headspace gas samples collected. See the expedition data directory under H002 / Curation.

3.7.3 Pore water

Field sampling

A total of 5 whole round samples (9 to 15 cm length) from cores UT-GOM2-1-H002-01CS, -02CS, -06CS, and -08CS were collected (Table 3.7.4).

Hole	Core	Section	Interval from (cm)	Interval to (cm)	Length (cm)	Depth top (mbsf)	Depth bottom (msbf)	Sample type	Date sampled	Time sampled
H002	01CS	1	5	20	15	409.40	409.55	Pore water	5/12/2017	13:45
H002	02CS	2	45	60	15	413.29	413.44	Pore water	5/12/2017	21:10
H002	06CS	4	72	81	9	427.50	427.59	Pore water	5/14/2017	8:40
H002	08CS	4	25	37	12	433.28	433.40	Pore water	5/14/2017	15:45
H002	08CS	1	31	57	26	430.99	431.25	Pore water	5/14/2017	17:18

Table 3.7.4 H002 Pore water samples collected. See the expedition data directory under H002 / Curation.

Contamination control

A total of 3 drilling fluid samples, timed with the collection of cores UT-GOM2-1-H002-01CS, -04CS, -07CS, at a frequency of approximately one sample per day during drilling (Table 3.7.5) were collected. A PCATS water sample associated with core 4CS was collected.

Hole	Core	Sample type	Date sampled	Time sampled
H002	01CS	Drilling fluid	5/12/2017	8:26
H002	04CS	Drilling fluid	5/13/2017	7:26
H002	07CS	Drilling fluid	5/14/2017	9:26
H002	04CS	PCATS water	5/13/2017	21:28

Table 3.7.5 H002 Drilling fluid samples collected. See the expedition data directory under H002 / Curation.

Analytical Results

Salinity in depressurized cores from H002 varies from 3 to 19 practical salinity units (psu) (Table 3.7.6). All of these samples were recovered from pressure cores that did not maintain pressure to the surface (see 3.3 Pressure Coring). The salinity in all samples is lower than average seawater salinity (35 psu)

(Figure 3.7.2). Sulfate concentrations ranged from 5.37 to 9.11 mM, indicating that each of the whole rounds were contaminated by drilling fluid during coring. All pore water geochemical data will be corrected for drilling fluid contamination based on the sulfate data and the drilling fluid composition. Due to the moderate drilling fluid contamination of H002 cores, the pore water Cl^- and salinity values reported herein are maximum values. Chloride concentrations range from 150 to 344 mM (26-61% of seawater value), and bromide concentrations range from 224-786 μM. The composition of the drilling fluid used when collecting core 1CS is also shown in Table 3.7.6.

Hole	Core	Section	Interval from (cm)	Interval to (cm)	Length (cm)	Depth top (mbsf)	Depth bottom (msbf)	Recovered volume (mL)	Salinity (psu)	Chloride (titration) (mM)	Chloride (IC) (mM)	Bromide (mM)	Sulfate (mM)	Notes
H002	01CS	1	5	20	15	409.40	409.55	8	8	150	148	0.7	6.7	Sample bag had a leak, likely exposed to O2 during storage. Silt w/interbedded clay
H002	02CS	2	45	60	15	413.29	413.44	1	3	-	-	-	-	Mainly silt
H002	06CS	4	72	81	9	427.50	427.59	2	14	-	279	0.5	5.4	Silt with clay transitions
H002	08CS	4	25	37	12	433.28	433.40	4.5	6	344	350	2.2	9.1	Silt with mm thick clay interbeds
H002	08CS	1	31	57	26	430.99	431.25	11	19	161	163	0.3	5.4	Sample not in core liner, compressed during transit to UW, clay with interbedded silt
H002	01CS	-	-	-	-	-	-	50	-	474	483	-	27.7	Drilling fluid sample

Table 3.7.6 H002 Pore water analysis from depressurized cores. All H002 Pore Water data can be found in the expedition data directory under H002 / Geochemistry / Pore Water.

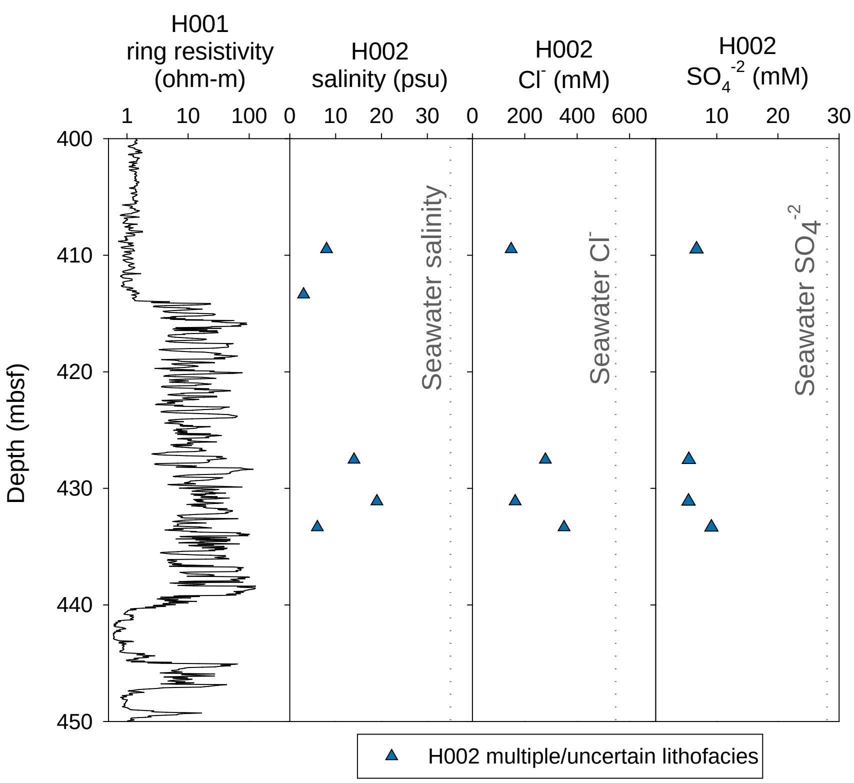

Figure 3.7.2 H002 Down core variation in salinity, chlorinity, and sulfate versus H001 LWD resistivity. Data points are shown with average seawater concentrations. See 3.6 Lithostratigraphy for a description of lithofacies. All H002 Pore Water data can be found in the expedition data directory under H002 / Geochemistry / Pre Water.

3.7.4 Microbiology

Field sampling

A total of 5 whole round samples were collected for microbiology from depressurized cores UT-GOM2-1-H002-01CS, -02CS, -06CS, and -08CS (Table 3.7.7), adjacent to pore water samples. All samples were stored frozen at -20 C for the duration of the on-board and dockside operations.

Hole	Core	Section	Interval from (cm)	Interval to (cm)	Length (cm)	Depth top (mbsf)	Depth bottom (mbsf)	Sample type	Date sampled	Time sampled
H002	01CS	1	20	35	15	409.55	409.7	Microbiology	5/12/2017	13:45
H002	02CS	2	60	75	15	413.44	413.59	Microbiology	5/12/2017	21:10
H002	06CS	4	62	72	10	427.4	427.5	Microbiology	5/14/2017	8:40
H002	08CS	4	9	25	16	433.12	433.28	Microbiology	5/14/2017	15:45
H002	08CS	1	31	57	26	430.99	431.25	Microbiology	5/14/2017	17:18

Table 3.7.7 H002 Whole round samples collected for microbiology. See the expedition data directory under H002 / Curation.

Contamination control

Splits of the same samples collected for characterizing drilling fluid and PCATS contamination of pore waters as described above were frozen for microbiological analysis (Table 3.7.5).

3.8. Wireline Logging

The initial goal of the wireline logging program was to acquire a full suite of key logs over the cored interval in H002. However, because of the limited success of pressure coring in the hole, H002 was not extended beyond the depth of the final pressure core, 8142 fbrf (2481.7 mbrf) (see 3.2 Operations). A consequence of this decision was that the deepest logging depth was above the top of the cored interval. Nonetheless, logging was required by regulation to survey the hole. Because the cored interval was not logged, the decision was made to run only a deviation survey and a minimal logging tool string (gamma ray and resistivity tools) for basic well characterization in H002. These limited logging operations saved rig time for future expedition activities.

3.8.1 Operations

The total depth of H002 was 8142 fbrf (2481.7 mbrf). After retrieval of the final core, the hole was conditioned for logging using 275 bbls of 10.5 ppg mud, and the bit was raised to 7680 fbrf. Following a toolbox safety meeting, preparation of the rig floor started at 19:00 h, 14-May-2017. Rig up of the tool string began at 19:50 h, and at 2010 h, the 17.25 meter long string made of the Enhanced Telemetry Cartridge (EDTC-B), the High Resolution Laterolog Array (HRLA) and the General Purpose Inclinometry Tool (GPIT) tools was assembled and ready to be checked on the rig floor. This tool string was run into the hole at 20:45 h, 14-May-2017.

The tool string was not able to move beyond 8057 fbrf. The hole had either a bridge or 85 ft of fill had accumulated at the bottom. Later, after logging, the drill pipe was lowered to TD, indicating that the obstruction was a bridge that had formed at this depth.

A repeat logging pass (called a repeat pass, because it does not cover the full length of hole) was acquired recorded from 8057–7806 fbrf, followed by a downlog from 7608–8057 fbrf. These two repeat passes confirmed the high quality of log data acquisition. The main pass began at 2300 h from 8057 fbrf and concluded at 2345 h. The tool string was then returned to the surface and rigged down; the rig floor was cleared for other operations at 0150 h, 15-May-2017. A detailed timing of the logging operations in H002 can be found in Table 3.1.1.

The seafloor depth was identified at 6719 fbrf using the gamma ray log.

Operations	Time	Depth (fbrf)	Comments
Rig floor preparation:	1900, 14-May		
Start tool string build up	1950		
Tool string check	2010		Length of tool string: 17.25 m (56.6 ft)
Run into hole	2045	0	
Troubleshooting winch	2145	5235	leaking hydraulic hose replaced at 2200
Slow down before flapper valve	2215	7565	slowing down to 1800 ft/hr to open flapper valve
First try opening flapper valve	2219	7695	valve did not open at first try
flapper valve opened	2225	7697	valve opened at speed of 3000 ft/hr
Tag bottom	2235	8057	bridge 97 ft above TD
Start pass1	2240	8057	pass 1 is a "repeat" pass recorded at 1800 ft/hr
End of pass 1	2250	7806	end of pass 1
Start of downlog	2250	7806	downlog recorded at 1800 ft/h
End of downlog	2300	8057	obstruction tagged at same depth as first pass
Start of pass 2	2300	8057	main pass, recorded at 1800 ft/hr
Entering drill string	2312	7755	top of tool through valve; slow down (1200ft/h) to enter
String inside pipe	2314	7695	GPIT switched to proper mode for survey in pipe
Increas speed	2330	7425	speed increased to 2200 ft/h
Tools across seafloor	2342	6719	Seafloor seen in gamma ray log
End of main pass	2345	6655	speed up to 6000 ft/h
Tools at surface	0059, 15-May	0	
Start rigging down tools	0055		
Tool string rigged down	0115		
Wireline out of top drive	0135		
Rig floor clear of logging	0150		

Table 3.8.1 Details of H002 Wireline Logging Operations.

3.8.2 Logging Results and Quality

The primary purpose of the limited logging operations in H002 was to record a survey of the deviation of the borehole. The GPIT tool utilizes a three-axis inclinometer, or accelerometer, and a three-axis magnetometer to define the tool axis with respect to the earth's gravity and magnetic field. Part of the procedure required to do this is to measure the spinning of the tool in the borehole and apply an algorithm that compensates for it. Also, to account for the influence of the pipe on the magnetic field measurement, a degraded algorithm was applied, which uses only the accelerometer once the tool string was inside the pipe. The results of the borehole deviation survey are shown in Figure 3.8.1. The well deviated slightly to the southwest, with a total lateral offset of about 10 ft at the bottom of the logged interval. The apparent bend in the well trajectory at ~7700 fbrf (~300 mbsf) may associated with the tool recording inside of the drill pipe with degraded resolution, and thus may, not accurately the apparent inclination of the well over this interval.

The well logs recorded during the main pass in H002 are displayed in Figure 3.8.2 and Figure 3.8.3. As shown in these figures, the data recorded over the three recording passes (repeat, downlog and main) are compared and agree well, overall. The three resistivity curves with increasing depth of penetration (RLA1-RLA5) and the main and repeat passes of the resistivity logs nearly overlay, suggesting that the borehole was in good condition during logging (Figure 3.8.2 and Figure 3.8.3). Also, Figure 3.8.2 illustrates the bridge encountered at the bottom of the hole. Furthermore, the overall consistency between the logs measured in H002 and the open-hole logs recorded in H001 indicate the high quality of these data (Figure 3.8.4). One noticeable difference between the log responses in these wells, however, is over the interval from ~7830-7865 fbrf (~338-350 mbsf), where high-angle, hydrate-filled fractures have been previously inferred to be present and may cause large lateral heterogeneity over short distances.

Comparison of the gamma ray log recorded through the pipe in H002 with the open-hole logs recorded in H001 during JIP Leg 2 also indicates overall agreement (Figure 3.8.5). Despite the attenuating influence of the pipe, the pipe junctions, and the bottom hole assembly, the gamma ray logs in both holes follow similar trends. A thin, low-gamma-ray layer at ~7454 fbrf (230 mbsf) observed immediately above the drill pipe was used define the top of Unit 2, as previously identified using the open hole logs in H001 (Guerin et al., 2012). This layer may correspond to a thin sand unit.

There are also important differences between the gamma ray in H002 and the open-hole gamma ray logs recorded in H001 during JIP Leg 2. For example, H002 shows a discrete coarsing-upwards interval from 385-390 mbsf surrounded by high-gamma-ray (clay-rich) sediment (Figure 3.8.4). In contrast, the gamma ray in H001 shows a fining upwards sequence that persists throughout the interval cored in H002 to ~382 mbsf. This observation suggests that the reservoir layers may not be laterally continuous even over the small distances between H001 and H002.

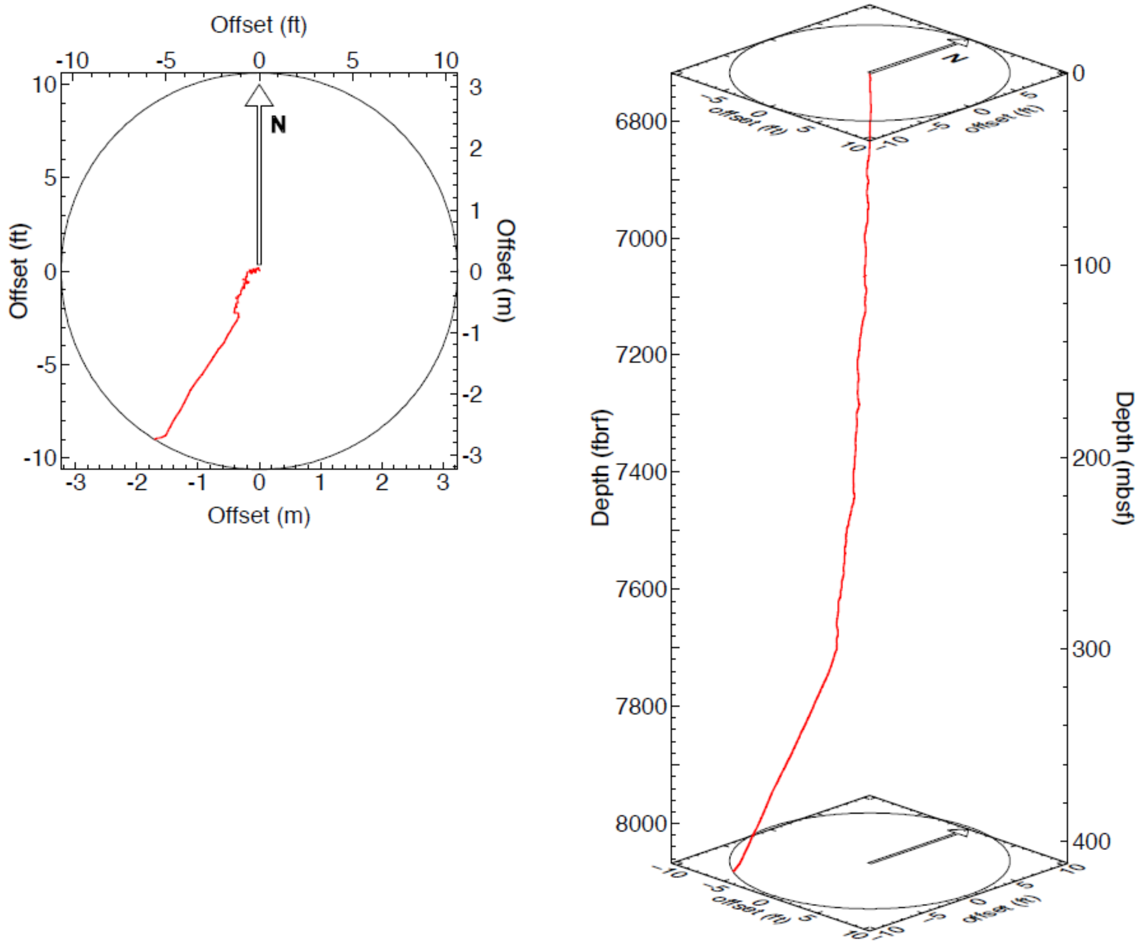

Figure 3.8.1 H002 Borehole deviation survey. All H002 survey data can be found in the expedition data directory under H002 / Wireline Logging.

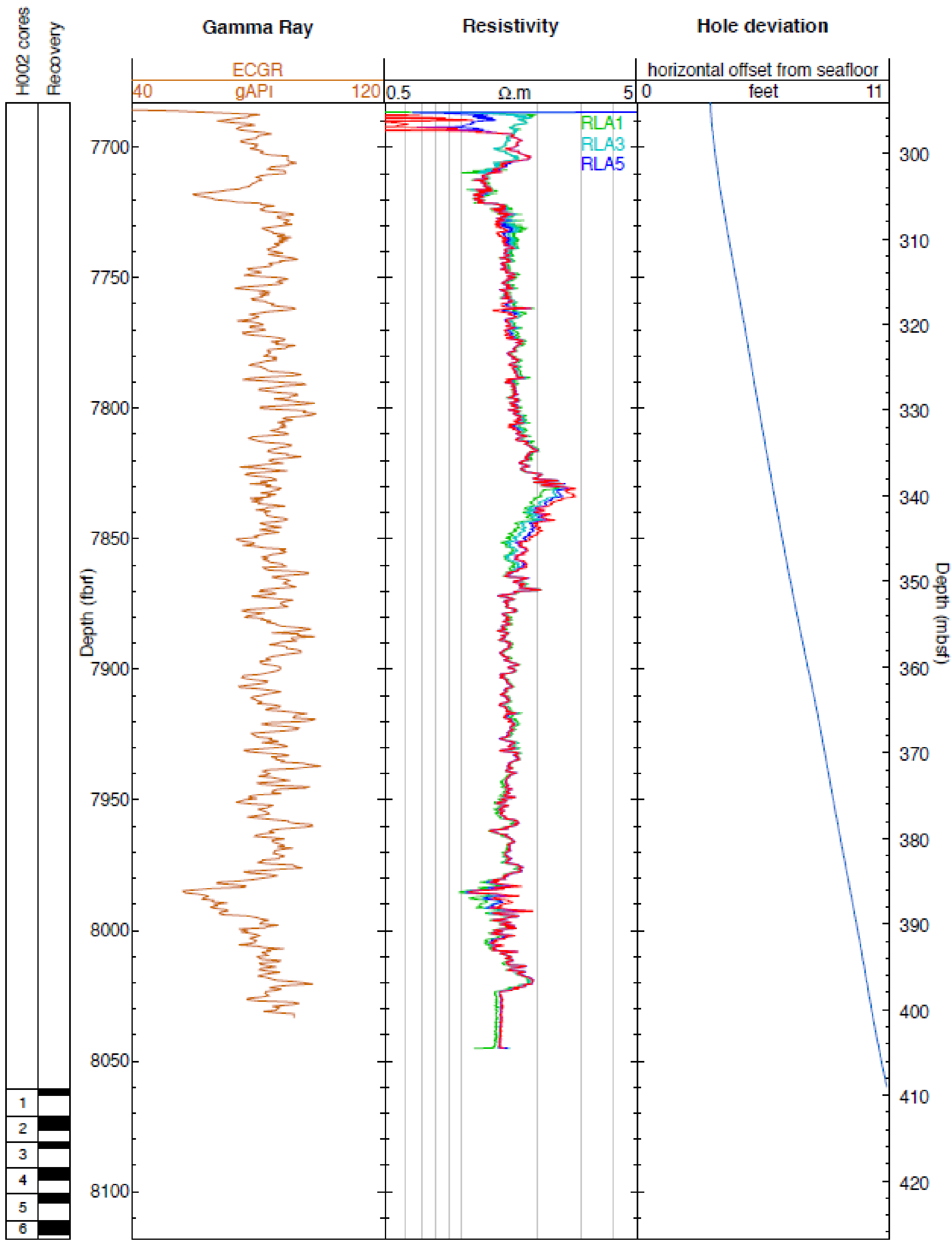

Figure 3.8.2 H002 recorded well logs and location of recovered core. All H002 survey data can be found in the expedition data directory under H002 / Wireline Logging.

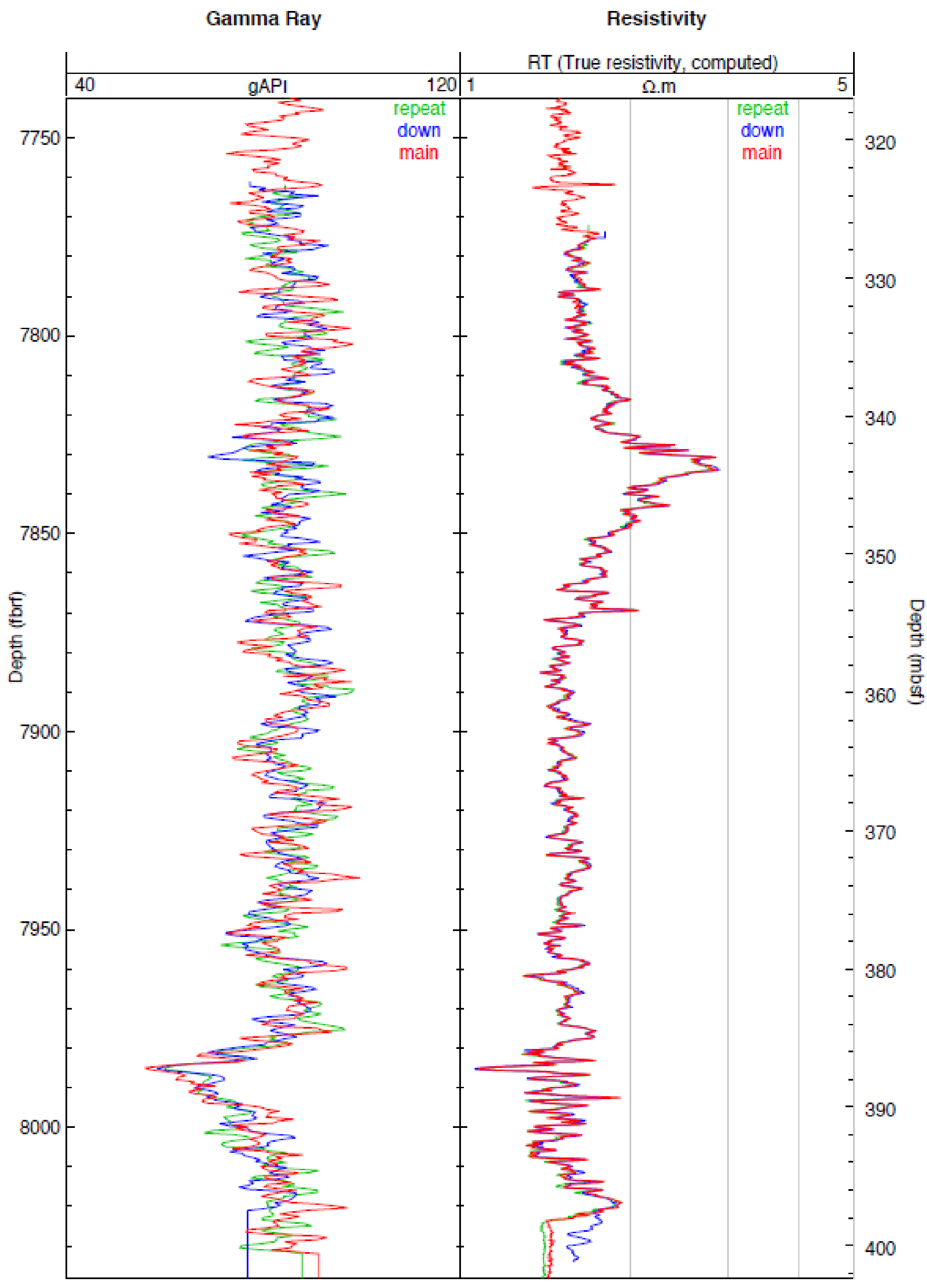

Figure 3.8.3 Comparison of H002 repeat, downlog and main well logging passes. All H002 survey data can be found in the expedition data directory under H002 / Wireline Logging.

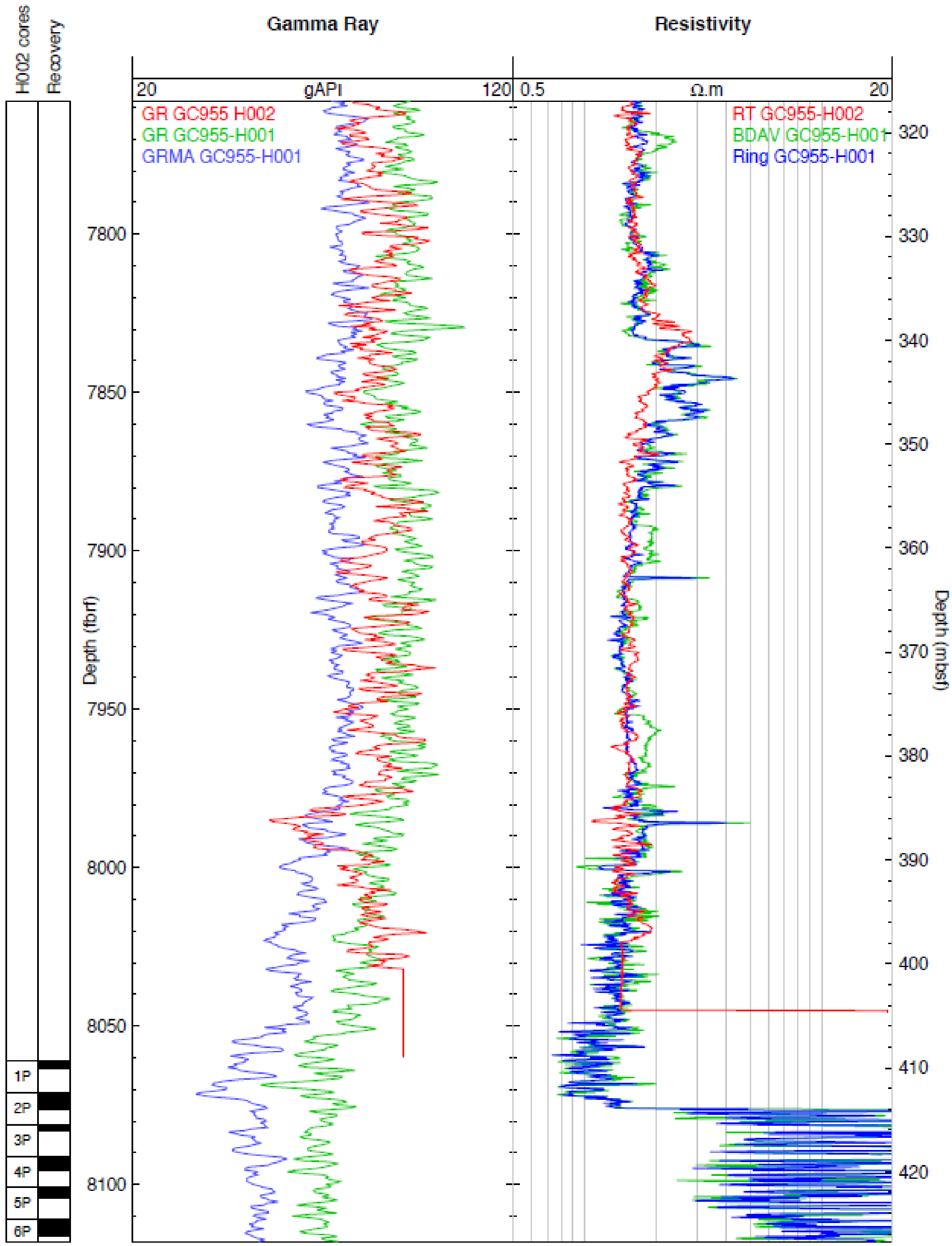

Figure 3.8.4 Comparison of logs from H002 and H001. (Guerin et al., 2012) All H002 survey data can be found in the expedition data directory under H002 / Wireline Logging.

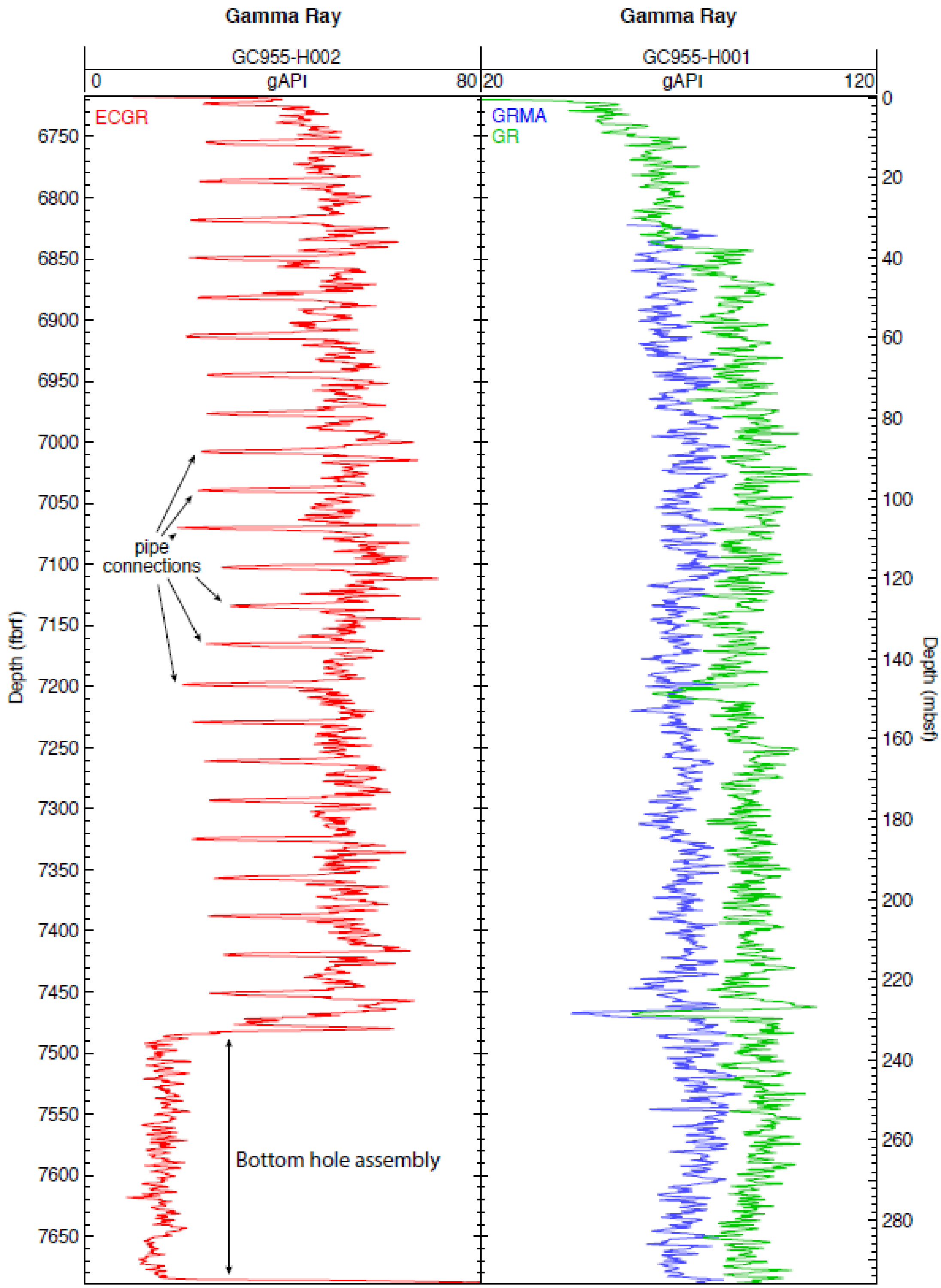

Figure 3.8.5 H002 gamma ray log recorded through the pipe versus H001 GR logs. (Guerin et al., 2012). All H002 survey data can be found in the expedition data directory under H002 / Wireline Logging.

3.9. References

Boswell, R., Collett, T. S., Frye, M., Shedd, W., McConnell, D. R., and Shelander, D., 2012, Subsurface gas hydrates in the northern Gulf of Mexico: Marine and Petroleum Geology, v. 34, no. 1, p. 4-30.

Collett, T. S., and Boswell, R., 2012, Thematic set on resource and hazard implications of gas hydrates in the Northern Gulf of Mexico: results of the 2009 Joint Industry Project Leg II drilling expedition, Marine & Petroleum Geology, Volume 34, p. 223.

Collett, T. S., Boswell, R., Frye, M., Shedd, W. W., Godfriaux, P. D., Dufrene, R. S., McConnell, D. R., Mrozewski, S., Guerin, G., Cook, A., Jones, E., and Roy, R., 2010, Gulf of Mexico Gas Hydrate Joint Industry Project Leg II: Logging-While-Drilling Operations and Challenges, Offshore Technology Conference.

Guerin, G., Cook, A., Mrozewksi, S., Collett, T., and Boswell, R., 2012, Gulf of Mexico Gas Hydrate Joint Industry Project Leg II: Green Canyon 955 LWD Operations and Results.

Munsell Color Company, Inc., 1994, Munsell Soil Color Chart (revised edition).